INCLUSION OF CELECOXIB IN MCM – 41 MESOPOROUS SILICA: DRUG
LOADING AND RELEASE PROPERTY

A THESIS SUBMITTED TO
THE GRADUATE SCHOOL OF NATURAL AND APPLIED SCIENCES
OF
MIDDLE EAST TECHNICAL UNIVERSITY

BY

ŞAHİKA GÜNAYDIN

IN PARTIAL FULFILLMENT OF THE REQUIREMENTS
FOR
THE DEGREE OF MASTER OF SCIENCE
IN
CHEMISTRY

JUNE 2014

Approval of the thesis:

INCLUSION OF CELECOXIB IN MCM – 41 MESOPOROUS SILICA: DRUG LOADING AND RELEASE PROPERTY

submitted by **ŞAHİKA GÜNAYDIN** in partial fulfillment of the requirements for the degree of **Master of Science in Chemistry Department, Middle East Technical University** by,

Prof. Dr. Canan Özgen
Dean, Graduate School of **Natural and Applied Sciences**   _____

Prof. Dr. İlker Özkan
Head of Department, **Chemistry**   _____

Assoc. Prof. Dr. Ayşen Yılmaz
Supervisor, **Chemistry Department, METU**   _____

Examining Committee Members:

Prof. Dr. Ceyhan Kayran
Chemistry Dept., METU   _____

Assoc. Prof. Dr. Ayşen Yılmaz
Chemistry Dept., METU   _____

Assoc. Prof. Dr. Emren Nalbant Esentürk
Chemistry Dept., METU   _____

Assoc. Prof. Dr. Sreeparna Banerjee
Biology Dept., METU   _____

Assoc. Prof. Dr. Gülay Ertaş
Chemistry Dept., METU   _____

Date: 17.06.2014

I hereby declare that all information in this document has been obtained and presented in accordance with academic rules and ethical conduct. I also declare that, as required by these rules and conduct, I have fully cited and referenced all material and results that are not original to this work.

Name, Last name: Şahika Günaydın

Signature:

ABSTRACT

INCLUSION OF CELECOXIB IN THE MCM – 41 MESOPOROUS SILICA:
DRUG LOADING AND RELEASE PROPERTY

Günaydın, Şahika

M. Sc., Department of Chemistry

Supervisor: Assoc. Prof. Dr. Ayşen Yılmaz

June 2014, 111 pages

Mesoporous silica particles have been used to enhance the biocompability of the drugs and provide control drug release. Celecoxib was chosen as a model drug which is poorly water soluble non-steroidal anti-inflammatory drug.

In this study, in order to determine the morphology effect on the drug loading capacity of the silica particles and release properties of the drug, MCM-41 particles were synthesized with different particle size, pore volume and surface properties. MCM-41-1 and MCM-41-2 labeled particles were nearly 50 nm with spherical shape and MCM-41-3 had ellipsoidal shape with nearly 500 nm particle diameter. In order to observe the template removal process on morphology of samples, acid extraction and calcination were performed. Boron doping of MCM-41 samples was prepared and borosilicate samples were obtained. Surfaces of samples were functionalized by post − grafting method with three different functional groups to observe the behavior of unfunctionalized and functionalized surfaces. Polyethylene glycol (PEG), luminescent groups and (3-Aminopropyl) triethoxysilane (APTES) were used in this way. Drug loading was examined in three different solvents, methanol, ethanol and

hexane, to observe the effect of polarity of solvent on the drug loading capacity of the carrier particles.

For the characterization process of pure and drug loaded samples, X-ray Diffraction (XRD), N_2 adsorption - desorption, Fourier Transform Infra-red (FTIR), Elemental Analysis, Scanning Electron Microscopy (SEM), Transmission Electron Microscopy (TEM), Ultra-Violet Spectrometry (UV-VIS), Zeta Potential and Thermogravimetric Analysis (TGA) were applied.

According to characterization process, Celecoxib remained in crystalline state in hexane and MCM-41-1 silica particles with highest pore volume held the highest amount of Celecoxib in it (29.51% by wt/wt). However, drug molecules were finely dispersed in ethanol and carrier particles held 25.95% Celecoxib in their pores and channels. It has been seen that functionalization could not increase the drug loading capacity of the MCM-41 particles.

The release experiments of the Celecoxib molecules in all samples were performed in phosphate buffer solution (PBS) pH=7.4 at 37 °C. Release rate of the drug molecules were also highly improved by using MCM-41 silica particles as drug carriers according to its commercial drug capsule, Celebrex. Sustained release was observed for all the samples. Celecoxib molecules loaded to carrier particles in ethanol were released faster in first six hours than hexane loaded samples. Among the silica samples, MCM-41-3 with average size released the lowest amount of drug in this time interval (63% in ethanol loaded and 59% in hexane loaded) and highest amount of release observed in borosilicate samples (87% in ethanol loaded and 66% in hexane loaded). These results confirm the potential of silica supports as drug delivery carriers for low water solubility drugs.

Keywords: Low water soluble drugs, MCM-41, drug delivery system, borosilicate and Celecoxib.

ÖZ

MCM-41 MEZOGÖZENEKLİ SİLİKA PARÇACIKLARINA SELEKOKSİB YÜKLEME ÇALIŞMALARI: İLAÇ YÜKLEME VE BIRAKMA ÖZELLİKLERİ

Günaydın, Şahika

Yüksek Lisans, Kimya Bölümü

Tez Yöneticisi: Doç. Dr. Ayşen Yılmaz

Haziran 2014, 111 sayfa

MCM-41 mezogözenekli silika parçacıkları, kontrollü ilaç salınımı ve ilaçların silika parçacıklarına yüklenme kapasitelerini arttırmak amacıyla kullanılmaktadır. Model ilaç olarak suda çözünmeyen, steroid yapıda olmayan, ateş düşürücü özellikteki Selekoksib kullanılmıştır.

Bu çalışmada, morfolojinin silika parçacıkların ilaç yükleme kapasiteleri ve Celecoxib moleküllerinin salınım özellikleri üzerindeki etkisini incelemek için, MCM-41 farklı parçacık boyutlarında, farklı gözenek hacimlerinde ve yüzey özelliklerinde sentezlenmiştir. MCM-41-1 ve MCM-41-2 olarak isimlendirilmiş parçacıklar küresel şekildedir ve 50 nm'den küçük parçacık boyutundadır. Oval şekildeki MCM-41-3 parçacıkları ise 500 nm çapındadır. Yüzey aktif maddeyi parçacıklardan uzaklaştırmak için kullanılan yöntemin morfoloji üzerindeki etkisini gözlemlemek için asit ekstraksiyon ve kalsinasyon kullanılmıştır. MCM-41 parçacıklarına bor eklenerek borosilikat parçacıkları elde edilmiştir. Ayrıca, fonksiyonlamış ve fonksiyonlanmamış yüzeylerin ilaç yükleme ve bırakma üzerindeki davranışlarını gözlemlemek için, parçacık yüzeyleri üç farklı fonksiyonel grup kullanılarak fonksiyonlanmıştır. Bunun için polietilen glikol (PEG), luminesans gruplar ve (3-Aminopropil) trietoksisilan (APTES) kullanılmıştır. İlaç yükleme

çalışmaları çözücünün polaritelerinin parçacıkların ilaç yükleme kapasiteleri üzerindeki etkisini gözlemlemek için üç farklı çözücü, metanol, etanol ve hekzan, kullanılarak gerçekleştirilmiştir. En son olarak kontrollü ilaç salınım çalışmaları yapılmıştır.

İlaç yüklenmiş ve yüklenmemiş parçakların karakterizasyonu X-Işınları toz kırınımı (XRD), N_2 adsorpsiyon-desorpsiyon, fourier-transform kızılötesi (FTIR), elemental analiz, taramalı electron mikroskobu (SEM), geçirimli electron mikroskobu (TEM), ultra-viyole spektroskopi (UV-VIS), zeta potansiyel ve thermo gravimetrik analiz (TGA) yöntemleri kullanılarak yapılmıştır. Karakterizasyon sonuçlarına göre, Selekoksib moleküllerinin hekzan içinde kristal yapıda kaldığı ve en büyük gözenek hacmine sahip MCM-41-1 silika parçacıklara en yüksek miktarda Selekoksib tutunduğu gözlemlenmiştir (%29.51). Ancak, ilaç molekülleri etanol içinde homojen şekilde dağılmış ve silika parçacıkların por ve kanallarına %25.95 oranında Selekoksib tutmuştur. Yüzey fonksiyonlamanın MCM-41 parçacıklarının ilaç yükleme kapasitelerini attırmadığı gözlemlenmiştir.

Selekoksib moleküllerinin salınım deneyleri fosfat tampon çözeltisinde pH=7.4 ve 37 °C gerçekleştirilmiştir. Selekoksib moleküllerinin salınım hızları ticari ilaç kapsülü Celebrex'e göre MCM-41 silika parçacıklarını kullanarak büyük oranda attırılmıştır. Salınım çalışmalarında, tüm örneklerde devamlı salınım gözlemlenmiştir. Etanol içinde parçacıklara yüklenen Selekoksib molekülleri hekzanda yüklenenlere göre ilk altı saatte daha hızlı salınmıştır. Ortalama parçacık boyutlarına sahip MCM-41-3 bu süre içinde en az miktarda ilacı yüzeyinden bırakmıştır (etanolde yüklenenler %63, hekzanda yüklenenler %59). En yüksek miktarda salınım borosilikat örneklerinde görülmüştür (etanolde yüklenenler %87, hekzanda yüklenenler %66). Bu sonuçlar silika parçacıkların düşük çözünürlükteki ilaçlar için geliştirilen ilaç taşıma sistemlerinde kullanılabileceğini doğrular niteliktedir.

Anahtar Sözcükler: Suda az çözünen ilaçlar, MCM-41, borosilikat, kontrollü ilaç taşıma sistemleri, Selekoksib.

To Gürol Günaydın, Emine Günaydın and Mediha Yılmaz…

ACKNOWLEDGEMENT

TABLE OF CONTENTS

LIST OF TABLES

TABLES

LIST OF ABBREVATIONS

MCM: Mobil Composition Matter

SBA: Santa Barbara Amorphous

PTES: Phenyltriethoxysilane

PEG: Polyethylene glycol

NSAID: Non-steroidal anti-inflammatory drug

XRD: X-Ray Diffraction

FTIR: Fourier-Transform Infra-Red Spectroscopy

TEM: Transmission Electron Microscopy

UV: Ultra-Violet

MCM-41-1@clx: Celecoxib loaded acid extracted MCM-41 particles

MCM-41-3@clx: Celecoxib loaded MCM-41 particles with larger particle size

CTAB: Cetyltrimethylammonium bromide

TEOS: Tetraethylorthosilicate

APTES: Aminopropyltriethoxysilane

COX: Cyclooxygenase

PBS: Phosphate Buffer Solution

TGA: Thermogravimetric Analysis

BET: Brunauer-Emmett-Teller

BJH: Barrett-Joyner-Halenda

SEM: Scanning Electron Microscopy

CLX: Celecoxib

MCM-41-1@clx: Celecoxib loaded calcined MCM-41 particles

B-MCM-41: Borosilicate

LIST OF FIGURES

FIGURES

CHAPTER 1

INTRODUCTION

Porous materials attract attention due to their functional network of channels and pores in different sizes. The function of these materials can be determined due to size of their pores. According to the definition of the International Union of Pure and Applied Chemistry (IUPAC), 3 different types of porous materials can be counted in this way; microporous, mesoporous and macroporous materials. While microporous materials have pore size smaller than 2 nm, pore size of macroporous material is larger than 50 nm. In this study, our main interest is the mesoporous materials with pore size ranging from 2 nm to 50 nm [1].

1.1 MESOPOROUS MATERIALS

Research interests in the field of porous materials started with conventional zeolites that have ordered micropores, good stability and high crystallinity. Discovery of zeolites created a lot of opportunities in the field of adsorption, separation, catalysis and storage. In spite of the large number of studies and advances made in this area, small pore size of the zeolites possessed a problem for many studies. As a result, in the early 1990s, with the studies in heavy petroleum conversion, scientists started to work on synthesis of materials with larger pore size and a new family of porous materials was introduced; M41S. This discovery is still counted as the milestone in the history of porous materials. Since then, mesoporous materials have attracted a lot of attention due to their ordered pore structure, uniform pore size, high internal surface area, good thermal and mechanical stability and ease of modification with different functional groups [2, 3].

1

It has been stated that mesoporous materials opened new horizons in the fields of membrane, catalysis, sensors, nanodevices, energy storage and conversion. However, in the 2000s, the importance of fields like nanomedicine and biomaterials has increased and scientists started to investigate in these areas. With the advancement in synthesis and modification of mesoporous materials, they started to be used in the fields of drug delivery. Their biocompability, nontoxicity, high loading capacity and thermal stability made mesoporous materials ideal carriers in drug delivery systems. So, in 2001 mesoporous materials started to be used as carriers in the delivery of ibuprofen drug by Vallet-Regi and his colleagues [4].

1.2 TYPES OF MESOPOROUS MATERIALS

1.2.1 M41S

After the introduction of M41S to the scientific studies as the first mesoporous material made from silica, a lot of developments have been made and important milestones have been achieved. Generally, M41S type mesoporous materials can be synthesized in alkaline conditions by using cationic surfactant and different types of mesoporous materials with different particle size, pore size, morphology, surface properties and structure have been synthesized. Types of M41S can be mentioned as MCM (Mobil Composition of Matter) and there are 3 types of it; cubic MCM - 48, hexagonal MCM - 41 and lamellar MCM – 50. With the slightly varying conditions in synthesis process such as temperature, pH, synthesis time, chain length of surfactant and auxiliary chemicals, different properties of mesoporous materials can be developed [5].

1.2.1.1 MCM-48

The main difference of MCM-48 among other mesoporous materials is its cubic arrangement with tridimensional pores. Important physical properties of MCM-48 are its high specific surface area and specific pore volume. These features make it perfect candidate for adsorbent in separation techniques and catalytic applications. However, due to its thin pore wall, its chemical and thermal stability is limited. Because of this stability problem, MCM-48 is less studied compared to MCM-41 type mesoporous materials [6].
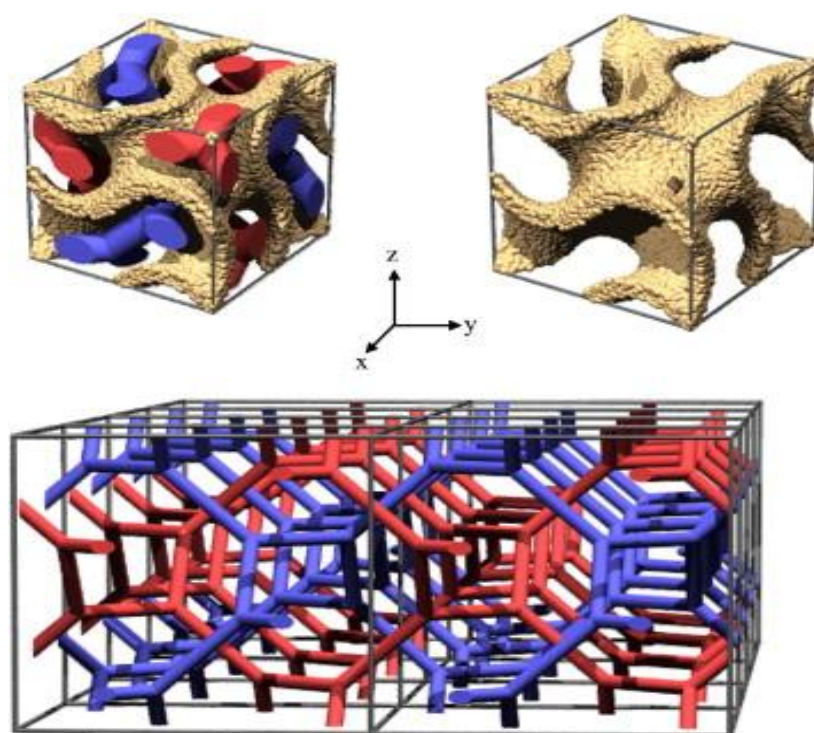
Figure 1: Cubic unit cell of MCM-48 [7]

1.2.1.2 MCM-50

Second member of M41S mesoporous materials is MCM-50. It has stabilized lamellar arrangement, with one-dimensional pores. Although its pore walls are thicker than MCM-48, its stability is also low. Moreover, its synthesis procedure is

slower and involves long stages. Due to its low stability and hardness of synthesis, it is the least studied mesoporous material among the others [8].

1.2.1.3 MCM-41

Among all M41S type mesoporous materials, silica based MCM-41 catches the attention of scientists most. Pore diameters of MCM-41 particles vary between 2 nm and 15 nm and their surface area reaches to 1000 m^2/g. Its hexagonal arrays of uniform, regularly ordered, one-dimensional cylindrical mesopores make MCM-41 ideal material for many studies in different fields. Ease of synthesis and modification has also improved the applicability of this promising mesoporous material. Although the number of the alternative synthesis procedures has been increasing day by day, basis of the original synthesis steps starts with combination of appropriate amount of silica source (e.g. Tetraethylorthosilicate), alkyltrimethyl ammonium halide surfactant (e.g. CTAB, Cetyltrimethylammonium bromide), base and water. In order to remove surfactant and obtain the mesoporous silica network, samples can be calcined at elevated temperatures or extracted in acidic solutions. By making small variations in synthesis process, MCM-41 in different morphologies like spheres, fibers, films and monoliths can be synthesized [9].
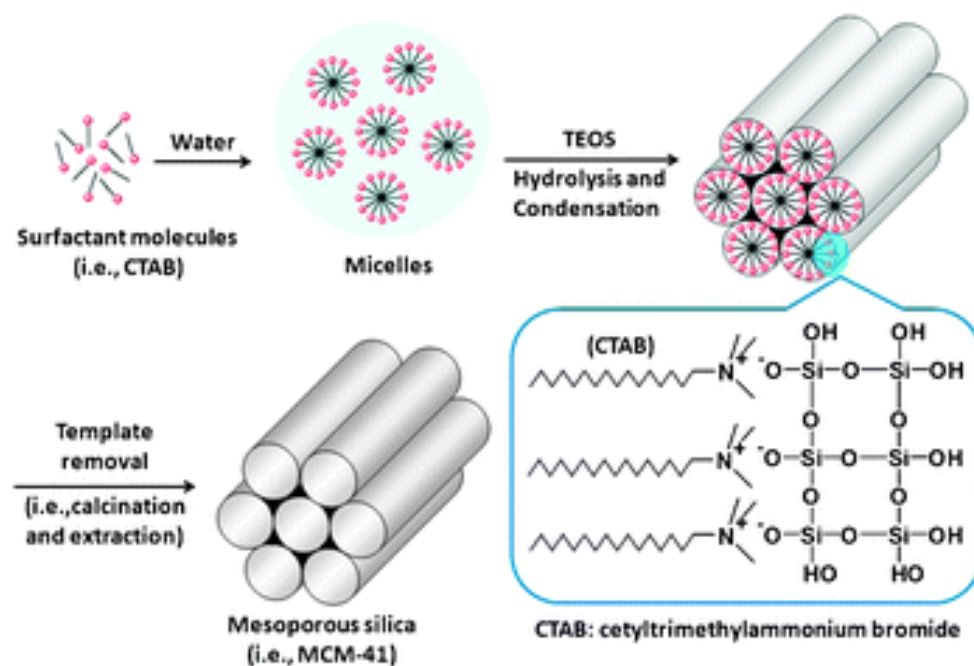
Figure 2: Scheme of the formation mechanism of MCM-41[10]

1.2.2 SBA

In order to improve the applicability of mesoporous materials in catalysis, separation processes and sensors, scientists started to work on a new mesoporous material with higher stability. On this way, Stucky and co-workers introduced SBA mesoporous material family that stands for Santa Barbara Amorphous. Difference of SBA family is their larger pore size and thicker pore walls in the range of 3.1 and 6.4 nm with respect to M41S mesoporous materials. By using non-ionic triblock copolymers instead of cationic surfactants under acidic conditions, mesoporous materials with high surface area, large pore size and high hydrothermal stability were synthesized. There are many different types of SBA materials such as SBA-15, SBA-16, SBA-11 and SBA-14, but SBA-15 is most widely used one among others [11].

1.2.2.1 SBA-15

These silica based mesoporous materials with hexagonal array of one-dimensional channels posses large pore size between 4 nm and 30 nm. If we replace the alkyltrimethyl ammonium halide surfactant in the synthesis procedure of MCM-41 with Pluronic 123 triblock copolymer and replace the base with acid, SBA-15 mesoporous material can be obtained. Their thicker pore walls make them hydrothermally and chemically more stable than M41S type. Due to this feature, SBA-15 silica materials more widely used as catalytic materials. [11].

Figure 3: Representation of pore arrangement of ordered SBA-15 silica material [12]

1.3 APPLICATION

Due to their unique features, mesoporous materials can be used in different fields. For instance, their large internal surface area and tunable pore volume allow them to incorporate active complexes in catalytic applications. Due to their non-toxic nature and hydrothermal stability, a lot of scientists use silica based mesoporous materials in biomedical studies such as imaging or disease treatment. One of the major application areas of them is adsorption. With large pore volume and flexibility, they can be used to absorb gases, liquids and heavy metals, and become a major component of environmental applications such heavy metal cation removal or sorption of organics from waste streams. In addition to these application areas, mesoporous materials can be modified or combined with different materials easily.

This feature broadens the application areas of mesoporous material. For example, when they are processed as thin films, mesoporous materials can be used in membrane separation that is used in biomedical sensors. Or, if they are processed as hollow tubules, mesoporous materials can find application in optics including lasers, light filters, sensors, solar cells, data storage [13, 14].

As we focused in this study, one of the promising usage areas of the mesoporous materials is drug delivery systems. Since the MCM-41 particles have been used as carrier in drug delivery systems since 2001, mesoporous silica materials attract lots of attention as drug carriers and controlled release systems. While high pore volume provides holding the required amount of drug particles, their ordered pore network allows controlled release of the drug in targeted area. During the delivery of drug in the body fluid, stability of the drug delivery system is maintained due to hydrothermal stability of silica mesoporous particles. These unique properties make them perfect carrier candidates in drug delivery systems. Due to the increasing number of the studies about the usage of the mesoporous materials in drug delivery systems, publications in this area have been increased. According to the Web of Science, 1400 papers have been published by 2011 with the keywords "mesoporous", "drug" and "delivery" [15, 16].

1.4 SURFACE FUNCTIONALIZATION

It has been reported that surface functionalization of mesoporous materials exhibits a lot of new approaches to scientific studies and these functionalization procedures are applicable. There are two ways of it; one-pot synthesis and post-grafting.

1.4.1 ONE-POT SYNTHESIS

Generally, in one-pot synthesis, all the precursors undergo reactions in one reactor. With this technique, organic functionalities are dispersed homogenously within the matrix. One-pot synthesis of mesoporous silica materials requires the co-

condensation between silica source and selected organotrialkoxysilanes (e.g. PTES ,phenyltriethoxysilane or APTES, aminopropyltriethoxysilane) in a compatible solvent. The siloxane precursors determine the structure, while the organosilanes contribute to build the structure and to functionalize the material surface. Drawback of this synthesis approach is to find a compatible solvent in which all the precursors are soluble [17, 18, 19].

1.4.2 POST – GRAFTING

This synthesis technique utilizes silanol groups of mesoporous silica as bonding sites to form linkage with organic functional groups. It consist two different steps; substrate preparation and post-grafting. In the first step, mesoporous silica is synthesized. In the following post-grafting step, the free silanol groups on the surface of the silica react with organosilane and they are replaced with organic functional groups. Many compounds such as transition metal halides, hydrides, alkoxides, complexes and functional silanes can be bonded onto the frameworks of mesoporous silica by this method. While the structure of the mesoporous material remains same, the thermal and hydrothermal stability can be increased [11].

1.4.3 TYPES OF SURFACE FUNCTIONALIZATION METHODS

There are different examples of surface functionalization types. For different application areas, mesoporous materials can be functionalized in different ways. For biomedical application, surface is generally functionalized with chemical groups that can form linkage with therapeutic agents. A lot of drug delivery, controlled release and imaging systems are set up with this approach. For example, Song et al [20] functionalized SBA-15 silica particles with amino groups to use them in controlled release of ibuprofen. These amino groups form an ionic interaction with the carboxy groups of ibuprofen drug. They reported that this functionalization resulted in increased drug loading and slower drug release. Alternatively, polymers can be used

in surface functionalization of mesoporous particles. For instance, silica particles can be pegylated. Pegylation is a process in which PEG (polyethylene glycol) is attached to another molecule with covalent bonding. PEG coated silica particles offers lots advantages. Firstly, PEG molecules prevent the aggregation of particles by the repulsion force. It provides a biocompatible and protective surface for bonding of therapeutic agents. PEG also protects the particles from elimination by the immune system in vivo [21]. Silica particles coated with phosphor shells such as $YVO_4:Eu^{3+}$ or $LaPO_4:Eu^{3+}$ can be used in biological labeling, imaging and drug delivery. Phosphor particles that are widely investigated show different optical properties with different size and morphology. By using silica particles, their morphology and size can be controlled easily and different types of photoluminescent property can be obtained [22]. Alternatively, mesoporous materials can be functionalized with magnetite materials such as Fe_3O_4. By this way, they provide magnetic responsivity and good biocompability. They can be used in diagnostic analysis, bio-separation and controlled release systems [23].

Functionalization with boron trioxide is another way to use silica mesoporous materials in different fields by adding boron atoms to silica network. After the functionalization process, borosilicate material that has high thermal and chemical resistance is obtained. This promising material can be used in variety of application areas in semiconductors, optical devices, biomedical fields as carrier in drug delivery systems, implantable medical devices or sensors [24].

If the mesoporous materials are wanted to be used as adsorbent, they can be functionalized with thiol and amino ligands. For example, in order to use silica particles as adsorbent for the removal of heavy metal ions from waste water, they should contain specific binding sites for these heavy metal ions. Liu et al. [25] reported that SBA-15 particles functionalized with 3-mercaptopropyltriethoxysilane shows specific affinity for binding of Hg^{2+}. On the other side, SBA- 15 functionalized with 3-aminopropylltriethoxysilane groups exhibited higher binding capacity for relatively harder metal ions such as Cu^{2+}, Zn^{2+}, Cr^{3+} and Ni^{2+}.

As it is mentioned above, mesoporous materials can be used as catalyst in different reactions. For this purpose, they can be functionalized with different chemicals. For instance, Das and his colleagues [26] functionalized MCM-41 particles with sulfonic acid and used them as catalyst in the condensation of phenol and acetone to synthesize Bisphenol-A that is an important raw material for polymer and resin production. They have found that synthesis reactions catalyzed with sulfonic acid functionalized MCM-41 particles showed high selectivity at relatively low reaction temperatures.

CHAPTER 2

CONTROLLED DRUG DELIVERY SYSTEMS

Drugs have being used for decades in order to improve health and living standards. The release of a drug in body can be divided into two groups according to US FDA (Food and drug administration); immediate release and modified release. In immediate release, drug is released immediately after intake takes place. However in modified release, drug is released some time after the administration. Modified release can be further classified as delayed release and extended release. In delayed release, drug is released short time after initial intake however in extended release; release of the drug is prolonged to reduce dosing frequency. Drug delivery systems are technologies, approaches or systems engineered in this way, for targeted delivery and controlled release of the therapeutic agents. Incorporation of therapeutic agents into the matrix of mesoporous materials offers lots of opportunities in drug delivery systems. They aim to improve the effectiveness of drug therapies and prevent harmful side effects. This can be achieved by controlling different aspects such as release profile, capacity to cross biological carriers, biodistribution, clearance, and stability. Drug delivery systems contain two main components; particulate carrier and associated therapeutics. Many different kinds of drugs can be used in drug delivery systems such as antibiotics or chemotherapeutics drugs [27, 28, 29].
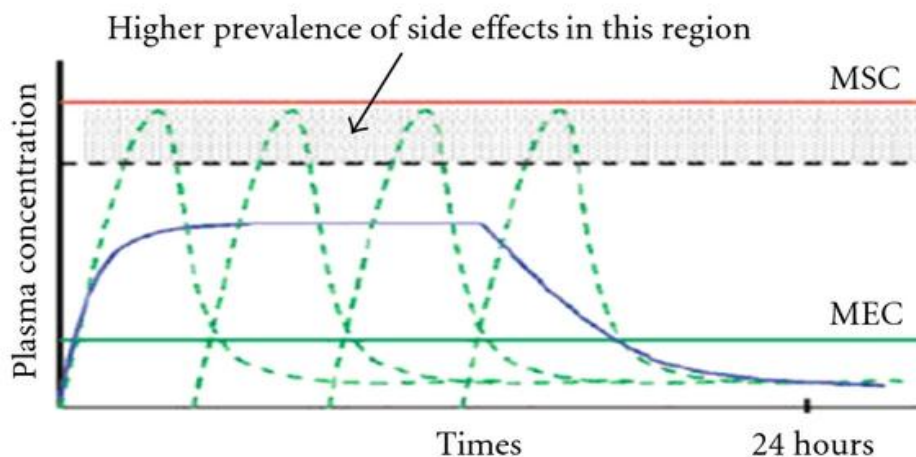
Figure 4: Release profiles of immediate release (green) and modified controlled release (blue) of a drug [29] (MSC: Minimum safe concentration, MEC: Minimum effective concentration)

There are different types of drug delivery systems being used and investigated. Although the purpose of the ongoing studies is same as improving the delivery and release of the drug, each one works with different carrier and different drug molecule. Ideal drug carrier in a drug delivery system should be non-toxic, biocompatible, non-immunogenic and biodegradable. In this way, different carriers can be used such as polymers, liposomes, lipoproteins. However, there are some limitations about these carriers such as premature degradation of the therapeutic agent, destruction of the polymeric system, poor chemical and thermal stability, non - homogeneous dispersion of the drug and rapid excretion through the system. Due to these limitations, mesoporous materials come forward as drug carriers with their unique properties [30].

A lot of factor affecting the drug delivery systems should be considered. Firstly, volume of pores of the mesoporous materials should be compatible with the size of the drug, so that drug adsorption and release can be controlled by size selectivity. For example, according to the study done by Horcajada, Rámila and Valet-Regi, aimed to explain pore size and release rate relation, as the pore size of the MCM-41 was decreased, the release rate of the ibuprofen drug molecules was decreased as well

[28]. Chemical interaction of pore walls and drug molecules should be also considered. For further applications, pore walls of the mesoporous material should be modified easily to maximize the adsorption and release of the drug molecules. Surface functionalization with different groups can change electrostatic, hydrophobic, hydrophilic forces and the adhesive interactions of drug and matrix that affect adsorption and release behavior of mesoporous materials. Biodegradability and biocompability are other two important key factors affecting the drug delivery systems [15, 31].

In traditional drug delivery systems like oral or intravascular delivery, drug is carried through the blood circulation. However most of the active molecules are released before reaching the target site and causes the side effects. One of the purposes of controlled drug delivery is to prevent these effects. To achieve this, drug release should be controlled and drug loss before the carrier reaches the target site should be avoided. This approach minimizes the toxicity and side effects [15].

CHAPTER 3

HYDROPHOBIC DRUGS

Although there are different ways of drug intake, oral administration is the most desired one, because it is simple, painless and easy to control the dosage. To deliver a drug molecule to the targeted area in the body in an effective way, bioavailability of the drug is the most important concern. To call a drug molecule as 'bioavaliable', it should have 3 important features; solubility, permeability and stability. However, it has been reported that 40% of the lately developed pharmaceutical agents are poorly water soluble or insoluble. So, enhancing solubility of a hydrophobic drug is an important subject in the way of developing and achieving optimum adsorption of a drug molecule. As it can be seen in the Figure 5, hydrophilic drug is dissolved in the gut lumen and dissolved small drug molecules get absorbed by the blood stream easily. However in Figure 6, hydrophobic drugs stay intact and cannot be absorbed due to insolubility [32, 33].
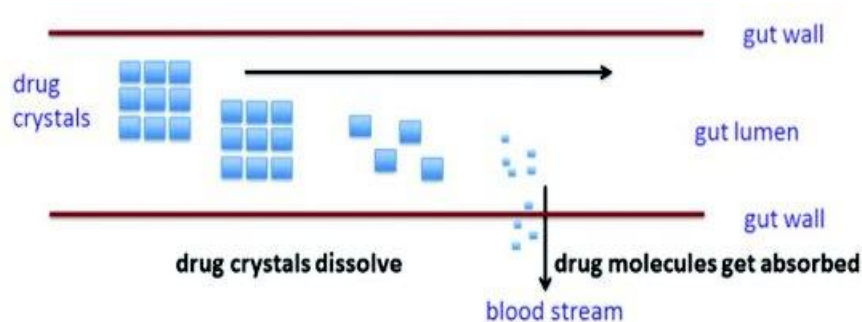
Figure 5: Water soluble drugs during the passage of gastrointestinal tract [33]
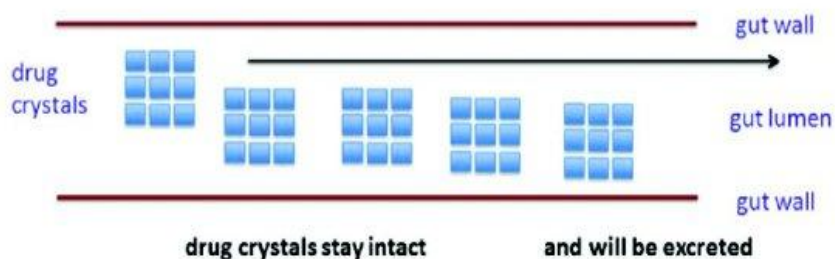
Figure 6: Water insoluble drugs during the passage of gastrointestinal tract [33]

'Hydrophobic drug' term generally can be defined as the molecules that are insoluble or poorly soluble in water. If drug is dissolved in a solvent as 1-10 mg/mL, it is said to be soluble. If it is dissolved as 0.1-1 mg/mL, it is slightly soluble. However if the amount of the dissolved drug is below 0.1 mg in 1 mL solvent, we can say that it is practically insoluble.

Poor solubility and dissolution rate of many drugs is a challenging task to overcome. Dissolution is the first step of adsorption of drug. In this way, aqueous medium of the blood and gastrointestinal tract provide an undesirable environment for dissociation and delivery of hydrophobic drugs. Insufficient solubility leads to the undesired pharmacokinetic properties and minimize the therapeutic effects of the drug molecules. Poorly soluble drugs can be eliminated from the gastrointestinal tract before dissolving completely and being absorbed. This may cause low bioavailability and poor dosage intake. Because of the hydrophobic drugs, solubilization of drug molecules and developing an efficient drug delivery system is an important task. There are lots of ongoing studies to improve the solubility and pharmacokinetic properties of this type of drugs [34].

3.1 FACTORS AFFFECTING SOLUBILIZATION OF HYDROPHOBIC DRUGS

Physical form of the drug, composition of the solvent medium and environmental conditions can be counted as the factors affecting the solubilization of the

hydrophobic drugs. Particle size is the most important factor influencing the solubilization. As the particle size of the drug decreases, its surface area increases. With the increasing surface area, drug particles can interact with solvent easily. When the temperature of the system is increased, solution that contains drug molecules absorbs energy and its solubility increases as well. The solubility of the drug increases when molecules have lower molecular weight and lower molecular size because larger molecules are more difficult to surround with solvent molecules. Polarity is the other factor affecting the solubilization of hydrophobic drug. The polar drug molecules have a positive and a negative end. If the solvent molecule is also polar then positive ends of solvent molecules will attract negative ends of drug molecules. This is a type of intermolecular force known as dipole-dipole interaction. Dipole-dipole interaction enhances the solubility of the hydrophobic drug molecules [35].

3.2 TECHNIQUES USED TO ENHANCE THE SOLUBILITY OF HYDROPHOBIC DRUGS

Due to the results of studies made in this area, limitation of poor solubility of drug can be overcome with different ways. One of them is self-emulsifying systems that accommodate hydrophobic drug molecules with mixtures of oils, surfactants and cosolvents. They use the formation of emulsion in the gastrointestinal tract. Drugs are generally in the form of soft or hard gelatin capsules. Drug molecules that show hydrophobic properties are generally lypophilic. Lipid based formulations are the key concept in this way. Due to the study done by Strickley [36] aimed to explain the properties of low solubility drugs, a lot of different excipients for preparing lipid-based formulations can be used such as dietary oils composed of triglycerides (e.g., vegetable oils), lipid soluble solvents (e.g., polyethylene glycol, ethanol, propylene glycol, glycerin), and various pharmaceutically-acceptable surfactants. However using an excipient limits some of the functions of the drug molecules. For example, this type of drugs cannot tolerate room temperature, and they should be kept in specific temperature conditions. Because of this, their chemical and physical stability

is low. Also, some of the synthetic excipients such as polyethylene glycol can irritate the gastro intestinal mucosa. On the other side, due to its ease to manufacture and simplicity, lipid based formulations are one of the most commonly used solutions to the low solubility problem of hydrophobic drugs [34, 35, 37].

Another way to enhance the solubility of hydrophobic drug molecule is reducing the particle size and increasing the surface area. Although it is a commonly used technique to improve the solubility of hydrophobic drugs, there are some limitations of it. Size reduction can be achieved by grinding or controlled crystallization. However, there is a practical limit of reducing the size of the molecules by these conventional ways. Also, using finely divided powders can be stated as a problem due to its controlling difficulties. Dosage form should be precise and it is hard to deliver these small drug molecules to the target site. Besides, due to the high surface charge of the drug molecules, there is risk of particle agglomeration. To reduce this risk, suitable excipients should be used in this technique [33, 37].

Solid dispersion is the other alternative way to improve the solubility of hydrophobic drugs. This technique not only increases the dissolution rate but also enhances the bioavailability of the drug. Due to the physical state of the drug and the carrier, different types of solid dispersions can be used in hydrophobic drug delivery. As it can be seen in the Figure 7, solid dispersion includes the formation of mixtures of drug and highly hydrophilic carrier, spray drying process and hot-melt extrusion. Drug particles are dispersed in matrix of the carrier and solution is formed. This solution is subjected to a drying process and hot-melt extrusion. While the solid dispersion based drug is delivered, carrier is dissolved in body and the drug is delivered as finely divided colloidal particles. By this way, crystalline drug is converted into the amorphous form. The resulting high surface energy form leads to increase in solubility. However there are some drawbacks of this technique. Firstly, it requires different steps of preparation and generally it is hard to prepare solution. Because the drug is hydrophobic and the carrier is hydrophilic, finding an appropriate solution that dissolves both components is difficult. Secondly, due to dependence of solid solution on manufacture conditions like temperature, heating

rate, mixing time and cooling method; reproducibility and stability of the technique is low. Also, some of the carriers that can be used in this technique exist in unstable state in solution and undergo some changes with time [38, 39].
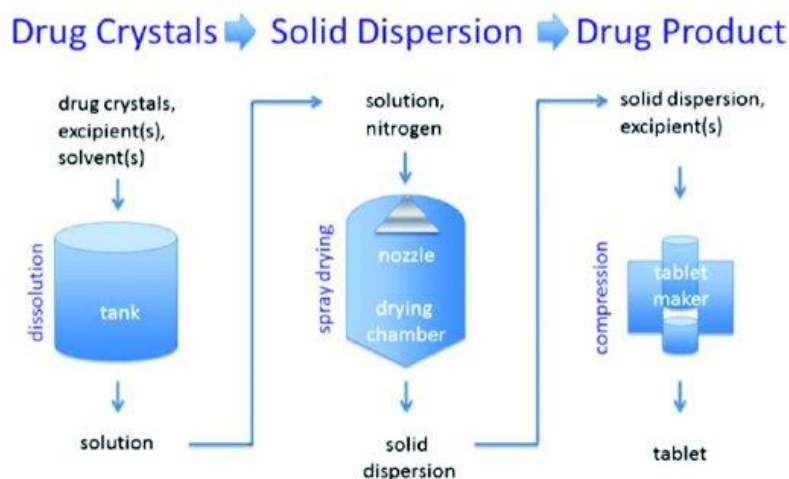
Figure 7: Manufacturing process of solid dispersion based drug [33]

Recently, another way of maximizing the solubility of a hydrophobic drug is using inorganic carriers such as silica. In this respect, hydrophobic drug can be molecularly dispersed in the arrays of pores in inorganic carrier. After the introduction of solvent to the pores in body, drug molecules are released. For example, as depicted in Figure 8, Mellaerts et al [40] used SBA-15 mesoporous silica as carrier in the delivery systems of hydrophobic drug, itraconazole. They found out that drug molecules were loaded into the pores of silica particles in 30% by weight. Release of the itraconazole from silica particles gave rise to supersaturation in gastric fluid and supersaturated concentrations were maintained for at least 4 h. There are a lot of different advantages of this technique. Firstly, tunable pore volume of silica particles allows capturing required amount of therapeutic agents. Generally, larger pore sizes than the drug molecule diameters are suitable for adsorption of drug molecules. Ordered pore network allows homogeneous drug load and release. Also silanol groups on the surface the silica particles can be functionalized. Their compositions, porosities and morphologies can be altered with small variation in synthesis process. Secondly,

19

silica particles are highly non-toxic and biocompatible [5]. Their chemical and physical stability are high under body fluid. Because of these advantages, inorganic carriers can be counted as the most advantageous drug delivery system for enhancing the solubility of hydrophobic drugs.
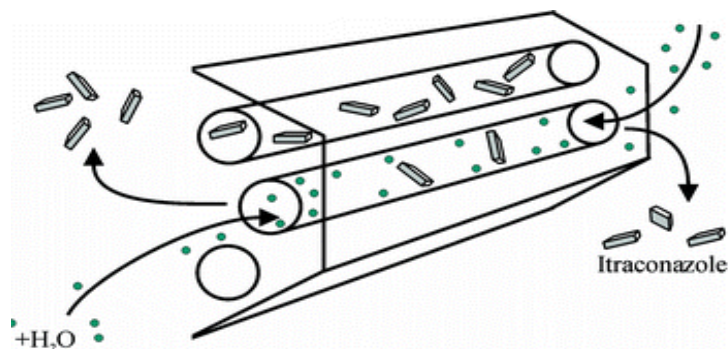
Figure 8: Enhanced release of itraconazole from SBA-15 resulting from the rapid influx and competitive adsorption of water [40]

3.3 CELECOXIB AND PHARMACOLOGY

Celecoxib is chemically designated as 4-[5-(4-methylphenyl)-3-trifluoromethyl)-1H-pyrazol-1-yl] benzene sulfonamide with the empirical formula $C_{17}H_{14}F_3N_7O_2S$, and molecular weight of 381.373 g/mol. It is a non-steroidal anti-inflammatory drug and generally used in the treatment of pain and inflammation. The most important property of Celecoxib is its high hydrophobicity. At pH 7 and $40^{o}C$, it is solubility in water is 0.003–0.007 mg/mL. Due to its water insolubility and high lipophilicity; it is classified as class II drug according to Biopharmaceutics Classification Scheme. It is also a weak acid with pKa≈11. [41].
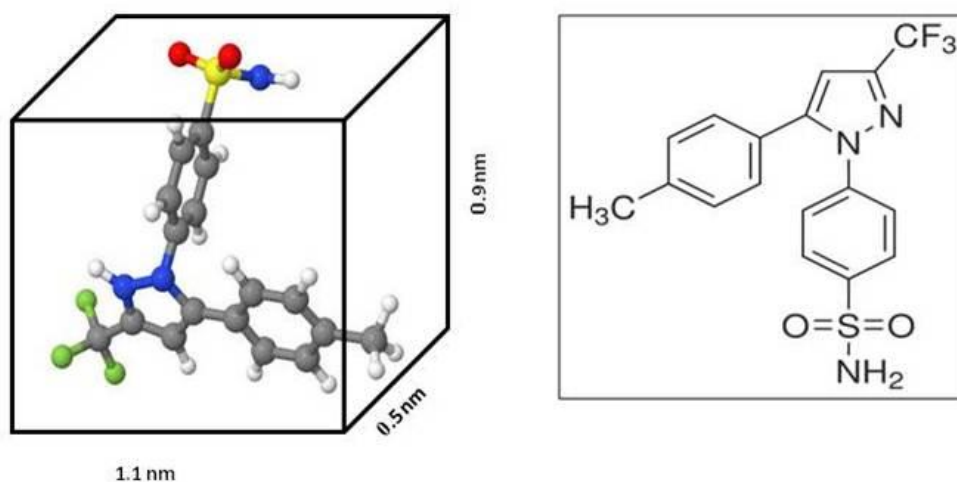
Figure 9: Structure and dimensions of Celecoxib, 4-[5-(4-methylphenyl)-3-trifluoromethyl)-1H-pyrazol-1-yl] benzene sulfonamide

Celecoxib selectively inhibits the Cyclooxygenase-2 enzyme. Cyclooxygenase (COX) is an enzyme that is responsible for converting arachidonic acid to the prostanoids that result in pain and inflammation. There are two different types of COX; COX-1 and COX-2. Traditional non-steroidal anti-inflammatory drugs (NSAID) are nonselective and inhibit both of the COX enzymes. However, inhibition of COX-1 can lead to NSAID toxicity and cause mucosal damage, ulceration and ulcer complication in the gastrointestinal tract. Celecoxib binds to hydrophilic side pocket region of the COX-2 with its polar sulfonamide side chain and this selectivity allows it to reduce inflammation and pain. It also minimizes adverse gastrointestinal effects that are common in traditional nonselective NSAIDs. Because of this, Celecoxib is safer than traditional NSAIDs because of its selectivity. Due to the analysis done in 2008, Celecoxib is the eighth most commonly advised arthritis drug among 8 million prescriptions written by rheumatologists from January to March 2008 [42, 43].

Although Celecoxib is the most advantageous NSAID among others, all the NSAIDs may rarely increase the risk of high blood pressure and heart diseases, especially for the patients with a heart problem or increased risk of heart diseases. Adverse effect of Celecoxib is generally known as heart or circulation problems such as heart attack or stroke, especially if you use it in long term. The FDA warned in 2005 regarding cardiovascular risks associated with Celecoxib and other NSAIDs. Withdrawal of some NSAIDs from the market raised the concerns about the potential risk of the drugs in this class. However, in 2006, Frank Andersohn and his colleagues made a nested case-control study by using the data from the UK General Practice Research Database. They worked with 469 674 cases and examined the effect of Rofecoxib, Etoricoxib and Celecoxib on the risk of ischemic stroke. 3094 ischemic stroke were identified. They found out that usage of Rofecoxib and Etoricoxib causes significantly increased risk of ischemic stroke in first 3 months of treatment. This high effect in the current usage of Celecoxib could not be observed. Percentage of nonfatal strokes was the same for Celecoxib 400 mg/day and placebo (both 0.4%). The increased cardiovascular risks of it became apparent after 12 months of treatment. Frank Andersohn and his colleagues concluded that NSAIDs may differ in their potential to cause harmful cardiovascular effects and Celecoxib is the safest one with respect to strokes [44].

Another study done by L. Chen and M. Ashcroft aimed to examine the adverse celebrovascular effect of NSAIDs. They worked with 88 116 patients and compared the celebrovascular risk of Celecoxib, Rofecoxib, Etoricoxib, Lumiracoxib with placebo drug. Due to results of the study, the proportions of patients experiencing celebrovascular diseases were not different from the patients taking placebo. They saw no evidence about the significantly increase risk of celebrovascular diseases when Celecoxib were taken in 200 mg/day [45].

In the purpose of the enhancing solubility and oral bioavailability of the Celecoxib, in 2009, Tan and colleagues [46] made a research and chose it as a model drug. They investigated the silica-lipid hybrid microcapsules that are composed of medium-chain triglycerides, lecithin and silica particles to encapsulate the Celecoxib

molecules. They observed increased release rate and better dissolution of drug. In addition to that, they increased the stability of it by this encapsulation technique. Zhao et al [47] made another research in 2012. They used fibrous ordered mesoporous carbon as drug carrier due to its high surface area, large pore volume and strong adsorption ability. It was reported that 1 g of mesoporous carbon was loaded with 0.599 g of Celecoxib. Besides they showed faster release rate and caused no damage to gastric mucosa. By using ethanol as a solvent in the loading process, they managed to change the crystalline state of the Celecoxib drug molecules to the non-crystalline and enhance the bioavailability.

3.4 AIM OF THE WORK

In this study, firstly our aim is to synthesize MCM-41 type silica particles with well-ordered array of pores and narrow particle size distribution. In order to compare morphology effect, two different diameter sizes of MCM-41 particles were used: MCM-41-1 and MCM-41-2 labeled particles have nearly 50 nm and MCM-41-3 has average size with nearly 500 nm particle. In order to investigate effect of boron doping to silica network boron added MCM-41 particles were prepared and labeled as B-MCM-41. Surface functionalization were performed for MCM-41 samples by post synthesis method adding PEG, APTES and YVO4:Eu luminescent groups to search behavior of unfunctionalized and functionalized silica surface. In the purpose of observing the effect of solvent on the loading efficiency of Celecoxib, 3 different solvent were used; methanol, ethanol and hexane. By this way, we wanted to control and enhance the release rate of this hydrophobic drug and improve its biocompability.

CHAPTER 4

EXPERIMENTAL

4.1 SYNTHESIS OF MCM-41

4.1.1 SYNTHESIS OF MCM-41-1 & MCM-41-2

With the synthesis procedure written by Zheng and his colleagues, 0.75 g CTAB (hexadecyltrimethylammonium bromide) was dissolved in 360 mL distilled water [48]. 2.0 mL 2.0 M NaOH solution, that was prepared with 8.0 g NaOH pellets and 100.0 mL distilled water, was added to catalyze the CTAB solution and temperature was increased to 80 °C. 3.75 mL TEOS (tetraethyl orthosilicate), which is source of silica, was added to the mixture under stirring drop by drop. This mixture was stirred for 2 hours at 80 °C. After the white precipitate formed in 2 hours, it was filtered with filter papers, washed with distilled water and dried at 50 °C overnight in the furnace.

When the dried sample was obtained, 1.0 g of the dried silica particle was taken for acid extraction and mixed with methanol and 37% HCl solution that is prepared with 100 mL methanol and 1 mL HCl. The mixture was mixed at 60 °C for 6 hours, filtered with filter paper and washed with distilled water. It was dried at 50 °C overnight in the furnace. By this way, surfactant was removed and silica network of the MCM-41-1 was obtained.

As an alternative method to remove the surfactant by acid extraction, calcination was used. White precipitate obtained in first step placed in the muffle oven inside the crucible. The ramp rate was 1°C / min. To remove the adsorbed water, after the temperature was reached to 160 °C, sample was heated at this temperature for 2 hours. Then, the temperature was increased to 550 °C and kept the sample at this

temperature for 6 hours. With this purification technique, MCM-41-2 particles were obtained.

The amounts of the chemicals used in the synthesis procedure are given in Table 1. All of the chemicals were used without further purification.
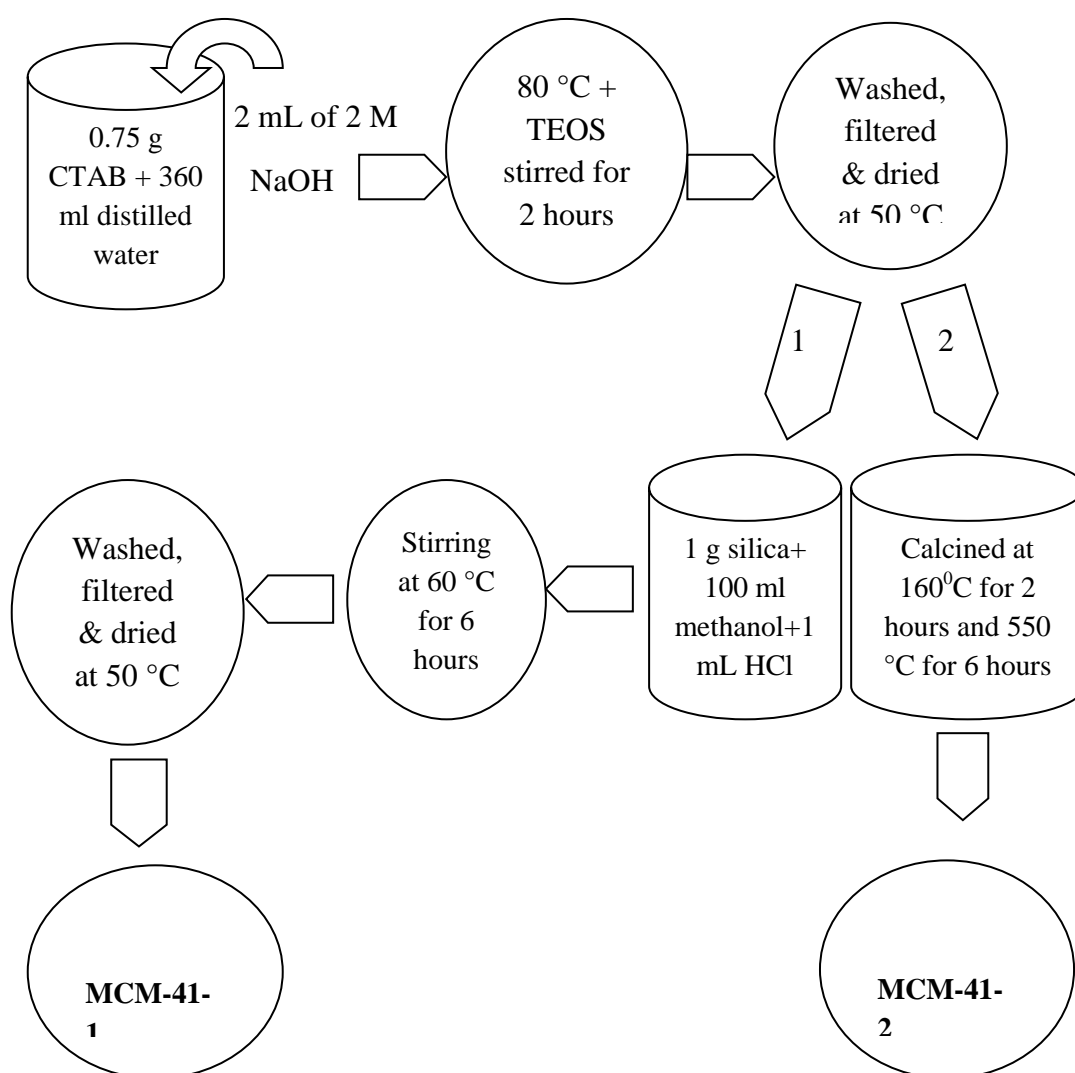
Figure 10: Schematic representation of synthesis of MCM-41-1 and MCM-41-2

Table 1: Precursors used for MCM-41-1 & MCM-41-2 synthesis

Chemicals	m(g) or V(mL)	Brand	d (g/mL)	MW (g/mol)
CTAB	0.75 g	Sigma - Aldrich	390.0	364.5
NaOH	8.00 g	Sigma - Aldrich	2.13	39.99
TEOS	3.75 mL	Aldrich	0.93	208.33
HCl	1.00 mL	Sigma - Aldrich	1.20	36.46
Methanol	100 mL	-	0.79	32.04
H_2O	460 mL	-	1.00	18.00

4.1.2 SYNTHESIS OF AVERAGE SIZE MCM-41

2.0 g CTAB was dissolved in 480.0 mL distilled water and 7.0 mL of 2.0 M NaOH was added under stirring. Solution was heated up to 80 °C and mixed for 30 minutes. After 10.0 mL TEOS was added to the mixture drop by drop, it was mixed for 2 hours at 80 °C. The white precipitate, formed in 2 hours, was filtered with filter paper, washed with distilled water and dried at 50 °C overnight in the furnace.

After it was dried, acid extraction was done to remove the surfactant. 1.0 g of MCM-41-3 sample was added to 100.0 mL ethanol and 1.0 mL 37% HCl and mixed at 60 °C for 6 hours. Sample was dried at room temperature again. By this synthesis procedure, average size MCM-41 silica particles in size of 500 nm labeled as MCM-41-3 was obtained.

4.1.3 SYNTHESIS OF BOROSILICATE

According to the procedure of Zhang et al., 0.64 g CTAB was dissolved in 32.0 mL distilled water. 10.0 mL 25% NH_3 solution, 14.5 mL acetone and 0.16 g boric acid was added [49]. The solution was mixed for 20 minutes. After 2.8 mL TEOS was added, solution was mixed for 2 hours. White precipitate was filtered with a filter

paper, washed with distilled water and dried in oven at 50 °C for overnight. In order to remove the surfactant, calcination was used. White precipitate placed in the muffle oven inside the crucible. The ramp rate was 1 °C/ min. After the temperature was reached to 160 °C, sample was calcined at this temperature for 2 hours to remove the adsorbed water. Then, the temperature was increased to 550 °C and kept the sample at this temperature for 6 hours. With this technique used to remove the surfactant, B-MCM-41 was obtained.

Table 2: Precursors used for B-MCM-41 synthesis

Chemicals	M(g) or V(mL)	Brand	d (g/mL)	MW (g/mol)
CTAB	0.64 g	Sigma - Aldrich	390.0	364.0
NH_3	10.0 mL	Sigma - Aldrich	0.73	17.0
Acetone	14.5 mL	-	0.79	58.0
Boric acid	0.16 g	Sigma - Aldrich	1.44	61.8
TEOS	2.80 mL	Aldrich	0.93	208.3

4.2 SURFACE FUNCTIONALIZATION

4.2.1 LUMINESCENCE FUNCTIONALIZATION OF MCM-41

According to the functionalization process done by Yu et al., 0.429 g Y_2O_3, 0.0352 g Eu_2O_3 and 0.232 g NH_4VO_3 were dissolved in 20 mL HNO_3 and this solution was added to 1:7 (v:v) water/ethanol solution [50]. 0.84 g citric acid as chelating agent and 2.85 mL PEG 400 (polyethylene glycol) (0.08 g/mL) were added to the solution. It was stirred for 1 hour. 0.5 g of MCM-41 silica particles was added and the

solution was mixed for another 3 hours. The final solution was filtered, washed with distilled water and dried at 50 °C overnight in the furnace. To remove the surfactant and adsorbed water, temperature was reached to 160 °C, sample was heated at this temperature for 2 hours. Then, the temperature was increased to 550 °C and kept the sample at this temperature for 6 hours. The ramp rate was 1 °C / min. It was expected that the silanol groups in the MCM-41 surface to be replaced with $YVO_4^+Eu^{3+}$ groups. In the Figure 11, formation process of luminescence functionalized MCM-41 particles is illustrated.
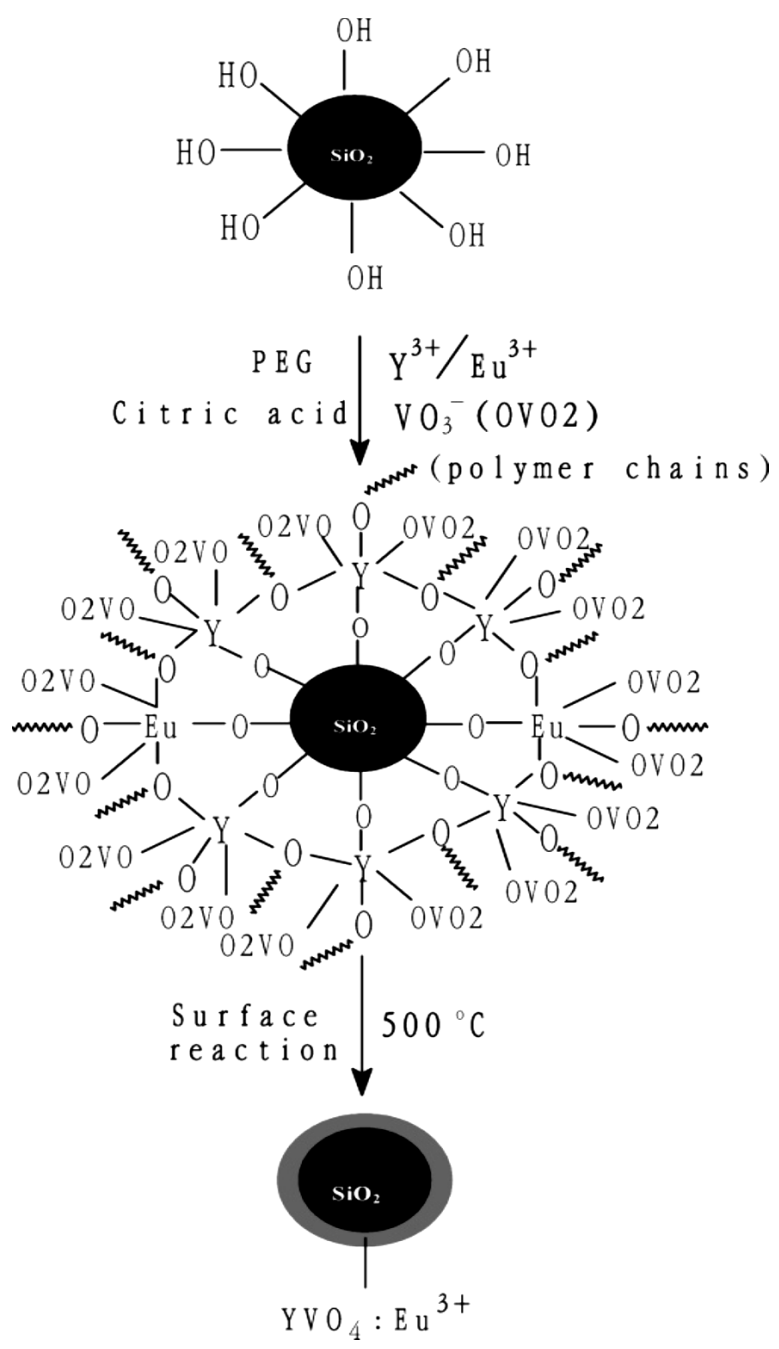
Figure 11: Schematic representation of formation Process of $YVO_4:Eu^{3+}$ functionalized MCM-41 particles [50]

Table 3: Precursors used for MCM-41 luminescence surface functionalization

Chemicals	m(g) or V(mL)	Brand	d (g/mL)	MW (g/mol)
Y_2O_3	0.429 g	Aldrich	5.03	225.8
Eu_2O_3	0.0352 g	Aldrich	7.42	351.9
NH_4VO_3	0.232 g	-	2.33	116.9
HNO_3	20.0 mL	Sigma - Aldrich	1.51	63.0
Citric acid	0.84 g	Sigma - Aldrich	1.50	210.1
PEG	2.85 mL	Merck	1.13	380.0
Ethanol	70.0 mL	-	0.79	46.0
H_2O	10.0 mL	-	1.00	18.0

4.2.2 ORGANIC FUNCTIONALIZATION OF MCM-41

In order to determine the effectiveness of APTES (3-Aminopropyl triethoxysilane, $H_2N(CH_2)_3Si(OC_2H_5)_3$) as an organic group in drug loading of MCM-41 particles, APTES in 3 different concentrations was grafted. For concentration in ratio of 1:1 APTES on MCM-41, 1.0 g MCM-41 and 1.0 mL APTES were mixed in 50.0 mL ethanol at 60 °C for 6 hours. As the ratio was increased, volume of APTES used increased. 2.0 mL APTES for 2:1 ratio and 3.0 mL APTES for 3:1 concentration were used. As depicted in Figure 12, the aim of the surface functionalization was to replace the silanol groups present in the pure sample with other organic functional groups by using alkoxysilanes. The samples were functionalized with post – grafting synthesis. In the Figure 12, the structure of the MCM-41 particles after the surface functionalization with APTES can be seen.
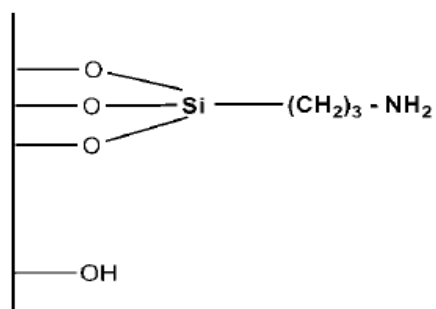
Figure 12: Surface of the MCM-41 after the functionalization by post - grafting synthesis using APTES

Table 4: Precursors used for MCM-41 organic functionalization

Chemicals	m(g) or V(mL)	Brand	d (g/mL)	MW (g/mol)
APTES	1 mL	Aldrich	0.95	221.4
	2 mL			
	3 mL			
Ethanol	50 mL	-	0.79	46.1

4.2.3 PEGYLATION FUNCTIONALIZATION

0.1 g MCM-41-2, 50.0 mL ethanol and 2.85 mL PEG was mixed for 3 hours at room temperature. Final white precipitate was filtered with filter papers, washed with distilled water and dried at 50 °C for overnight in the furnace.

4.3 CELECOXIB LOADING

Celecoxib loading was examined in three different ways; drug was loaded the MCM-41 silica particles in different ratios; 1:1, 1:2, 1:4 and 2:1 (w:w). For Celecoxib: MCM-41 particles in 1:1 ratio, 0.1 g MCM-41 and 0.1 g Celecoxib were mixed in

50.0 mL appropriate solvent for 48 hours at ambient temperature. For sample in 1:2 ratio 0.1 MCM-41 and 0.05 g Celecoxib were mixed in solvent. Sample in 1:4 ratio was prepared with 0.1 g MCM-41 and 0.025 g Celecoxib and 2:1 ratio was prepared with 0.1 g MCM-41 and 0.2 g Celecoxib. Prepared samples were washed with ethanol and dried at ambient temperature. In this way, three different solvents were used to see the solvent effect on the drug loading; methanol, ethanol and hexane. As source of Celecoxib, Celebrex 200 mg capsules in the brand of Pfizer were used.

Table 5: Precursors used for Celecoxib loading to MCM-41

Chemicals	m(g) or V(mL)	Brand	d (g/mL)	MW (g/mol)
MCM-41	0.1 g	-	-	60.00
Celecoxib	0.1 g	Pfizer	-	381.7
	0.05 g			
	0.025 g			
	0.2 g			
Methanol		-	0.79	32.04
Ethanol	50 mL	-	0.79	46.07
Hexane		Merck	0.65	86.18

4.4 CELECOXIB RELEASE

Firstly, the PBS (phosphate buffer solution) in pH 7.4 was prepared for the release experiments. For this purpose, two different phosphate salts were used: K_2HPO_4 and KH_2PO_4. 13.97 g K_2HPO_4 and 2.69 g KH_2PO_4 were dissolved in 1.0 L distilled water. The pH of the prepared solution was adjusted to 7.4 to simulate the pH of the intestine. Then 0.5 g MCM-41 samples loaded with Celecoxib were added to the 50 mL PBS. Each of the prepared solutions was mixed at 37 °C in order to simulate the

body temperature. The amount of Celecoxib released from the silica particles was calculated according to the concentration change within 6 hours. The concentration measurements were completed within 30 minutes, 1 hour, 2 hours, 4 hours and 6 hours.

Table 6: Precursors used for celecoxib release from MCM-41

Chemicals	m(g) or V(mL)	Brand	d (g/mL)	MW (g/mol)
K_2HPO_4	13.97 g	Riedel - Haën	2.44	178.30
KH_2PO_4	2.69 g	Merck	2.34	136.02
H_2O	1.0 L	-	1.00	18.00

CHAPTER 5

CHARACTERIZATION

5.1 POWDER X-RAY DIFFRACTION (XRD)

Powder XRD patterns of the samples were recorded under ambient conditions at 0.9 – 80 and 10 – 900 (2θ) with the resolution of 0.05 by using Rigaku X-ray Diffractometer with a Miniflex goniometer which was operated at 30 kV and 15 mA. The source of the X-ray radiation was Cu Kα (λ =1.54Å). The scanning mode was selected as continuous scanning.

5.2 ELEMENTAL ANALYSIS

The samples were examined with CHNS-932 (LECO) elemental analyzer at the METU Central Laboratory to obtain the percentages of the carbon within each sample. The carbon measurements were completed twice to obtain adequate results.

5.3 THERMOGRAVIMETRIC ANALYSIS (TGA)

The thermogravimetric analysis was completed by using Perkin Elmer Thermogravimetric Analyzer at METU Chemistry Department. The measurements were completed under air at temperatures between 30 and 600 °C with the heating rate of 10 °C/ min.

5.4 UV - VIS SPECTROSCOPY

UV analysis was used to make quantitative determination. For this way, Beer-Lambert law $(A=\varepsilon.b.c)$ is the common method to determine the concentration of species in solution. (A: absorbance ε: molar absorptivity coefficient b: path length of the sample c: concentration). During the loading and release process of Celecoxib, CARY 5000 UV - VIS - NIR Spectrophotometer was used in the wavelength of 254 nm.

5.5 FOURIER - TRANSFORM INFRA - RED SPECTROSCOPY (FTIR)

In the IR spectra of the samples, Bruker IFS 66/S ATR spectrometer was used in the range of 500 and 4000 cm^{-1}. Each sample was characterized before and after the loading of Celecoxib. To control the effect of solvent, each silica sample was characterized after being mixed in ethanol for 2 days.

5.6 NITROGEN - SORPTION

The N_2 adsorption - desorption measurements were examined with Quantachrome Autosorb-6 at the METU Central Laboratory. Before the measurement, each sample with Celecoxib was outgassed at 50 °C for 16 hours and samples without drug were outgassed at 110 °C for 16 hours. The specific surface areas were calculated using multiple point Brunauer - Emmett - Teller (BET) method. The pore size distributions were calculated using desorption branches of the isotherms by Barrett - Joyner - Halenda (BJH) method.

5.7 SCANNING ELECTRON MICROSCOPY (SEM)

The SEM analyses were obtained with QUANTA 400F Field Emission SEM instrument with 1.2 nm resolution at METU Central Laboratory.

5.8 TRANSMISSION ELECTRON MISCROSCOPY (TEM)

For the TEM analysis, JEOL JEM 2100F STEM was used. The analysis was completed at the METU Central Laboratory. JEOL JEM 2100F Field Emission Gun was used during the experiments. The pure samples were operated at 80 kV and after functionalization the samples were analyzed at 120kV. Before the analysis, MCM-41 silica particles dispersed in ethanol in the Elma S 30 H ultrasonic bath for 15 minutes.

5.9 ZETA POTENTIAL

Zeta potential measurements were done by using Malvern Zetasizer Nano ZS instrument in the METU Chemistry Department. Distilled water used as solvent. To disperse the silica particles in water, they were mixed at 35 °C and ultrasonicated in Elma S 30 H ultrasonic bath for 30 minutes.

CHAPTER 6

RESULTS & DISCUSSION

6.1 POWDER X-RAY DIFFACTION PATTERN OF MCM-41 PARTICLES

XRD (X-Ray diffraction) was completed in order to have some information about the order of pores of the MCM-41 crystals. In this technique, atoms in the crystal state cause diffraction in the incident light. Small angle XRD patterns of MCM-41 and MCM-41 loaded with drug in the ethanol solvent can be seen in the Figure 13, 14, 15 and 16. An example indicating the small angle XRD pattern which defines the order of pores in mesoporous silica was depicted in Appendix part.
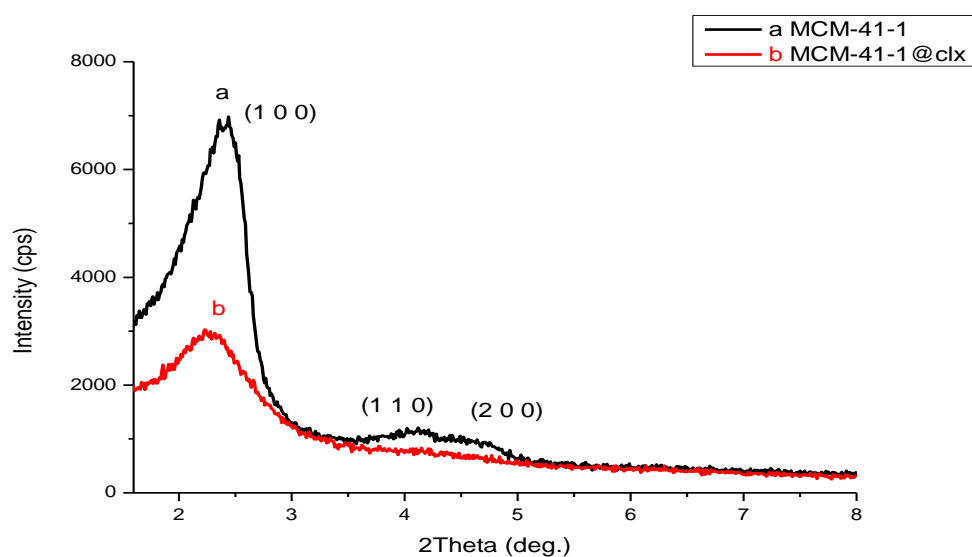
Figure 13: Small angle powder XRD patterns of a) MCM-41-1 b) MCM-41-1@clx in ethanol
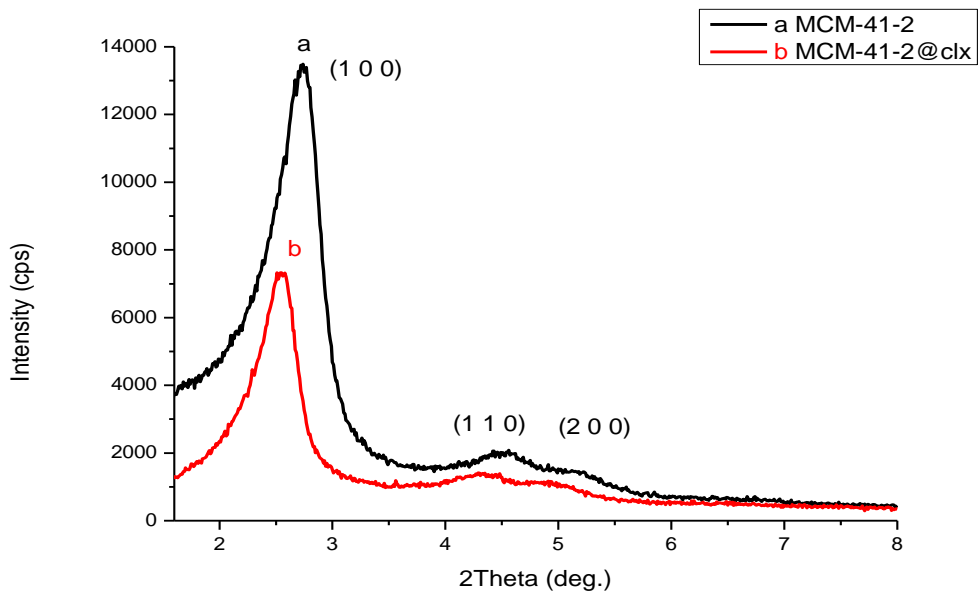
Figure 14: Small angle powder XRD patterns of a) MCM-41-2 b) MCM-41-2@clx in ethanol
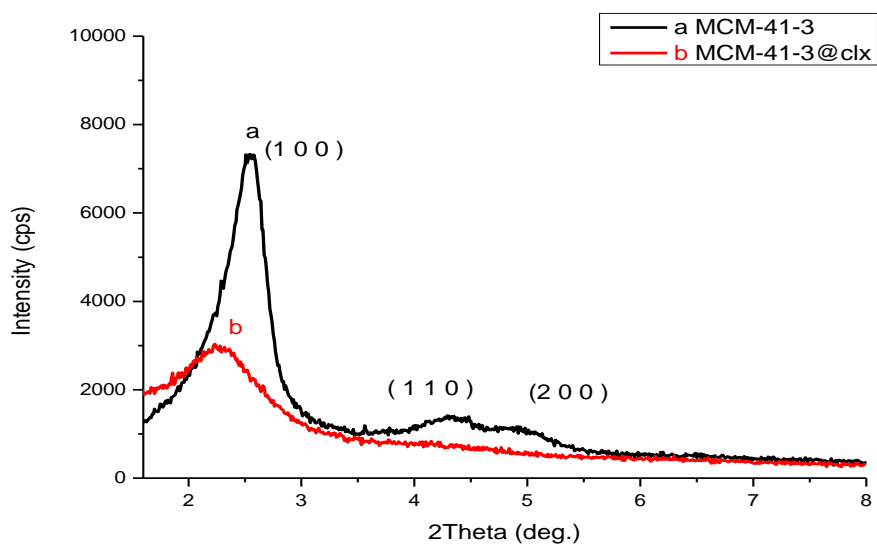
Figure 15: Small angle powder XRD patterns of a) MCM-41-3 b) MCM-41-3@clx
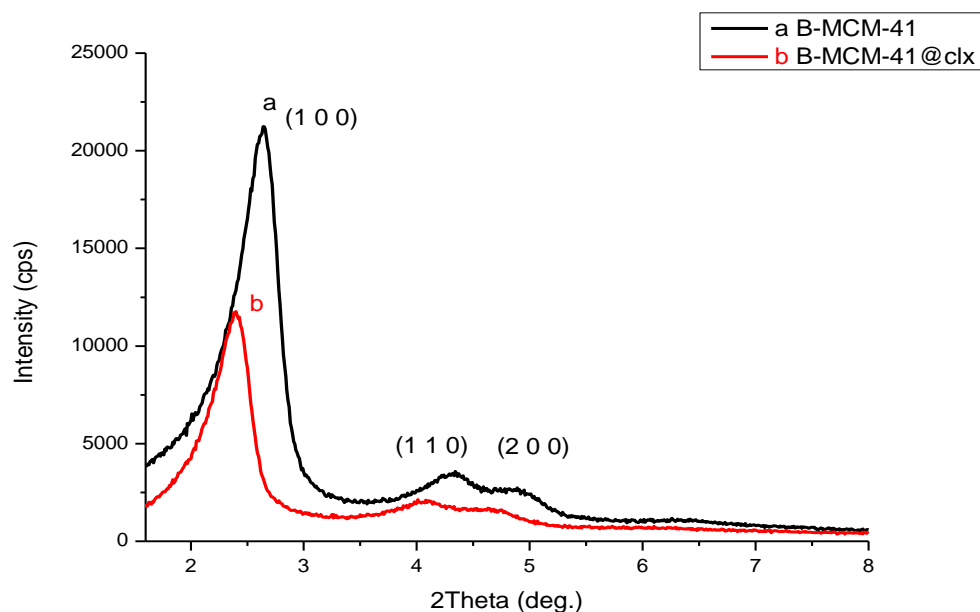
in ethanol

Figure 16: Small angle powder XRD patterns of a) B-MCM-41 b) B-MCM-41@clx in ethanol

Table 7: d spacing values and unit cell parameters of MCM-41 particles examined in ethanol

	(h k l)	d (Å)		a (Å)	
		Bare	**With Drug**	**Bare**	**With Drug**
MCM-41-1	(100)	36.2	39.4	41.8	45.5
MCM-41-2	(100)	31.9	34.7	36.8	40.1
MCM-41-3	(100)	35.2	36.9	40.6	42.6
B-MCM-41	(100)	34.5	35.9	39.8	41.5

MCM-41 particles exhibit a very intense diffraction peak between $2\theta= 2$ and 2.5 degrees and two different peaks with lower intensity at $2\theta= 4$ and 5 degrees. All the sample patterns show these characteristic diffraction peaks of a 2-D hexagonal lattice structure. XRD patterns of MCM-41 materials are hexagonally ordered with the space group p6mm [51]. It indicates well ordering of the hexagonal mesophase of the

samples. The diffraction peaks are assigned to the planes as (100), (110) and (200) respectively. After the drug loading process, these peaks could be seen again. It means that ordered hexagonal mesoporous structure of MCM-41 samples was preserved after Celecoxib loading.

Table 7 shows the d spacing values and unit cell parameters of the most intense peak in XRD patterns of MCM-41 samples calculated by using Bragg Law ($\lambda=2d.\sin\theta$) and the unit cell parameter, a, of the most intense peak assigned as (100) was calculated by using $a = 2d/\sqrt{3}$. It could be stated that all the data increased after drug loading process as expected due to the drug adsorption.

Compared to MCM-41 particles, intensities of XRD peaks of drug loaded MCM-41 silica particles are lower due to Figure 16. There is small shift to lower 2theta degree in the maximum point of peaks after drug loading. While decrease in intensities of peaks can be explained with decrease in order, small shifts indicate the change in unit cell parameters. Order may be caused by location of the Celecoxib drug molecules into the pores and channels of the MCM-41 particles. Although the mesoporous structure was preserved after drug loading process, a decrease in order due to drug loading was occurred. In the Figures 17, 18, 19 and 20, wide angle XRD patterns of MCM-41 and drug loaded MCM-41 in the ethanol as solvent can be seen.
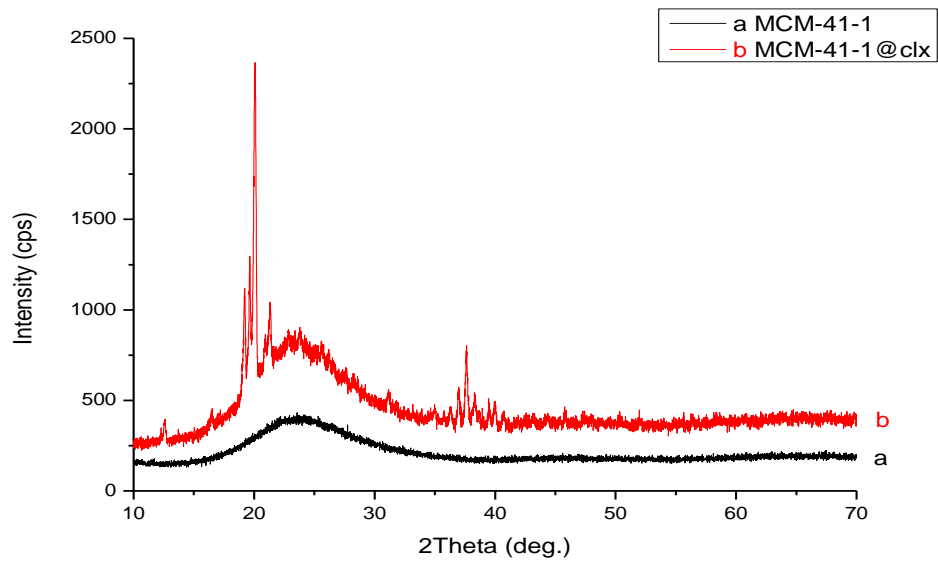
Figure 17: Wide angle powder XRD patterns of a) MCM-41-1 b) MCM-41-1@clx in ethanol
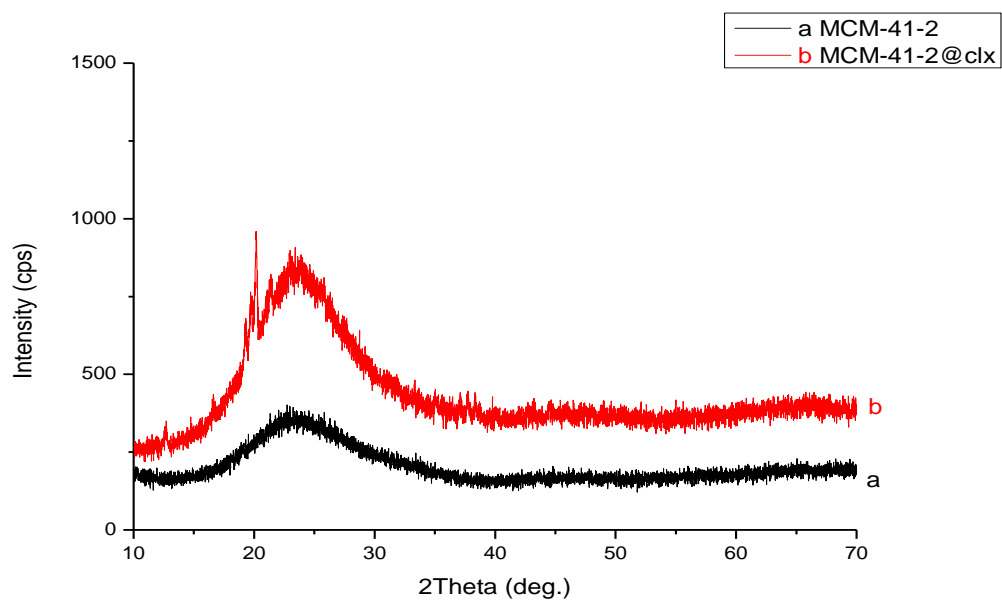
Figure 18: Wide angle powder XRD patterns of a) MCM-41-2 b) MCM-41-2@clx in ethanol
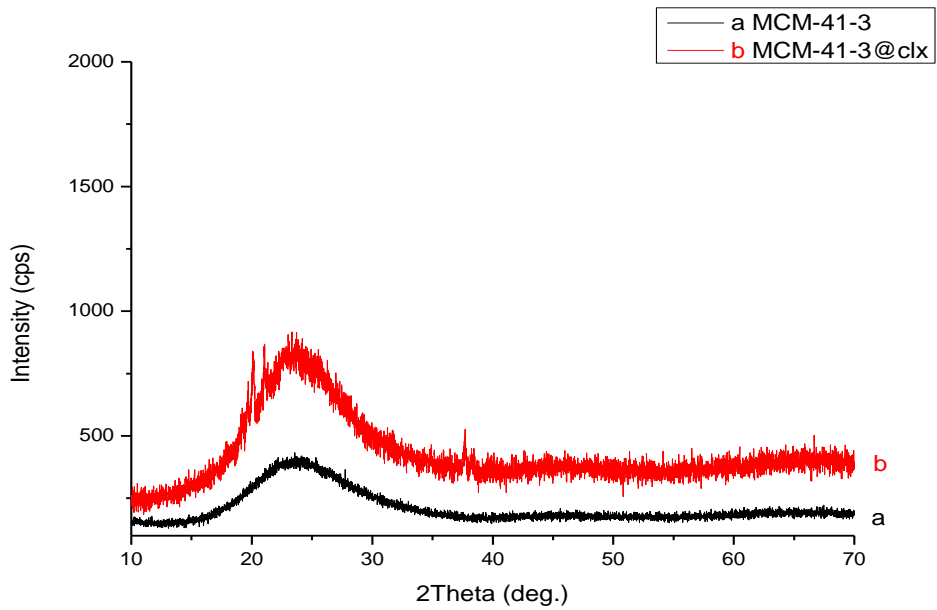
Figure 19: Wide angle powder XRD patterns of a) MCM-41-3 b) MCM-41-3@clx
in ethanol
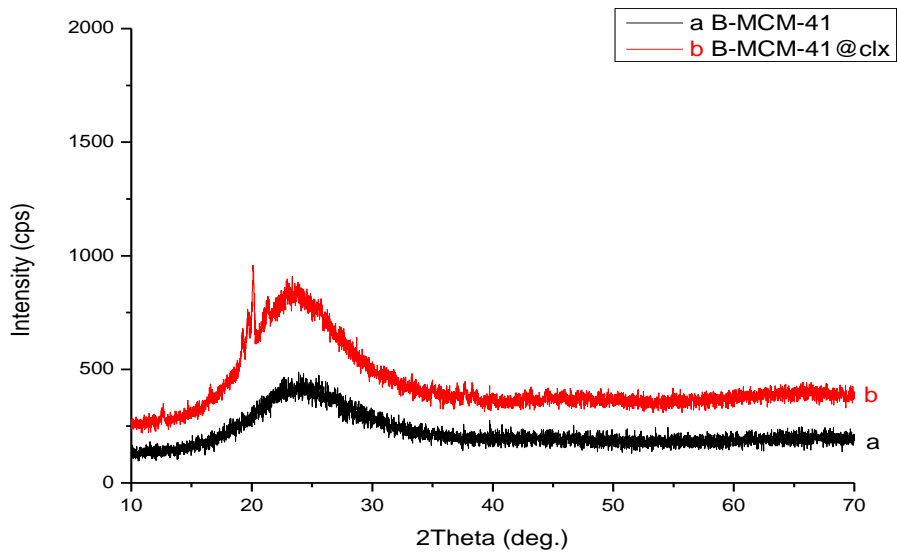
Figure 20: Wide angle powder XRD patterns of a) B-MCM-41 b) B-MCM-41@clx
in ethanol
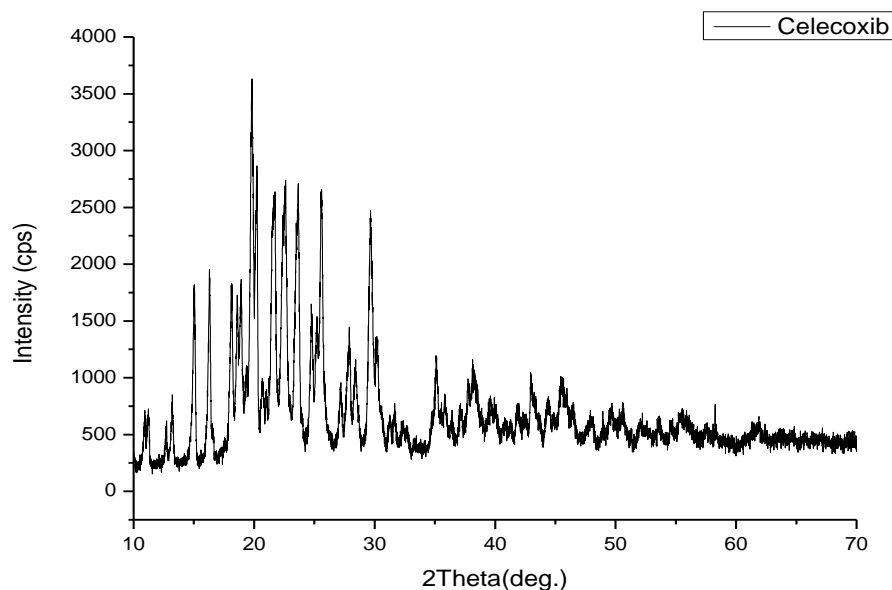
Figure 21: Wide angle powder XRD of Celecoxib

According to XRD patterns of MCM-41 samples, it can be recognized that broad peak between 20 and 30 degrees was preserved after Celecoxib loading. This peak is the characteristic diffraction peak of a 2D hexagonal lattice structure in the wide angle spectrum and it indicates the drug loaded MCM-41 samples remained in 2D hexagonal lattice structure. Difference between the XRD patterns of MCM-41 and drug loaded MCM-41 is the presence of the sharp peaks at 20 degree that are the characteristic peaks of Celecoxib according to Figure 21. While a decrease in the intensities of characteristic peaks in small angle XRD patterns can be explained as the loading of Celecoxib to the pores and channels of MCM-41 samples, presence of the peaks at 20 degree can be explained as the adsorption of Celecoxib to the outer pores on surface of the samples as crystalline form. Figure 22, 23, 24 and 25 show the small angle XRD patterns of MCM-41 and MCM-41 drug loaded in the hexane as solvent.

45
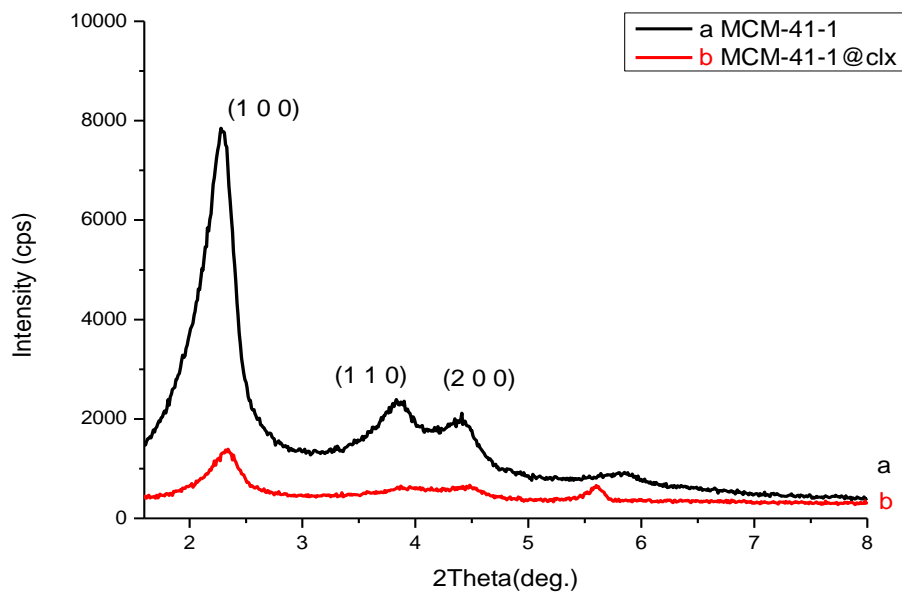
Figure 22: Small angle powder XRD patterns of a) MCM-41-1 b) MCM-41-1@clx in hexane
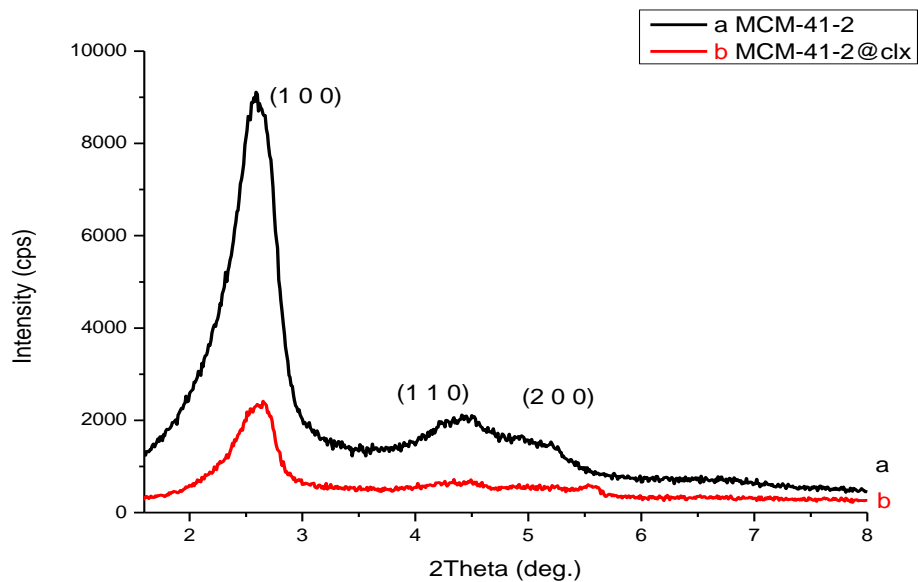
Figure 23: Small angle powder XRD patterns of a) MCM-41-2 b) MCM-41-2@clx in hexane
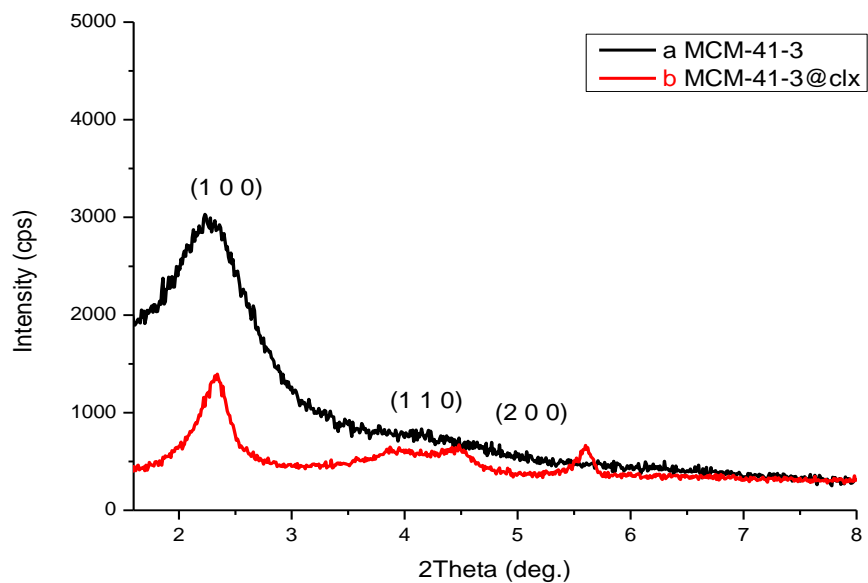
Figure 24: Small angle powder XRD patterns of a) MCM-41-3 b) MCM-41-3@clx
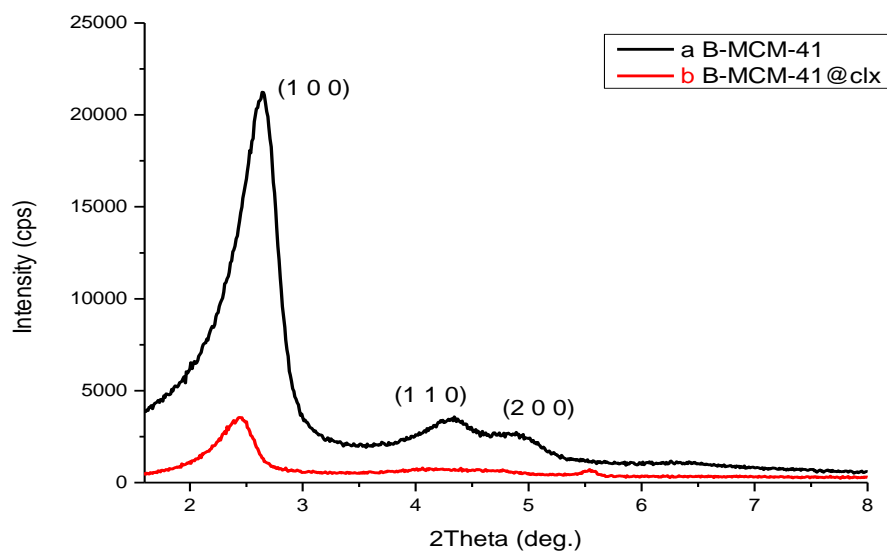
in hexane

Figure 25: Small angle powder XRD patterns of a) B-MCM-41 b) B-MCM-41@clx
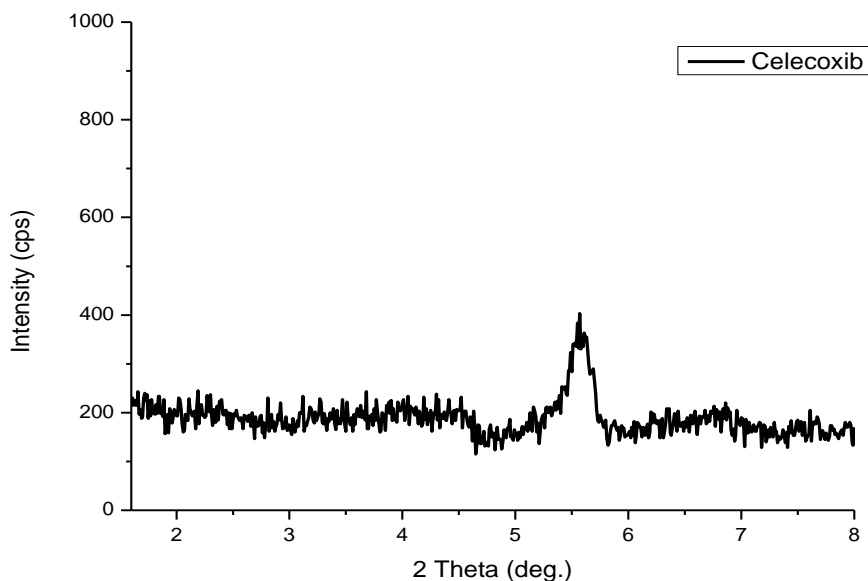
in hexane

Figure 26: Small angle powder XRD pattern of Celecoxib

Table 8: d spacing values and unit cell parameters of MCM-41 particles examined in hexane

	(h k l)	d (Å)		a (Å)	
		Bare	**With Drug**	**Bare**	**With Drug**
MCM-41-1	(100)	36.2	36.8	41.8	42.5
MCM-41-2	(100)	31.9	34.2	36.8	39.5
MCM-41-3	(100)	35.2	36.3	40.6	41.9
B-MCM-41	(100)	34.5	37.4	39.8	43.2

When the small angle XRD patterns of MCM-41 samples were investigated, decreases in the intensities of the characteristic peaks of 2-D hexagonal lattice structure were seen again. Although this lattice structure was kept after drug loading process in hexane, it can be said that a decrease due to drug loading to the channels

48

and pores was occurred. However this time, the peak that is the only peak at the 5.5 degree in the small angle XRD pattern of Celecoxib was seen in the XRD patterns of drug loaded MCM-41 samples. Celecoxib drug molecules probably stayed in crystalline state in the process of drug loading in hexane and attached to the outer pores on surface of the samples. The unit cell parameters and d spacing values of the XRD patterns of MCM-41 samples, data increased after drug loading process due to the adsorption of drug molecules to the pores and channels of carrier particles. Figure 27, 28, 29 and 30 refer to wide angle XRD patterns of MCM-41 samples drug loaded in hexane.
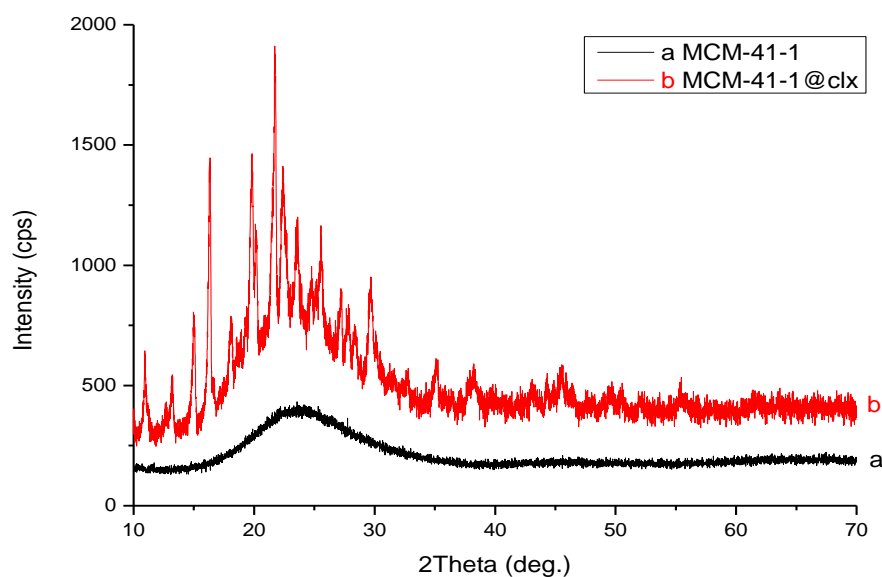
Figure 27: Wide angle powder XRD patterns of a) MCM-41-1 b) MCM-41-1@clx in hexane
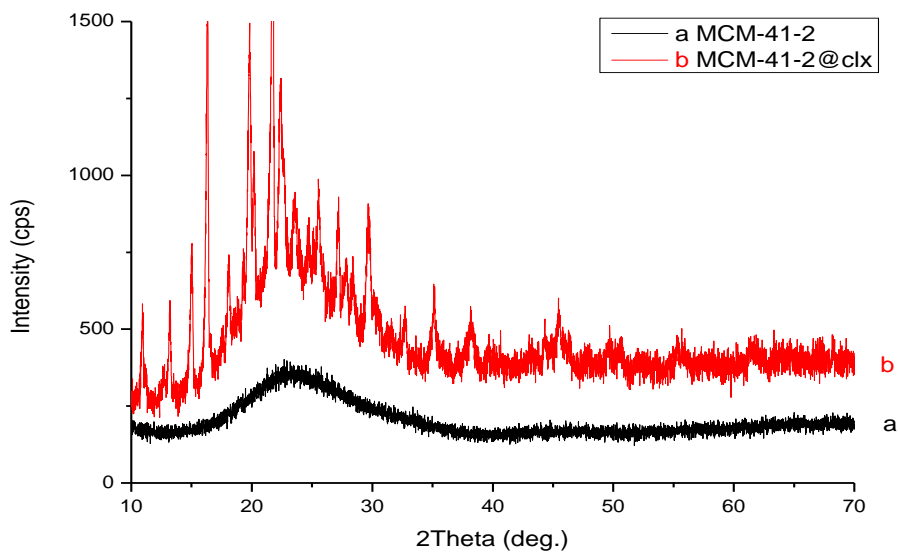
Figure 28: Wide angle powder XRD patterns of a) MCM-41-2 b) MCM-41-2@clx in hexane
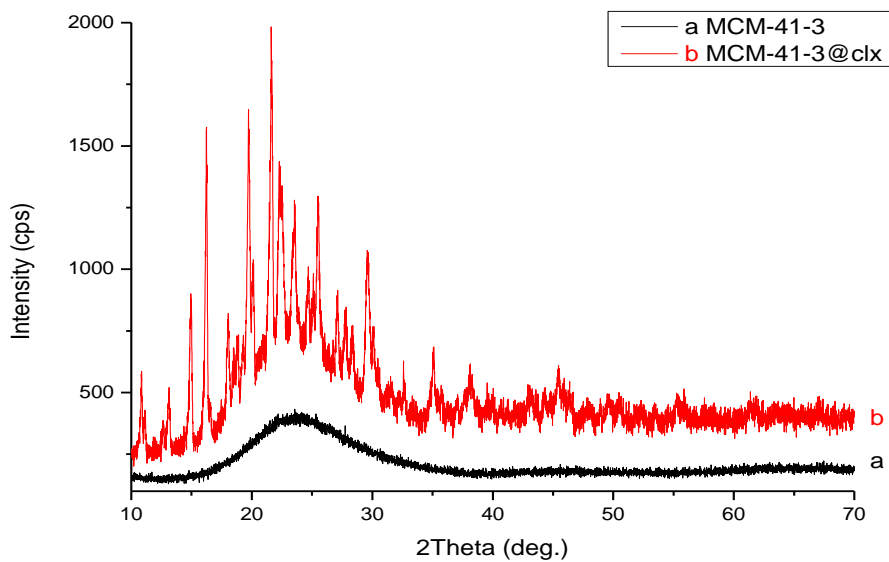
Figure 29: Wide angle powder XRD patterns of a) MCM-41-3 b) MCM-41-3@clx in hexane
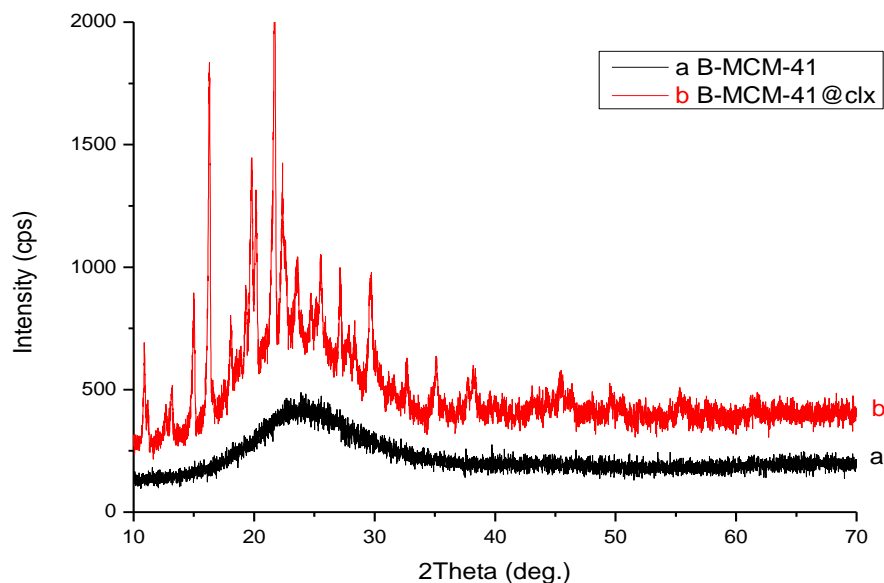
Figure 30: Wide angle powder XRD patterns of a) B-MCM-41 b) B-MCM-41@clx in hexane

XRD patterns of MCM-41 drug loaded in hexane showed almost all of the peaks of Celecoxib wide angle XRD pattern. Crystalline state of the drug molecules probably was maintained and adsorbed on the outer surface of the carrier in hexane. Due to these drug molecules in the crystalline state attached to surface of the MCM-41, all of the characteristic peaks of Celecoxib were seen in the XRD patterns of drug loaded MCM-41 samples in hexane.

6.2 FTIR ANALYSIS

MCM-41 samples, MCM-41 samples mixed with solvents and MCM-41 samples loaded with Celecoxib in these solvents were analyzed in FTIR analysis in order to investigate the infrared spectra. While observing the effect of solvent on the MCM-41 samples, solid samples were mixed in solvent for 2 days as it was done in the drug loading process but this time it was done without adding drug. Figure 31, 32, 33 and

51

34 indicate the FTIR spectra of MCM-41 samples that were examined with ethanol as solvent. Figure 35 shows the FTIR spectrum of Celecoxib.
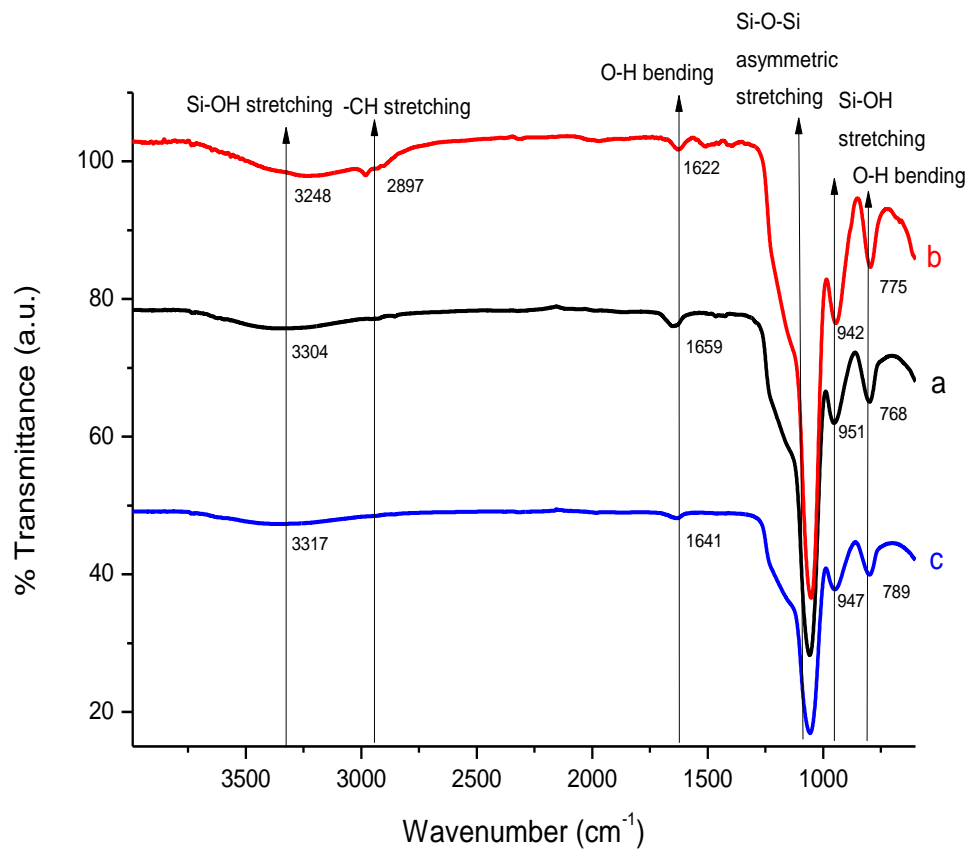
Figure 31: FTIR spectra of a) MCM-41-1 b) MCM-41-1 mixed in ethanol and c) MCM-41-1 drug loaded in ethanol
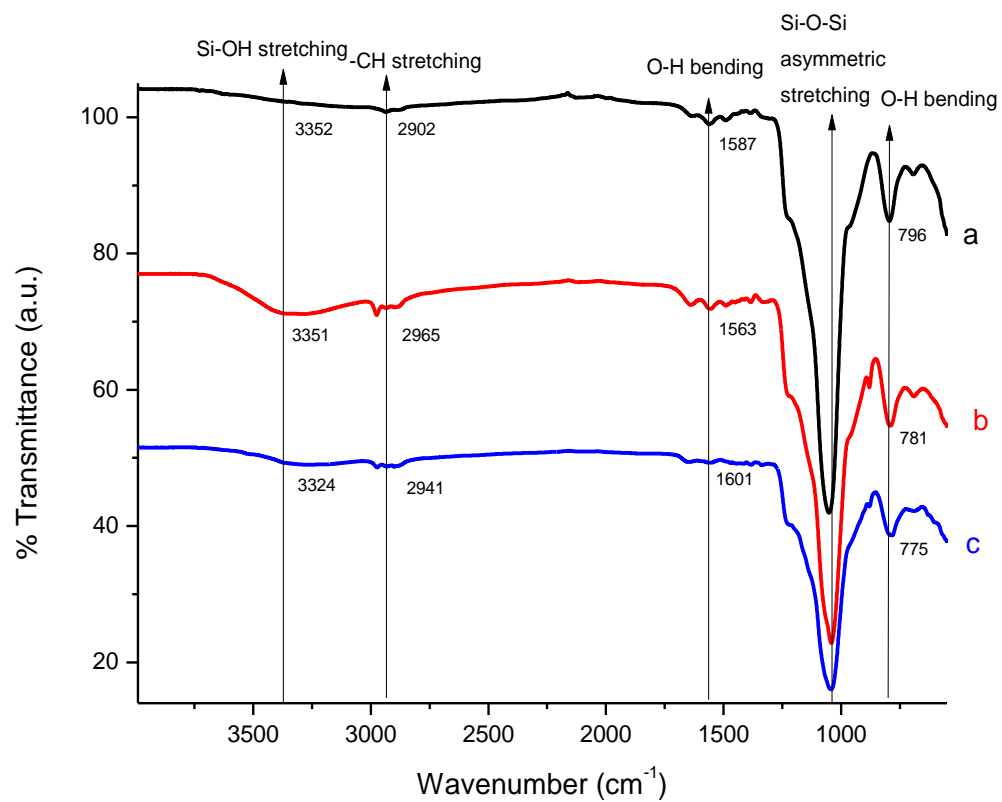
Figure 32: FTIR spectra of a) MCM-41-2 b) MCM-41-2 mixed in ethanol and c)
MCM-41-2 drug loaded in ethanol
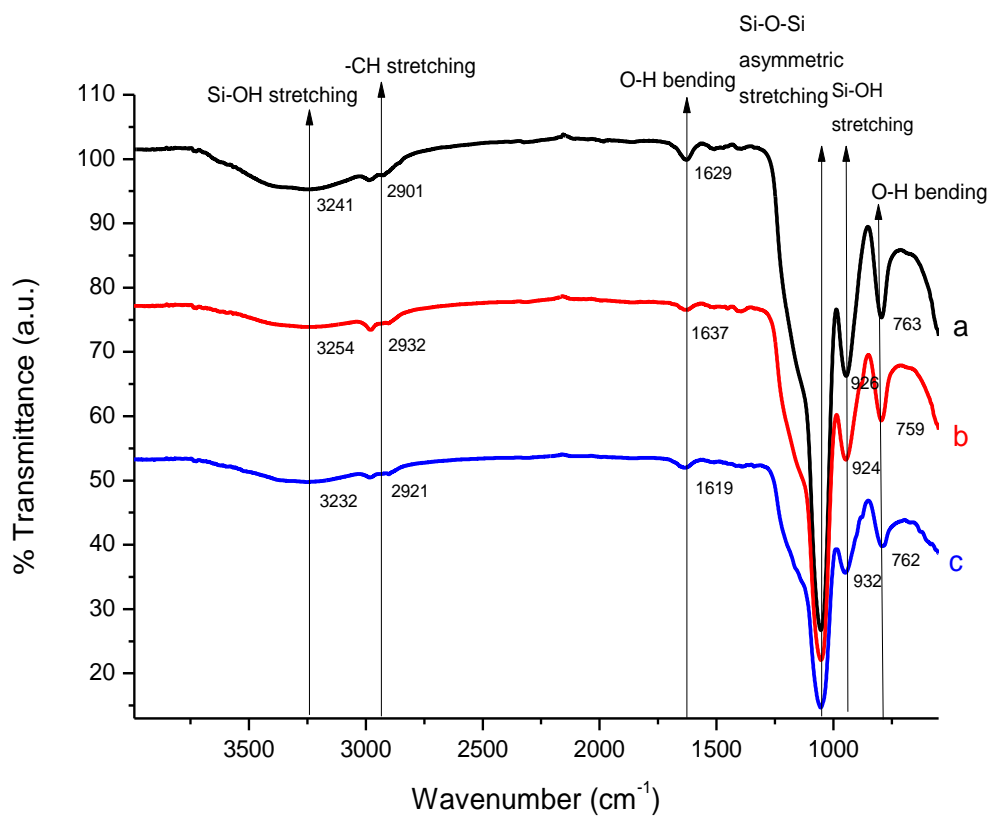
Figure 33: FTIR spectra of a) MCM-41-3 b) MCM-41-3 mixed in ethanol and c) MCM-41-3 drug loaded in ethanol
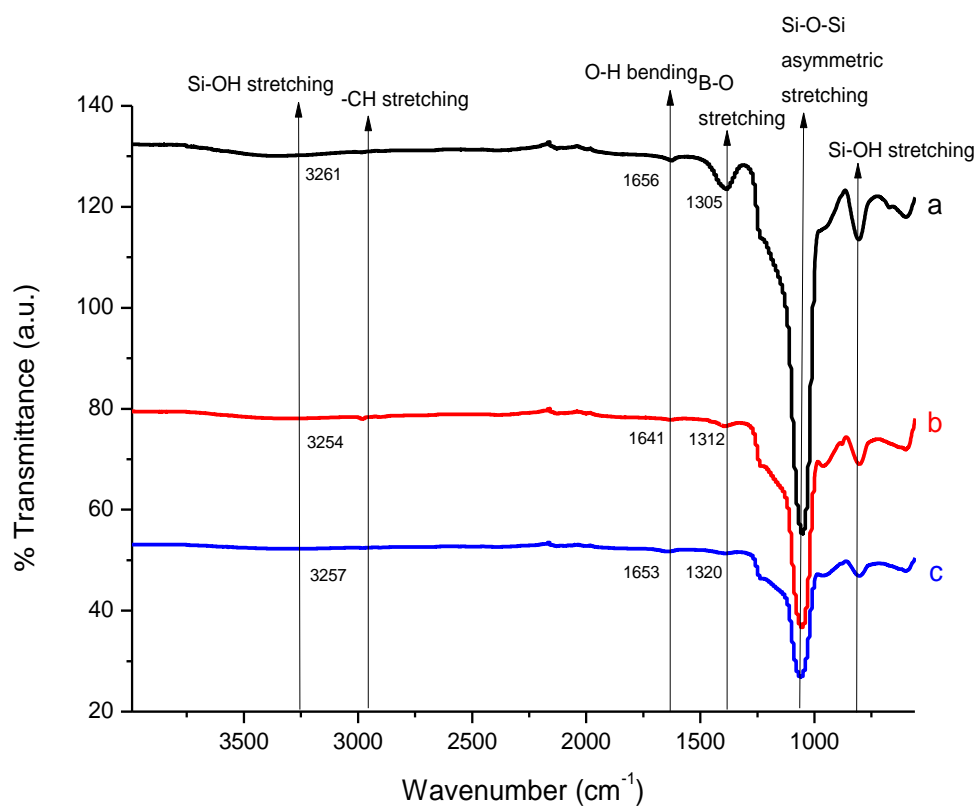
Figure 34: FTIR spectra of a) B-MCM-41 b) B-MCM-41 mixed in ethanol and c) B-MCM-41 drug loaded in ethanol
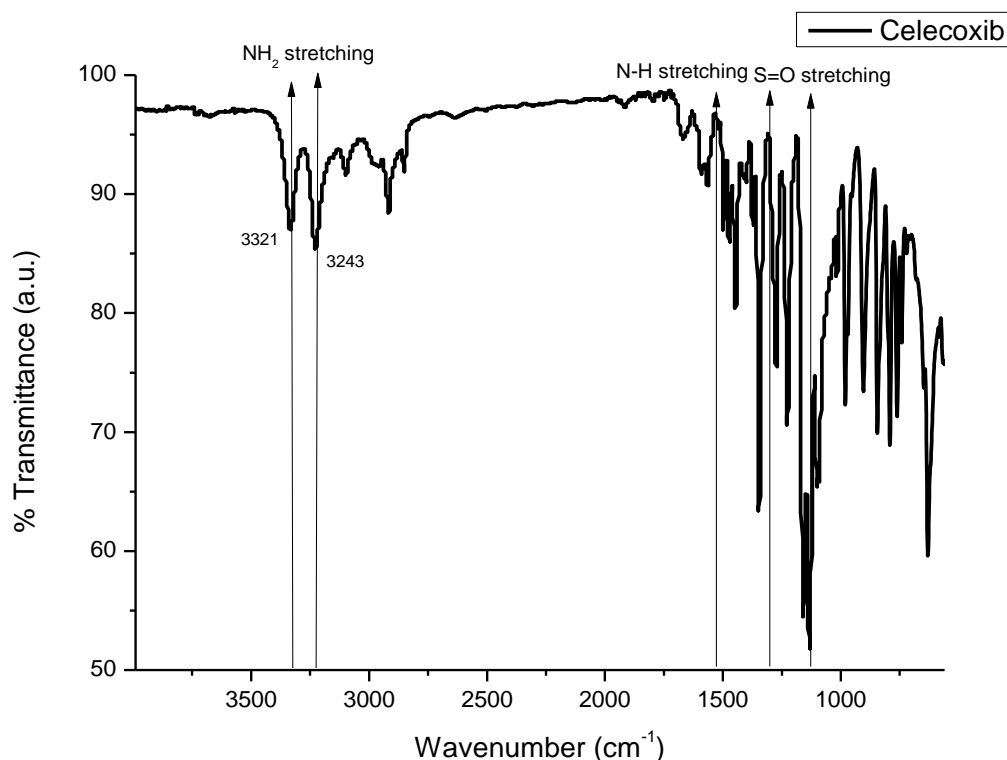
Figure 35: FTIR spectrum of Celecoxib

Comparing the FTIR spectra of MCM-41 samples, all of them may seem similar. All MCM-41 samples showed the wide adsorption bands in the range of 3750 – 3000 cm^{-1}. This indicates the –OH stretching due to silanol groups on the MCM-41 and adsorbed water. There was a small peak at 2900 cm^{-1}. According to Song et al [20] this peak corresponds to –CH stretching of CH$_2$ or CH$_3$ that may be due to surfactants that could not removed by calcination or acid extraction process. Due to this remaining surfactant in the MCM-41 samples, the peak at 2900 cm^{-1} might be seen. O-H bending can be seen at 1600 cm^{-1}, this small peak is due to molecular water adsorbed on the silica surface. Surface of the MCM-41 is covered with silanol groups and these are water adsorption sites. While the sharper band at around 1100 cm^{-1} is attributed to the Si-O-Si asymmetric stretching, band at around 950 cm^{-1} could be assigned as the Si-OH stretching due to silanol groups on the surface. It can

be seen that Si-OH stretching band at 950 cm^{-1} is not present in the calcined samples; MCM-41-2 and B-MCM-41. Elevated temperature may damage these silanol groups. The peak attributed to O-H bending due to silanol groups on the surface was seen at around 750 cm^{-1} [52].

Celecoxib shows a double sharp peak at 3321 and 3243 cm^{-1} that indicate the NH$_2$ stretching in the range of 3200 and 3500 cm^{-1}. While Single peaks in the range of 1500 and 1600 cm^{-1} indicate the N-H stretching, peaks in the range of 1150 and 1350 show the presence of sulfonyl groups of sulfonamide in Celecoxib [51]. In the comparison of mixture of MCM-41 and ethanol with MCM-41, there is no important difference. Figure 36, 37, 38 and 39 show the FTIR spectra of MCM-41 samples that were loaded with drug in hexane.
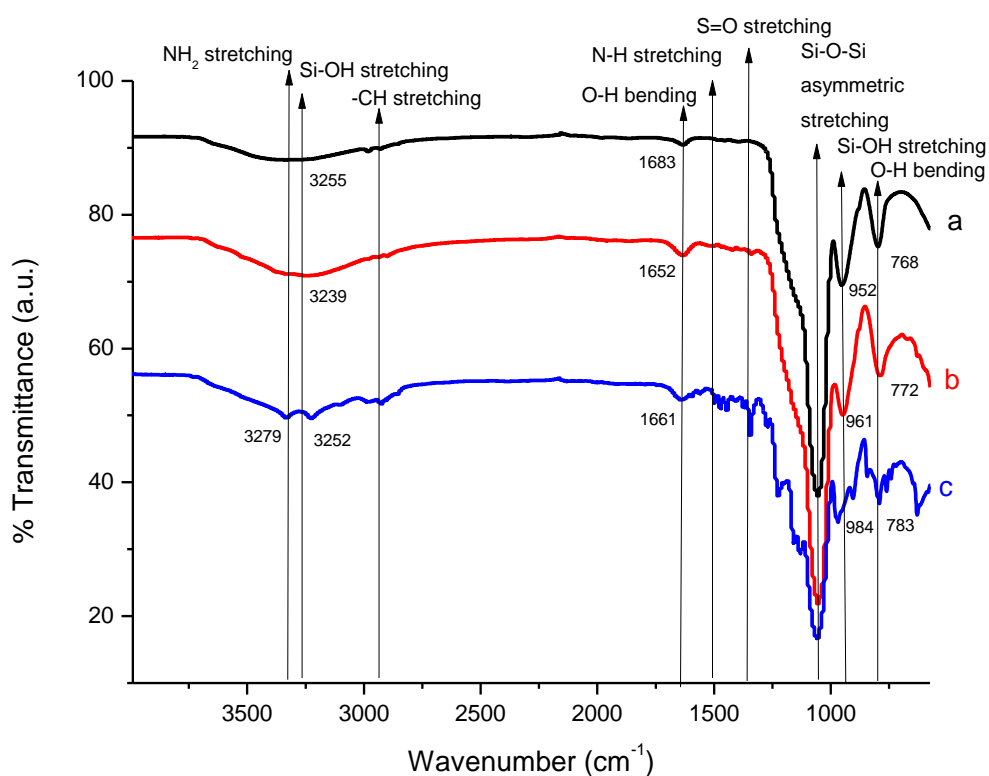
Figure 36: FTIR spectra of a) MCM-41-1 b) MCM-41-1 mixed in hexane and c) MCM-41-1 drug loaded in hexane

57
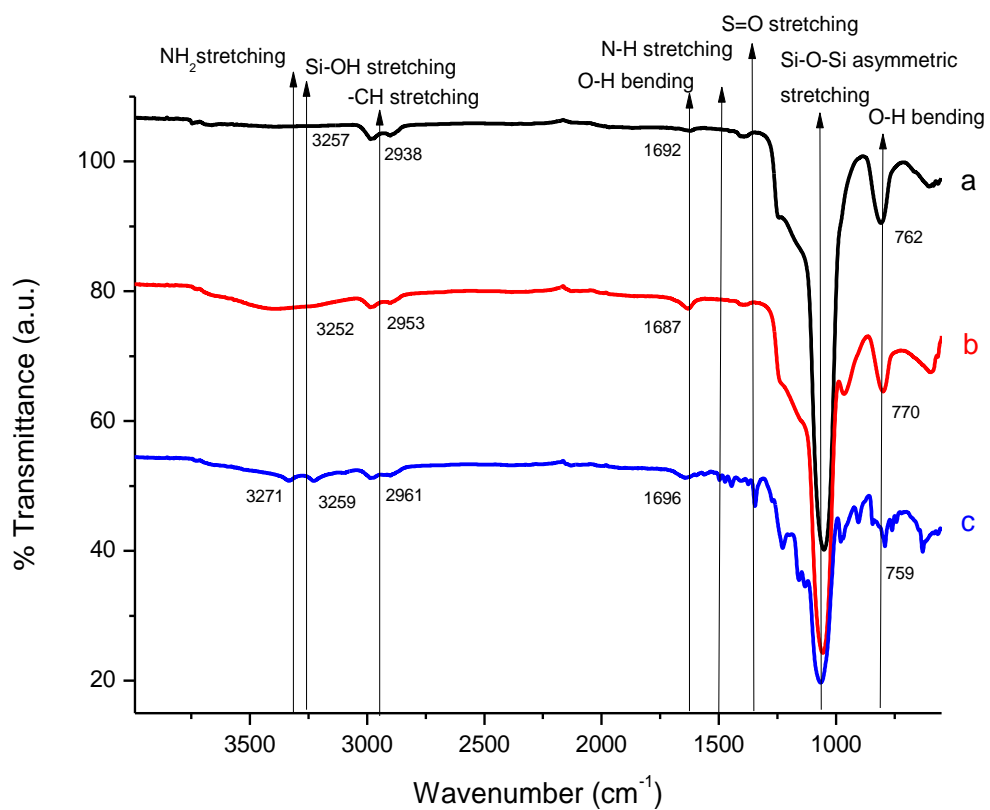
Figure 37: FTIR spectra of a) MCM-41-2 b) MCM-41-2 mixed in hexane and c)
MCM-41-2 drug loaded in hexane
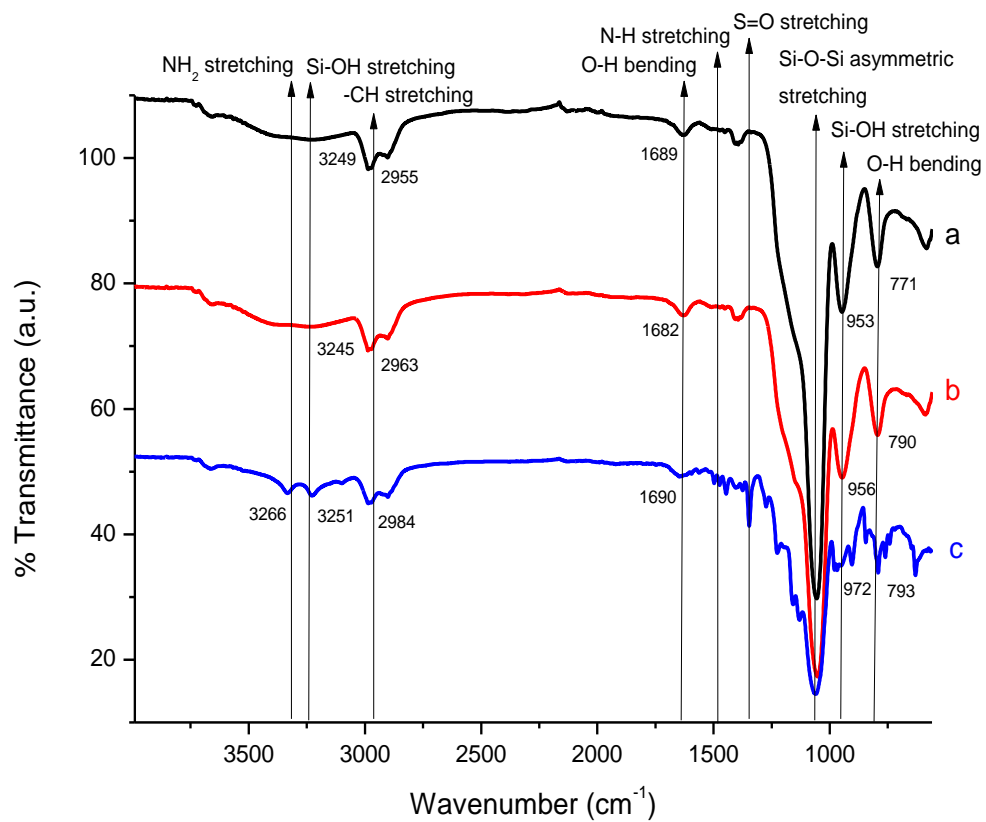
Figure 38: FTIR spectra of a) MCM-41-3 b) MCM-41-3 mixed in hexane and c) MCM-41-3 drug loaded in hexane
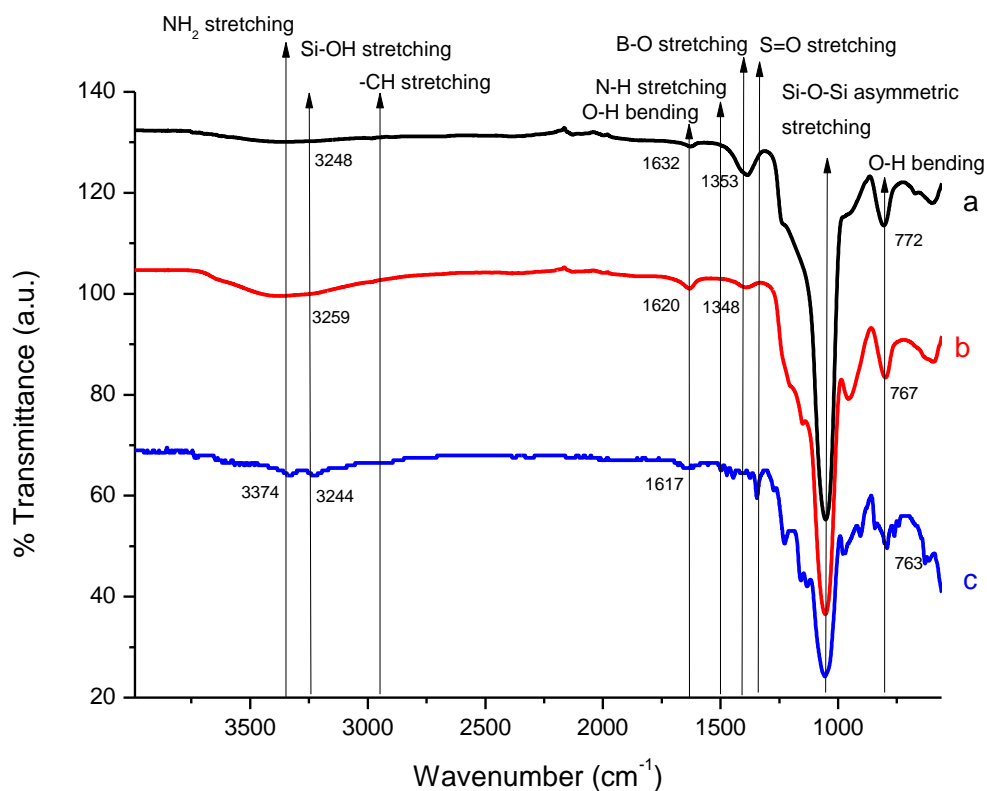
Figure 39: FTIR spectra of a) B-MCM-41 b) B-MCM-41 mixed in hexane and c) B-MCM-41 drug loaded in hexane

When the FTIR spectra of MCM-41 samples examined in hexane were investigated, characteristic peaks of Celecoxib that indicate the NH_2, N-H and S=O stretching can be seen. That shows that drug did not dissolved and adsorbed mostly on the outer pores on the surface of the MCM-41 samples in hexane and characteristic peaks of drug was seen easily in the surface characterization by FTIR spectrum. However, drug molecules that encapsulated in the inner pores of MCM-41 in ethanol and could not be seen in FTIR spectrum.

6.3 N$_2$ - ADSORPTION - DESORPTION ANALYSIS

6.3.1 BET THEORY

BET (Brunauer–Emmett–Teller) theory aims to investigate surface and pore characteristics of a porous material. The volume of gas adsorbed or desorbed on the solid surface is measured at constant temperature and different pressures. By this way, one can get information about surface area of the porous material, volume and diameter of pores. Brunauer-Emmett-Teller method was used. The purpose of this analysis in this study is to observe effect of Celecoxib loading on the surface area and pore sizes. Figure 40, 41, 42 and 43 depict the BET isotherms MCM-41 samples loaded with Celecoxib in hexane [53]. BET isotherms of MCM-41 particles examined in ethanol can be seen in appendix part.
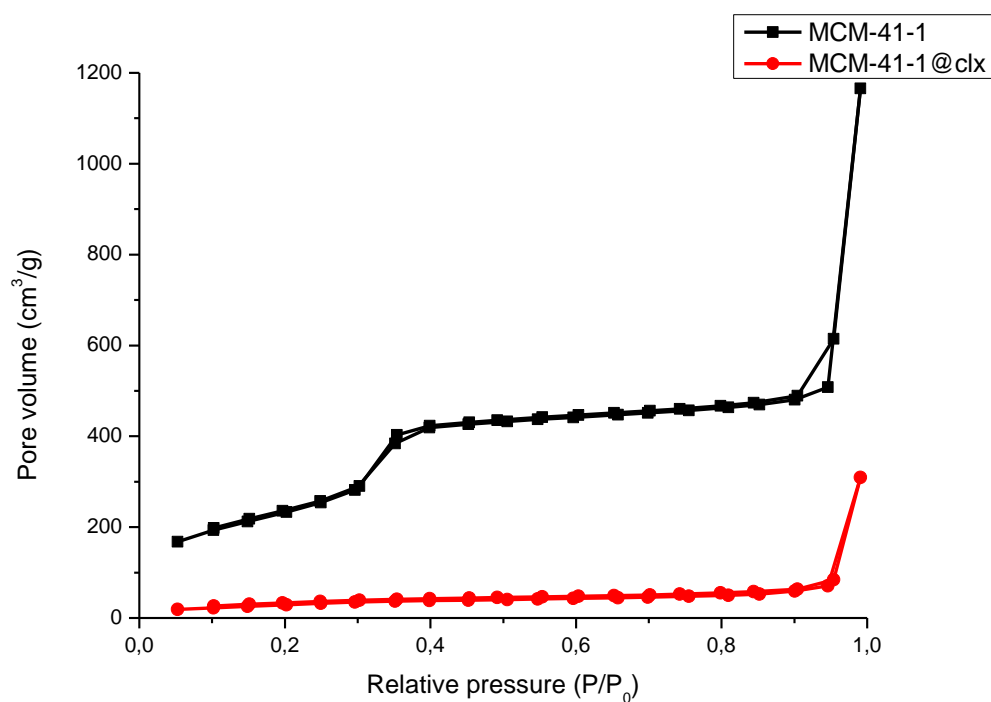
Figure 40: BET isotherms of MCM-41-1 and MCM-41-1@clx in hexane
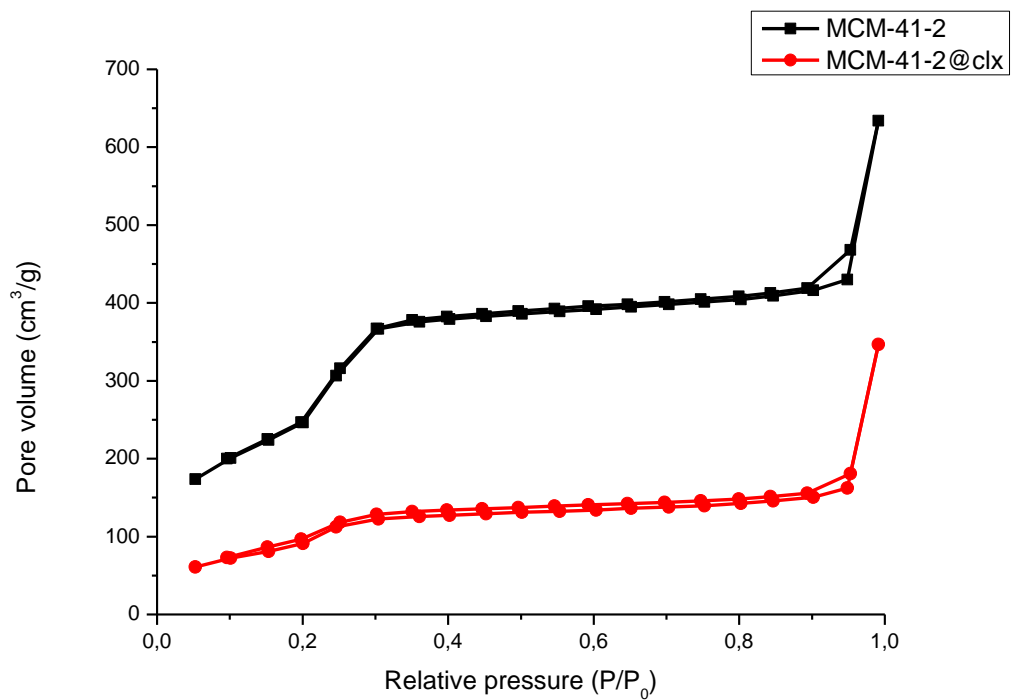
Figure 41: BET isotherms of MCM-41-2 and MCM-41-2@clx in hexane
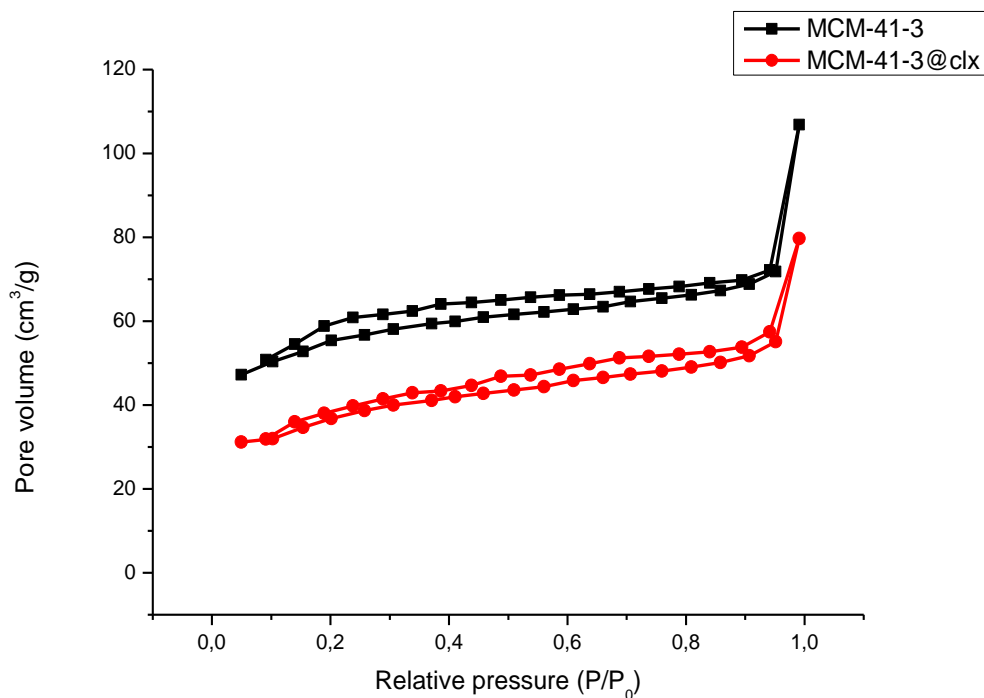
Figure 42: BET isotherms of MCM-41-3 and MCM-41-3@clx in hexane
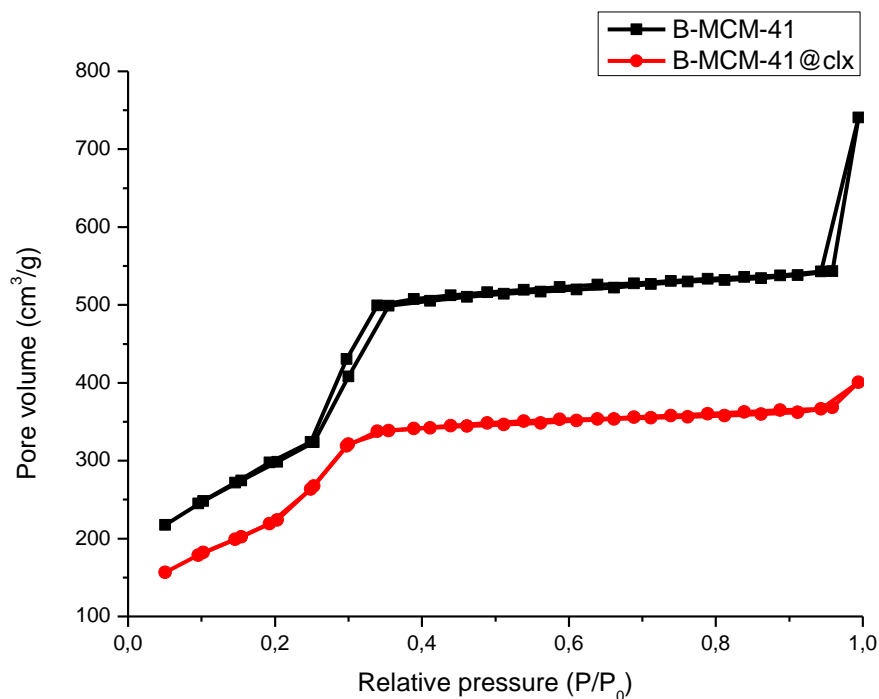
Figure 43: BET isotherms of B-MCM-41 and B-MCM-41@clx in hexane

All the MCM-41 samples exhibited the type IV BET isotherms that show the presence of mesoporous characteristic. For type IV isotherm, in the low relative pressures, gas fills the mesopores until the sharp increase at around $P/P_0 = 0.3$. Monolayer adsorption followed by multilayer formation of nitrogen occurs in the flatter region between the relative pressure at 0.3 and 0.9. After that point, nitrogen starts to be condensed in the capillary pores of porous material at pressures below the saturation pressure. The sharp increase at the pressure about 0.9 indicated the narrow pore size distribution and highly ordered mesostructured [20].

As it can be noticed from the BET isotherms of MCM-41 samples, all the adsorption – desorption processes are reversible. According to different studies made in this field, width of hysteresis loop gives lots of information about the quality of the porous material such as uniformity. Pores that are not uniform contain condensed nitrogen and prevent the capillary evaporation from different parts. This causes the formation of large hysteresis loops and irreversibility in BET isotherms. Hysteresis

loops are narrow in this analysis that can be explained with uniformity of pores and channels in MCM-41 samples. These trends in results can be seen in the samples loaded with drug in hexane that can be explained with stability of pores. After Celecoxib loading process, pores preserved their uniformity and did not degrade [54]. According to Ravikovitch et al [55] size of the hysteresis loop decreases with decreasing pore size. Due to results, pores of MCM-41 samples had 2 – 3 nm in diameter. Due to these small pores, hysteresis loop may be narrow. Exceptionally, MCM-41-3 has relatively broadened hysteresis loop and irreversibility. This sample probably has not the same uniformity as other samples have.

In order to analyze the porosity and surface area of MCM-41 samples before and after Celecoxib loading in detail, Table 9 shows the pore volume, pore diameter and surface area data of MCM-41 examined in ethanol and Table 10 shows the data of MCM-41 loaded with drug in hexane.

Table 9: Pore volume, pore diameter and surface area of MCM-41 samples before and after Celecoxib loading in ethanol

	MCM-41-1		MCM-41-2		MCM-41-3		B-MCM-41	
	Bare	With drug	Bare	With Drug	Bare	With Drug	Bare	With Drug
Pore volume (cm^3/g)	1.146	1.124	2.087	1.451	0.125	0.0917	1.203	0.663
Pore diameter (nm)	1.438	2.487	2.459	2.201	1.439	2.522	2.443	2.463
Surface area (m²/g)	763.9	457.5	1020	704.1	320.0	127.1	1095	816.6

Table 10: Pore volume, pore diameter and surface area of MCM-41 samples before and after Celecoxib loading in hexane

	MCM-41-1		MCM-41-2		MCM-41-3		B-MCM-41	
	Bare	**With drug**	**Bare**	**With drug**	**Bare**	**With drug**	**Bare**	**With drug**
Pore volume (cm^3/g)	1.868	0.488	1.045	0.557	0.118	0.091	0.758	0.226
Pore diameter (nm)	2.736	1.952	2.181	2.204	1.952	3.125	2.440	2.185
Surface area (m²/g)	861.8	114.5	907.3	336.3	191.8	39.36	912.0	243.8

According to N_2 adsorption - desorption results, it can be seen that all the pore volumes were decreased after Celecoxib loading process. This can be explained with successful adsorption of drug molecules into the pores and channels of MCM-41 silica particles. Same decrease can be seen in surface area of the samples. After drug loading process, Celecoxib drug molecules filled the pores and channels and adsorbed on the outer surface of dispersed particles that lead to decrease in surface area. Alternatively, during the loading process in solvent, dispersed particles might agglomerate. It probably caused to decrease in surface area. Besides, it can be said that pore diameter are not directly related with the particle size. MCM-41-1 and MCM-41-2 particles are smaller in particle diameter. MCM-41-2 and B-MCM-41 are synthesized to be larger in size shows smaller surface area. However, there is no significant difference between the pore diameters and pore volumes of them. MCM-41-3 shows even relatively smaller pore volume that can be explained with the surfactant that could not be removed during acid extraction process.

When the pore diameters were analyzed, a decrease was observed in cell parameters indicating the successful grafting in the internal surface of the MCM-41 particles. However, MCM-41-2 and MCM-41-3 samples showed an increase in hexane, pore diameters of MCM-41-1, MCM-41-3 and B-MCM-41 increased in ethanol. For example, for samples in hexane, although this increase is negligible in MCM-41-2 samples, pore diameter of MCM-41-3 particles increased to 3.125 nm from 1.952 nm after Celecoxib loading. This may be because of the adsorption of drug molecules to the outer surface of the MCM-41-3 sample. However, due to Kruk et al [54] and many other studies aimed to investigate the exact pore diameter of porous materials, data given in N_2 adsorption - desorption results are core diameter and do not reflect the actual pore size. Because, it examines the inner free space in the pore that is not filled with adsorbate during the adsorption process or emptied by capillary evaporation during the desorption process. Another important point worth to mention is that N_2 adsorption – desorption analysis uses Kelvin equation in order to determine the pore diameter assuming that all the pores are cylindrical and homogeneous in shape.. Kelvin equation can be written as $\ln(P/P_0) = 2\gamma V_m/rRT$ where P is the actual vapour pressure, P_0 is the saturated vapour pressure, γ is the surface tension, V_m is the molar volume of the liquid, R is the universal gas constant, r is the radius of the droplet and T is temperature. In contrast to assumptions made during this analysis, Kaminsky and his colleagues [56] say that each pore is filled with adsorbate discontinuously and incompletely. Due to these results, it is possible to see some deviations in data reflecting pore diameters and therefore, it is not that easy to make an observation by this way. Nevertheless, N_2 adsorption - desorption process is still the most practical way.

6.3.2 BJH METHOD

BJH (Barrett-Joyner-Halenda) method is used to investigate the pore size distribution of the porous materials. As it was mentioned in the previous part, pore size calculation in the N_2 adsorption - desorption analysis is based on the Kelvin equation. Although there may be some deviations in the pore diameter data, in order

to make an observation about the pore size distribution, it is the easiest and practical way. Figure 44, 45, 46 and 47 show the pore size distribution of MCM-41 and MCM-41 samples loaded with Celecoxib.
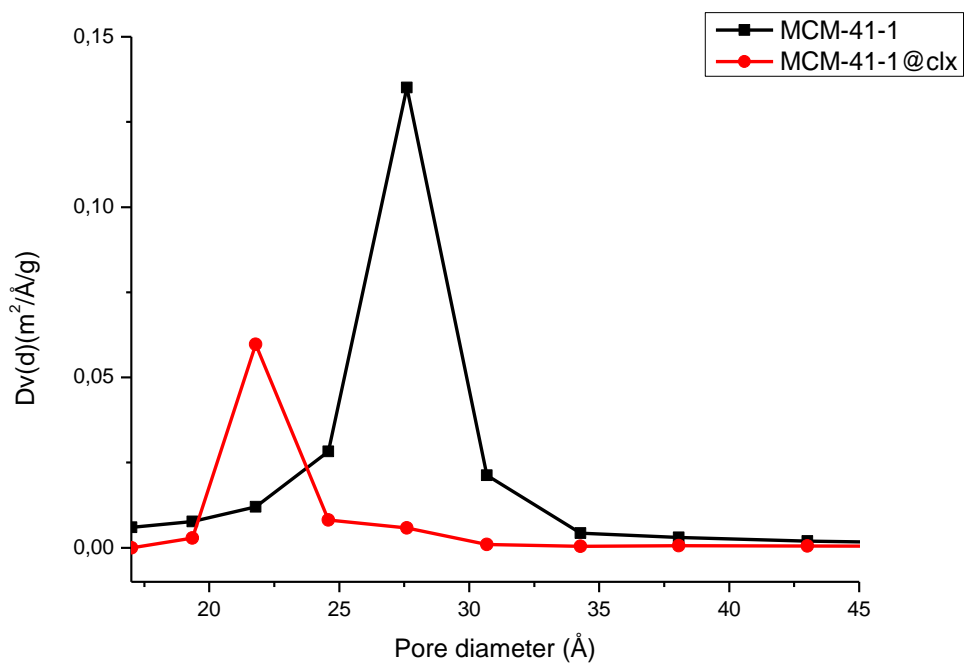
Figure 44: Pore size distribution of MCM-41-1 and MCM-41-1@clx in hexane
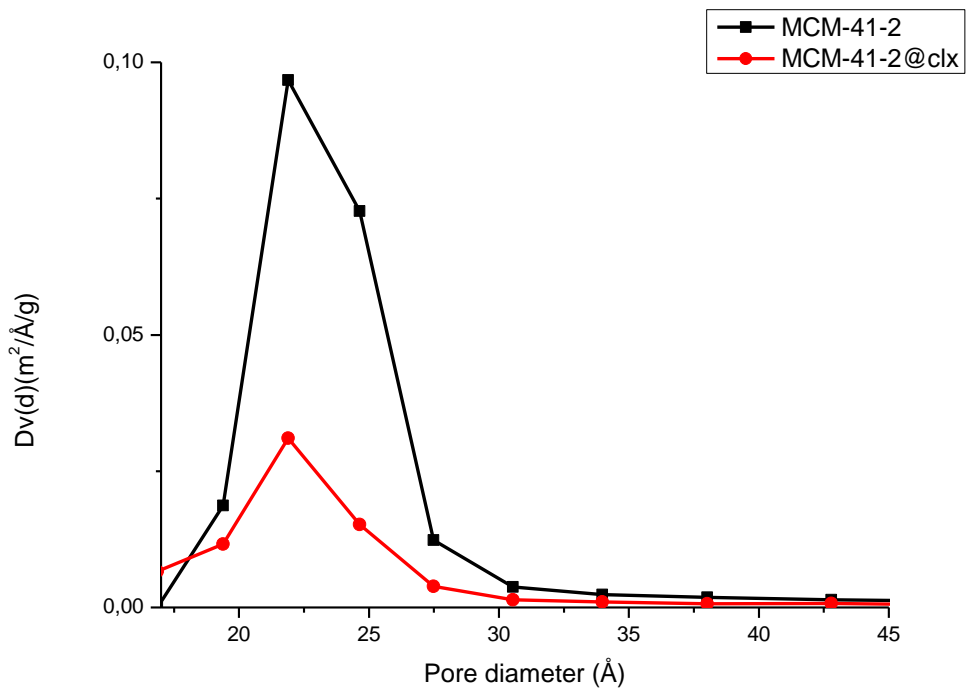
Figure 45: Pore size distribution of MCM-41-2 and MCM-41-2@clx in hexane
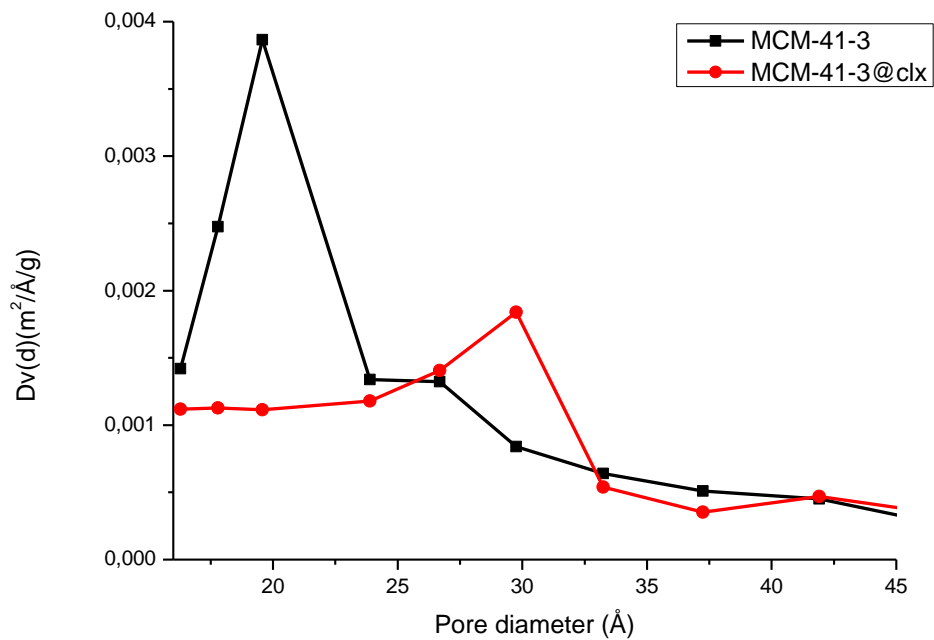
Figure 46: Pore size distribution of MCM-41-3 and MCM-41-3@clx in hexane
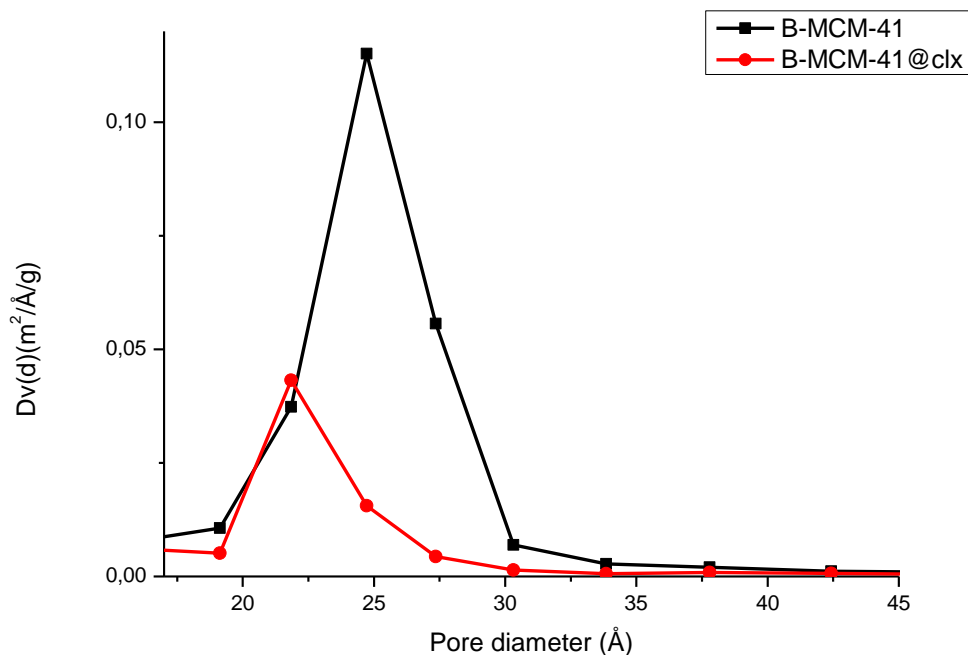
Figure 47: Pore size distribution of B-MCM-41 and B-MCM-41@clx in hexane

Due to pore size distribution calculated by using BJH method, all the MCM-41 samples show narrow pore size distribution in the range of 2 nm and 3 nm.

6.4 TEM ANALYSIS

The aim of the TEM analysis is to investigate the details of MCM-41 silica particle structure before and after Celecoxib loading. In all the reports and studies about the MCM-41, it has been said that MCM-41 has hexagonal arrays of uniform, regularly ordered, two-dimensional cylindrical mesopores. The TEM images of MCM-41 silica particles that can be seen in the images below prove this statement [9]. Figure 48, 49, 50 and 51 show the TEM images of MCM-41 samples in scale bar of 50 nm.
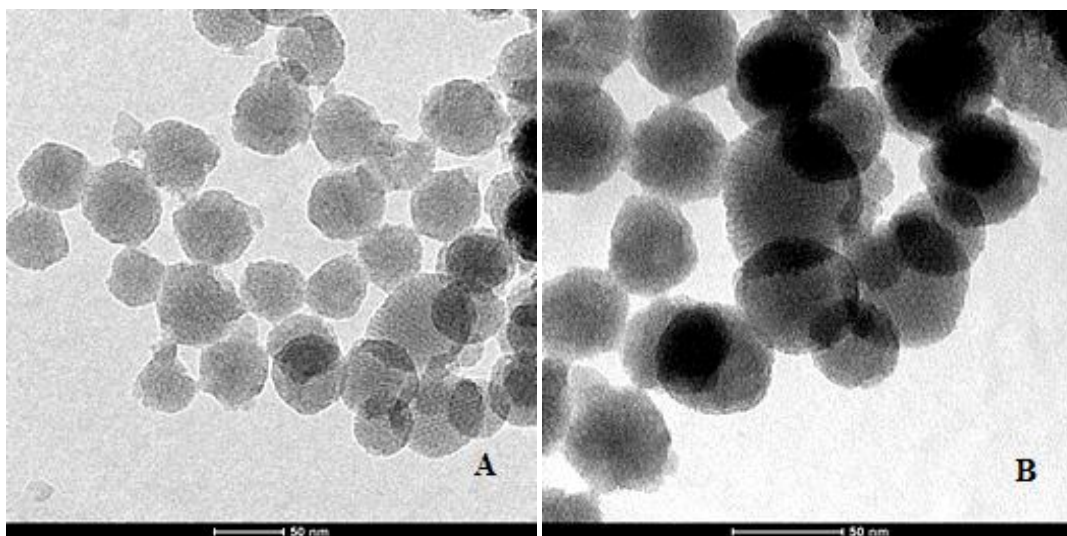
Figure 48: TEM images of A) MCM-41-1 and B) MCM-41-1@clx in ethanol

According to TEM images in the scale bar of 50 nm, MCM-41-1 silica particles are spherical in shape. They seem to have the diameter in size about 30-40 nm before being loaded with Celecoxib and well ordered hexagonal array of pores. However

after drug loading process, diameters of MCM-41-1 particles were increased and pores became less visible. Adsorption of the Celecoxib drug molecules to the pores and channels of MCM-41 and surface of the carrier particles may increase pore volumes and particle diameter. Another reason of this increase may be the swelling of the particles during the drug loading process in the solvent. TEM images reveal that the MCM-41-1 samples preserve the hexagonal mesoporous structure after drug loading process.
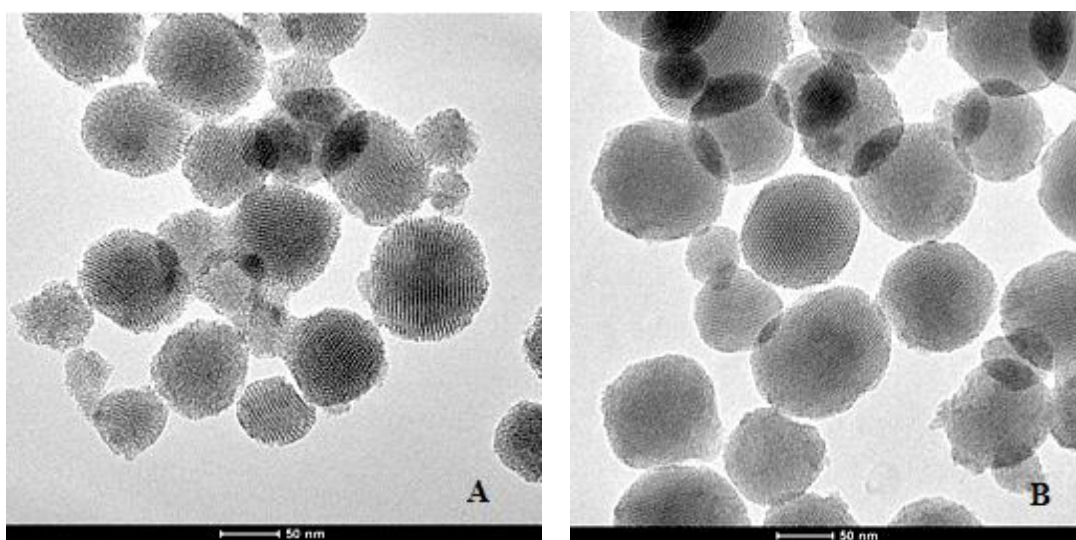
Figure 49: TEM images of A) MCM-41-2 and B) MCM-41-2@clx in ethanol

Due to the TEM images in Figure 49, MCM-41-2 particles are spherical like MCM-41-1 particles. It can be seen that samples that were calcined show more ordered array of hexagonal pores when it is compared with MCM-41-1. Elevated temperature probably enhanced the porous structure of the silica and resulted in highly ordered hexagonal pores and honeycomb structure in TEM images. After drug loading process, they also still exhibited the ordered pores.
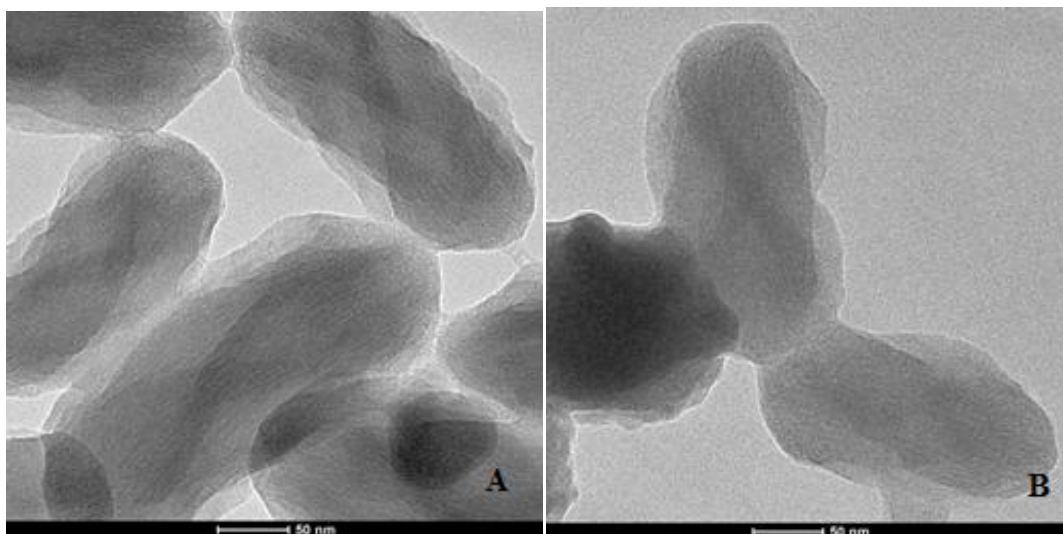
Figure 50: TEM images of A) MCM-41-3 and B) MCM-41-3@clx in ethanol

MCM-41-3 samples are different than other MCM-41 samples in many aspects as it can be seen Figure 50. Firstly, these particles are in ellipsoidal shape. After drug loading process they preserved this morphology. In the synthesis procedure of MCM-41-3, slightly high concentration of CTAB probably results in the formation of larger particle size and different morphology. Secondly, in TEM images, pores and channels could not be seen easily before drug loading. Finally, MCM-41-3 silica particles have larger diameter than MCM-41-1 and MCM-41-2.
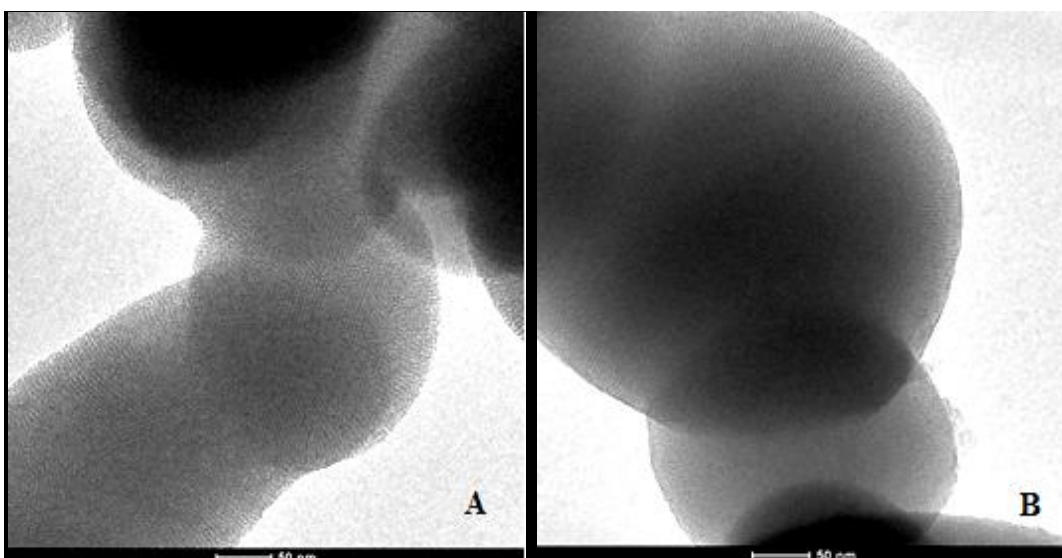
Figure 51: TEM images of A) B-MCM-41 and B) B-MCM-41@clx in ethanol

MCM-41 sample with the largest diameter is borosilicate. The diameter of one particle is about 400 nm. As it was showed in Figure 51, they are spherical in shape. Due to calcination process, particles of B-MCM-41 have ordered array of pores and channels that can be seen easily in TEM images. After drug loading process, these pores and channels were probably filled with drug molecules and could not be seen easily in TEM images.

6.5 SEM ANALYSIS

SEM analysis aims to observe the particle size uniformity and have information about the morphology of MCM-41 silica particles before and after drug loading process. Figure 52, 53, 54 and 55 show the SEM images of MCM-41 and drug loaded MCM-41 particles.
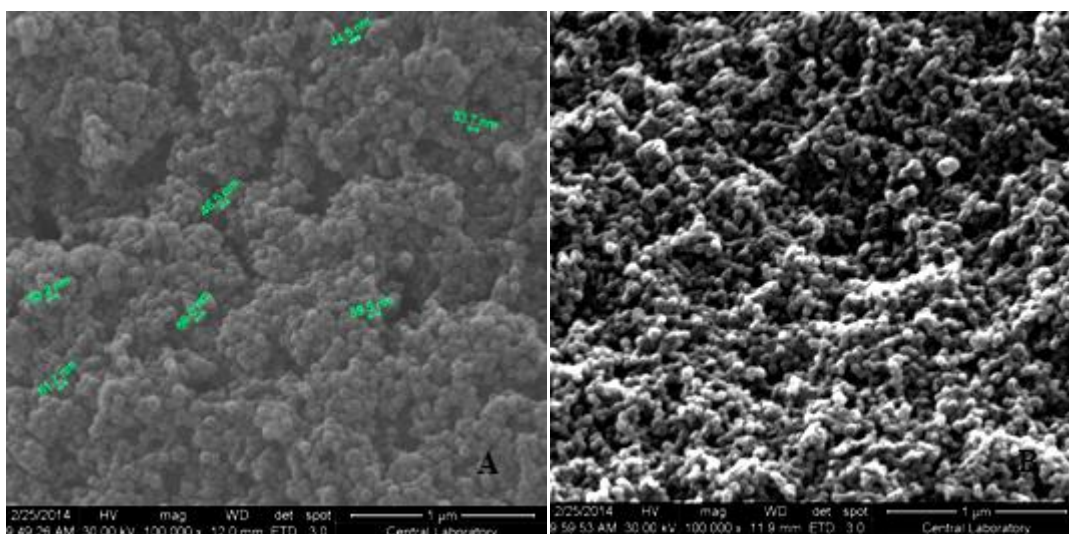
Figure 52: SEM images of A) MCM-41-1 and B) MCM-41-1@clx in ethanol

Due to the SEM images of MCM-41-1 silica particles before and after drug loading, particle sizes range from 40 nm to 80 nm. They are all in spherical shape. SEM images illustrate high degree of homogeneity in particle size and morphology. Morphology of the MCM-41-1 particles remained unchanged after Celecoxib loading.
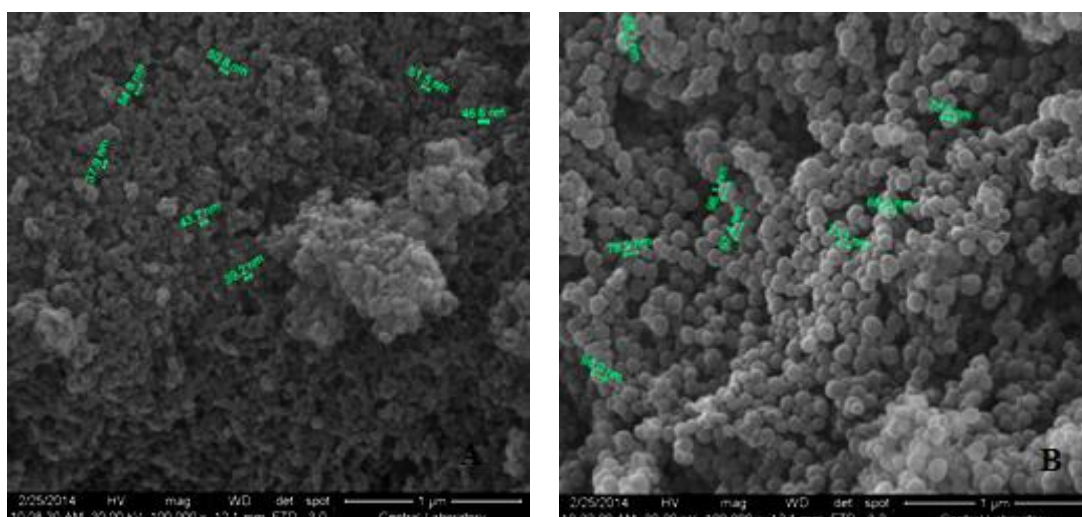
Figure 53: SEM images of A) MCM-41-2 and B) MCM-41-2@clx in ethanol

In the SEM images of MCM-41-2 silica particles, narrow pore size distribution could be seen. Spherical shape of the particles remained same after Celecoxib loading process. While the particles sizes before being loaded with Celecoxib range from 30 to 60 nm, their size diameter had increased to about 60-90 nm. As it was mentioned in the TEM analysis, this increase may be due to the encapsulation of the Celecoxib drug molecules in the pores and channels of MCM-41-2.
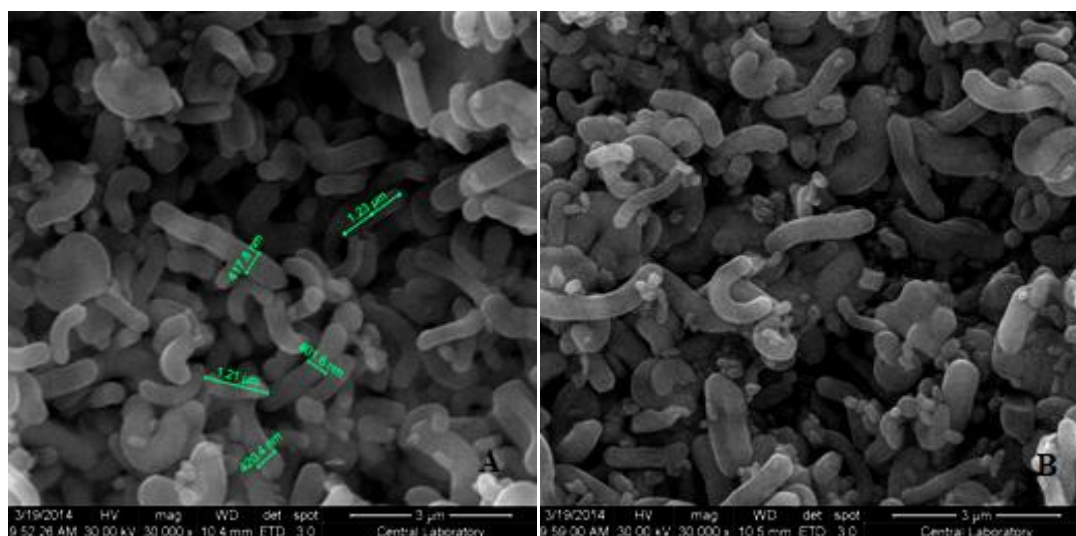
Figure 54: SEM images of A) MCM-41-3 and B) MCM-41-3@clx in ethanol

Morphology of MCM-41-3 particles is different than others. They are in ellipsoidal shape. As it can be seen in the SEM images, particles sizes of MCM-41-3 are larger than the other silica particles. While their lengths reached to 1.3 μm, their widths were in the range of 400-500 nm. However, pore size distribution is larger with respect to MCM-41-1 and MCM-41-2. Also homogeneity could not be seen in the particle size and morphology.
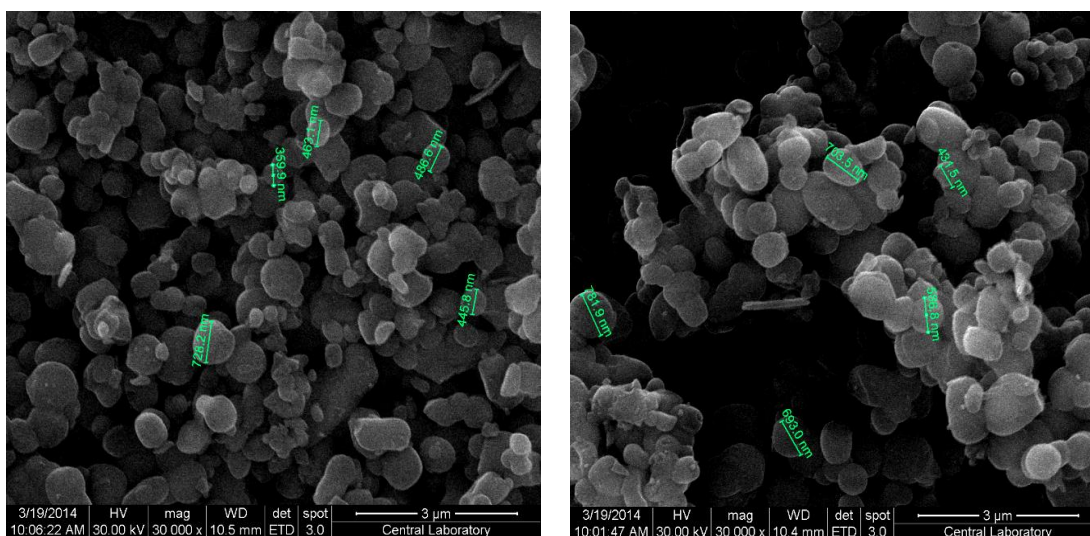
Figure 55: SEM images of B-MCM-41 and B-MCM-41@clx in ethanol

Borosilicate samples were spherical in shape in SEM images. They preserved this morphology after Celecoxib loading. Particle sizes of B-MCM-41 were larger, in the range of 400 nm to 700 nm. Their pore size distribution was larger like MCM-41-3. High homogeneity in the particle size and morphology in the SEM images of MCM-41-1 and MCM-41-2 could be seen in SEM images of MCM-41-3 and B-MCM-41. Larger particle size may be the main reason of decrease in homogeneity. As the particle sizes increases, regularity in the particles probably decreases.

6.6 ZETA POTENTIAL

Zeta potential measurements aim to have information about the surface properties of MCM-41 silica particles by using electric potential. It gives information about the electrical charge of the surface. For this purpose 0.001 g MCM-41 sample was suspended in 50 mL deionized water. Table 11 shows the zeta potentials of MCM-41 silica particles in pH 7.4.

Table 11: Zeta potential of MCM-41 samples

Sample	Zeta potential (mV) in deionized water at pH 7.4
MCM-41-1	-6.74
MCM-41-2	-2.94
MCM-41-3	-2.55
B-MCM-41	-31.7

Although there are small differences between them, all MCM-41 samples exhibit negative surface charge. This proves the presence of the negatively charged silanol groups on the surface of the MCM-41 samples [54]. However, surface of the borosilicate is highly negative with zeta potential -31.7 mV. This value is more negative than the other zeta potentials of MCM-41 samples. This may be due to high electronegativity of boron in the borosilicate.

6.7 ELEMENTAL ANALYSIS

Elemental analysis is a process in which elemental composition of the samples can be identified. By this method, qualitative and quantitative determination can be done. It enables to determine the empirical formula of the compound. It commonly includes the observations of mass fractions of carbon, hydrogen and nitrogen in the sample. We used elemental analysis because our model drug, Celecoxib, contains carbon. Amount of drug loaded to silica particles calculated due to elemental analysis results can be seen in the Table 12.

According to the Table 12, analysis of the samples in which the ethanol was used as a solvent in the drug loading process shows the highest amount of loaded Celecoxib. This can be explained with the solvent effect. Polarity of the solvent used in drug

loading process plays the most important role in the drug loading efficiency. -OH groups on the surface of the MCM-41 silica particles make surface polar and provide linkage with drug molecules. Polar solvents can form competitive adsorption with drug molecules and causes lower degree of drug loading. In this way, two different solvents that are different in degree of polarity were used; methanol and ethanol. So, ethanol that has longer alkyl chain and less polarity showed higher ability to hold Celecoxib as it can be seen in elemental analysis results [16]. After this observation, it was decided to use hexane due to its nonpolarity and see the effectiveness of solvent effect in the drug loading capacity.

Another observation is that MCM-41 silica particles that are not functionalized held the highest amount of Celecoxib. While 1 g drug loaded YVO4:Eu functionalized MCM-41-1 particle contains 0.1579 g Celecoxib in maximum with ethanol as solvent, 1 g MCM-41-1 with no functionalization contains 0.264 g Celecoxib. MCM-41-1 with organic functionalization with APTES contains 11.78% Celecoxib; pegylated MCM-41-1 contain 15.50% Celecoxib. The first possible reason of this decrease in drug loading is reduction of surface area by the surface modification. Secondly, this may be due to the effect of surface chemistry. The major force of drug loading is the interaction between surface of the carrier and drug molecules. Surface of the MCM-41 silica mesoporous carriers is covered with OH groups. After surface functionalization, electrostatic and hydrophobic interactions on the surface change and drug loading efficiency can increase or decrease with surface functionalization. If the hydrogen bond is the main form of the interaction between Celecoxib molecules, functionalization with PEG, APTES and YVO_4:Eu groups may hinder the interaction among silanol groups and Celecoxib molecules. Another reason may be the degradation of the pore framework caused by the surface functionalization process.

It can be seen that while MCM-41-1 holds 26.4% Celecoxib, MCM-41-2 holds relatively lower amount of drug; 18.98%. As it was mentioned in the experimental part only difference between these MCM-41 particles was the way applied to remove the surfactant. Possible reason of this decrease in the drug holding capacity of

calcined MCM-41 is the agglomeration of the particles at elevated temperature and reduction in the surface area. During the acid extraction, MCM-41 silica particles probably dispersed homogeneously in the methanol and HCl solution. Alternatively, elevated temperature may lead to decomposition in the silanol groups on the surface of the MCM-41 particles, this may cause decrease in drug loading capacity also.

Due to the drug loading results, it can be recognized that MCM-41 silica particles prepared with the 1:1 (wt: wt) ratio with Celecoxib in the drug loading process held the highest amount of drug than the other ones in 2:1 and 4:1 ratio. With the purpose of the maximizing the amount of Celecoxib in the MCM-41 silica particles, MCM-41-1 was mixed with Celecoxib in 1:2 (wt: wt) ratio, however desired results could not be seen. While MCM-41-1 in 1:1 ratio held 26.40% Celecoxib, MCM-41-1 in 1:2 ratio held 25.37%. Due to the steric effects, highest efficiency in the drug loading was seen in MCM-41 prepared with Celecoxib in 1:1 (wt: wt) ratio. After this result, other drug loading processes had been carried out with MCM-41 particles and Celecoxib in 1:1 (wt: wt) ratio.

Although reasonable and desired results were obtained in the elemental analysis, loaded amount of Celecoxib in the silica particles was also calculated by using UV-VIS results. Because, loading process of drug was performed in solvent and Celecoxib might be lost during the filtration process.

Table 12: Amount of drug loaded to silica particles calculated due to elemental analysis results

METHANOL			
MCM-41-1	**MCM-41-2**	**MCM-41-3**	**B-MCM-41**
Bare: 7.05%	Bare: 6.75%	Bare:1.78%	Bare: 4.21%
YVO_4:Eu functionalized: 1:1: 4.51% 1:2: 4.21% 1:4: 2.73%	YVO_4:Eu functionalized: 1:1:6.02% 1:2: 3.80% 1:4: 3.22%	YVO_4:Eu functionalized: 1:1: 5.68% 1:2: 3.87% 1:4: 3.56%	
Aptes functionalized: 1:1: 0.64%	2Aptes functionalized: 1:1: 4.32%	2Aptes functionalized: 1:1: 2.56%	
2Aptes functionalized: 1:1: 1.00%			
3Aptes functionalized: 1:1: 0.04%			
ETHANOL			
MCM-41-1	**MCM-41-2**	**MCM-41-3**	**B-MCM-41**
Bare: 26.40%	Bare:18.98%	Bare:19.48%	Bare: 16.21%
YVO_4:Eu functionalized: 1:1: 15.79% 1:2: 8.36% 1:4: 5.46%	YVO_4:Eu functionalized: 1:1: 13.57% 1:2: 5.96% 1:4: 2.51%	YVO_4:Eu functionalized: 1:1: 8.97%	
2Aptes functionalized: 11.78%	2Aptes functionalized: 10.28%	2Aptes functionalized: 8.93%	
Pegylated: 15.50%	Pegylated: 13.92%		

6.8 UV ANALYSIS

6.8.1 CELECOXIB LOADING

In the purpose of calculating the amount of Celecoxib loaded to MCM-41 silica particles, standard solutions were prepared with 5 mL solvent in the concentrations of 8×10^{-5}, 16×10^{-5}, 25×10^{-5}, 30×10^{-5} and 45×10^{-5} M. The measurements were recorded between 200-800 nm. The absorbance values at 254 nm were used for the all calculations of the concentration of Celecoxib. The absorbance values and concentrations of these standard solutions were used to plot the calibration curve. Slope of the curve indicated the molar absorptivity coefficient as 76.776 for ethanol and 87.814 for hexane. Their calibration curves can be seen in the Figures 56 and 57.
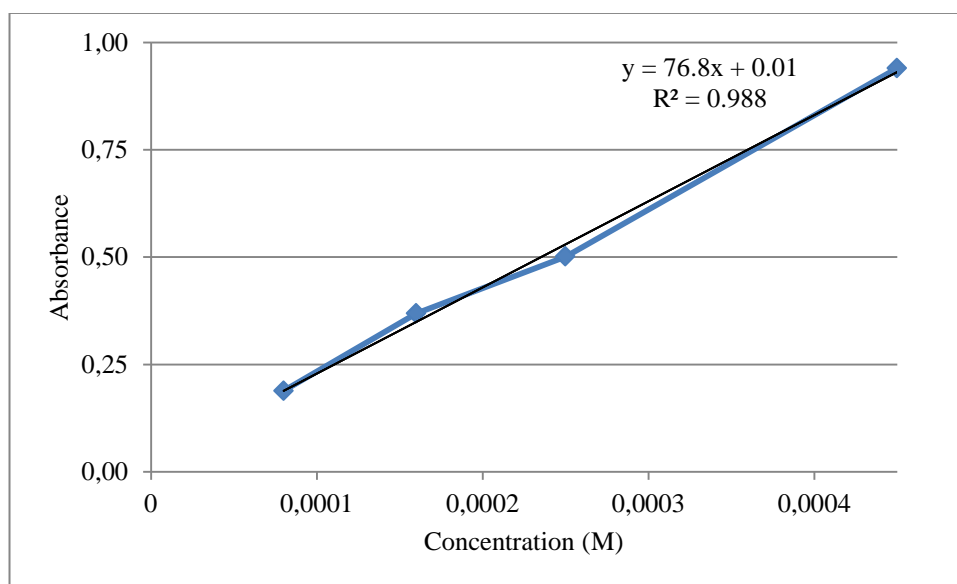
Figure 56: Calibration curve of loading process of Celecoxib in ethanol
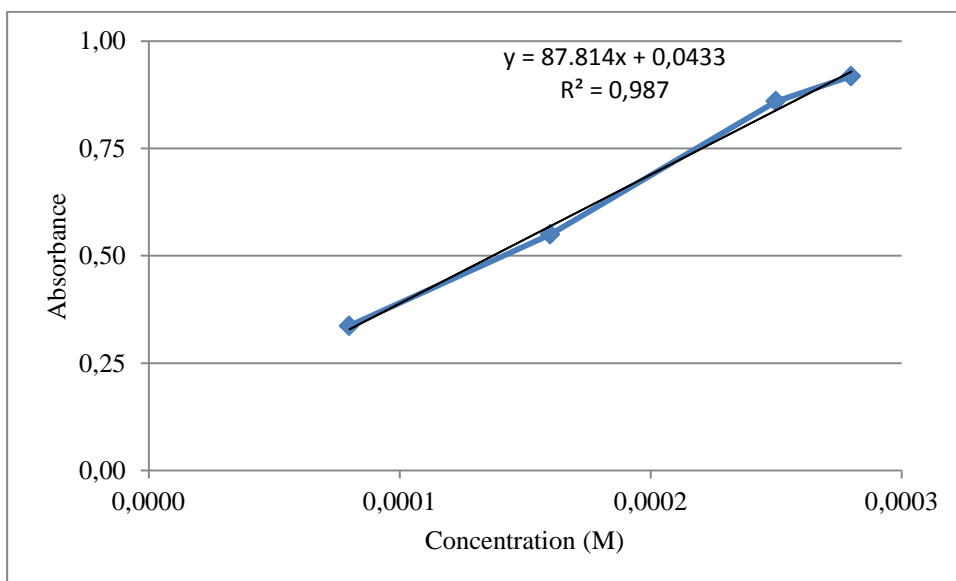
Figure 57: Calibration curve of loading process of Celecoxib in hexane

As it was mentioned in the experimental part, after 100 mg Celecoxib was mixed with 50 mL solvent, it was washed and filtered. The filtrate was analyzed in UV analysis. Due to residual amount of Celecoxib concentration in the filtrate, amount of Celecoxib loaded to MCM-41 were calculated by using Beer-Lambert law. Calculation of the % Celecoxib loaded to MCM-41-1 particles in hexane was shown in the Appendix part as an example. Table 13 shows the absorbance values and the % loaded Celecoxib to MCM-41 carrier particles in ethanol. Table 14 shows the the absorbance values and the % loaded Celecoxib to MCM-41 carrier particles in hexane.
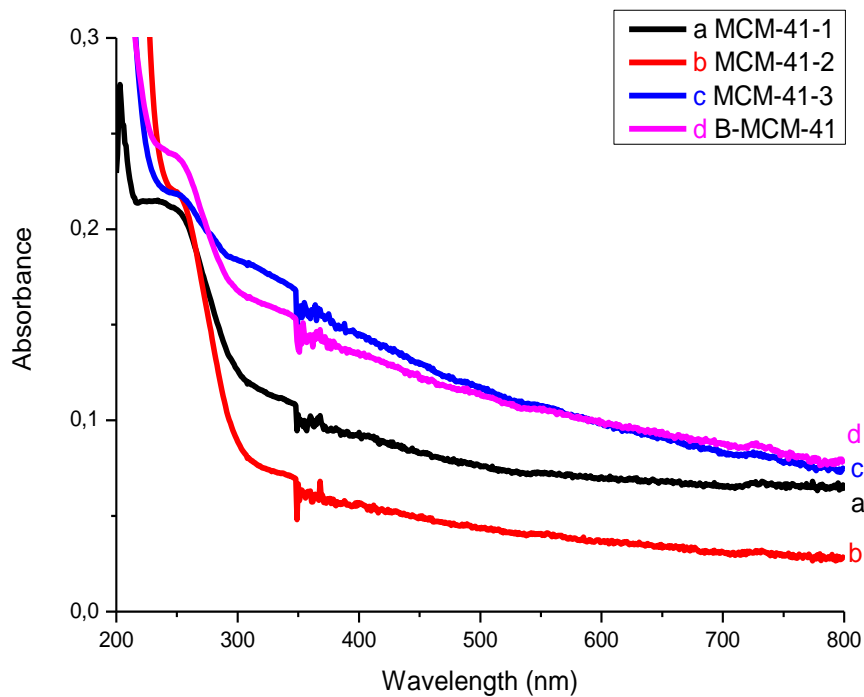
Figure 58: UV graph of a) MCM-41-1 b) MCM-41-2 c) MCM-41-3 d) B-MCM-41 in ethanol in the loading process

Table 13: Absorbance values and % loaded Celecoxib in ethanol

	Absorbance	**% Loaded Celecoxib**
MCM-41-1@clx	0.2087	25.95%
MCM-41-2@clx	0.2228	20.95%
MCM-41-3@clx	0.2108	25.21%
B-MCM-41@clx	0.2334	17.57%
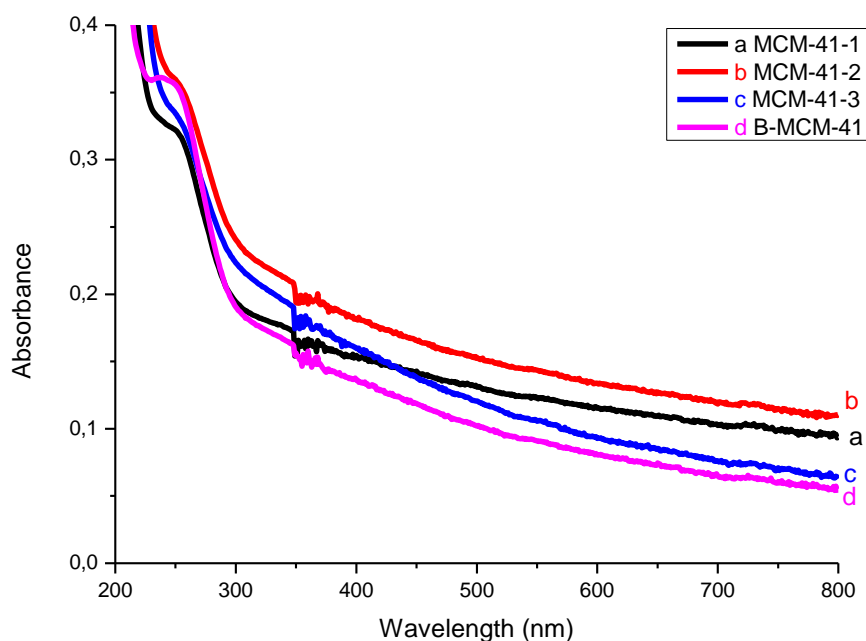
Figure 59: UV graph of a) MCM-41-1 b) MCM-41-2 c) MCM-41-3 d) B-MCM-41 in hexane filtrate in the loading process

Table 14: Absorbance values and % loaded Celecoxib in hexane

	Absorbance	**% Loaded Celecoxib**
MCM-41-1@clx	0.3246	29.51%
MCM-41-2@clx	0.3549	22.92%
MCM-41-3@clx	0.3289	25.58%
B-MCM-41@clx	0.3505	23.89%

Calculation results of the amount of Celecoxib loaded to silica particles due to UV results are confirmative with the values of elemental analysis. Due to the drug loss in the filtration process, higher degree of loading capacity has been seen in the UV measurements.

According to UV results, it can be seen that shape and particle diameter do not affect the drug loading capacity of the MCM-41 silica particles. There are no significant differences in the amount of loaded drug to MCM-41-1, MCM-41-2 silica particles that are spherical in shape with smaller pore diameter, and MCM-41-3 in ellipsoidal shape, B-MCM-41 in spherical with larger diameter. However, it can be recognized that MCM-41-1 particles that have largest pore volume held the highest amount of Celecoxib. This proves the encapsulation of drug molecules into the pores of samples. Besides, borosilicate sample held the lowest amount of drug that can be explained with its highly negative surface. It can be seen that solvent effect is another important force affecting the drug loading capacity of the MCM-41 particles. While MCM-41 particles that were loaded with Celecoxib in ethanol held 25.95% drug at maximum, this value increased to 29.51% in MCM-41 particles that were loaded with Celecoxib in hexane. Polar solvents such as methanol and ethanol formed competitive adsorption with drug molecules and decreased the degree of drug loading capacity; however hexane that shows no polarity increased the amount of Celecoxib loaded to MCM-41 particles by the –OH groups on the surface [16].

6.8.2 CELECOXIB RELEASE

The UV analysis for the release experiments were completed within six hours. For each measurement the 10 mL sample taken for the analysis was replaced with fresh medium of PBS (phosphate buffer solution). As it was done in the UV measurements in drug loading process, standard solutions in different concentrations were prepared and their absorbance values at 254 nm were used to plot calibration curve of Celecoxib in PBS. Slope of the curve in Figure 60 was used as molar absorptivity coefficient in Beer-Lambert law.
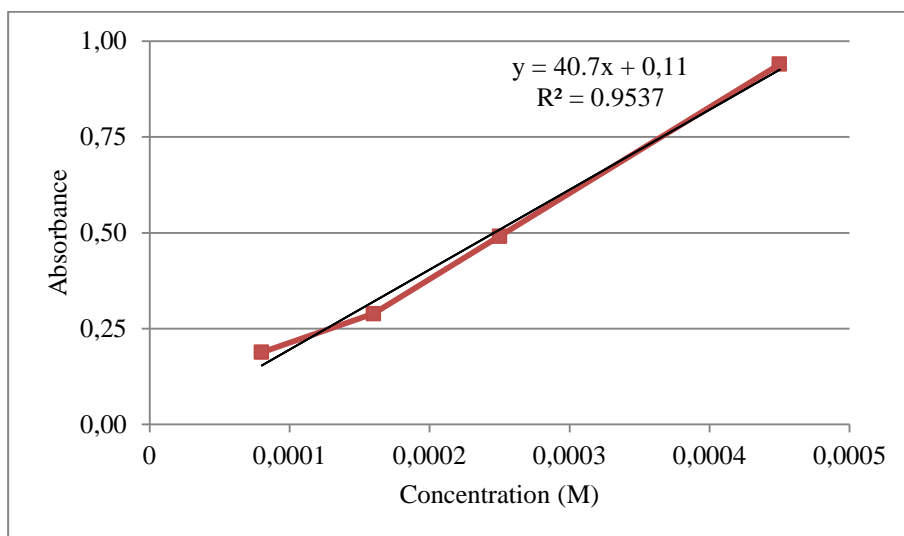
Figure 60: Calibration curve of release process of Celecoxib in PBS

The release experiments by UV analysis were completed three times to obtain adequate results. Table 15, 16 and 17 show the percentage of remaining Celecoxib released from the MCM-41 loaded with drug in the solvent of ethanol. Table 18, 19 and 20 show the percentage of Celecoxib released from the MCM-41 loaded with drug in hexane. The concentration measurements were completed within 30 minutes, 1 hour, 2 hours, 4 hours and 6 hours. Figure 61, 62 and 63 indicate the amount of Celecoxib released to the phosphate buffer solution from 1.0 g of MCM-41 loaded with Celecoxib in ethanol within 6 hours. Figure 64, 65 and 66 refer to the amount of Celecoxib released from 1.0 g of Celecoxib loaded MCM-41 in hexane within 6 hours.

Table 15: % Released Celecoxib of MCM-41 silica particles loaded with drug in ethanol within 6 hours and errors

Time(min)	MCM-41-1	MCM-41-2	MCM-41-3	B-MCM-41	Celebrex
0	0	0	0	0	0
30 min	20.85%	20.97%	16.74%	31.02%	9.34%
1 hour	18.77%	23.64%	16.30%	31.79%	7.49%
2 hour	22.58%	22.61%	15.99%	33.61%	9.83%
4 hour	23.83%	27.61%	13.35%	30.70%	9.88%
6 hour	28.35%	28.49%	26.04%	38.90%	9.49%
Total	**72.83**%	**75.82**%	**62.48**%	**86.78**%	**38.32**%
%Error	**2.68**%	**5.61**%	**8.10**%	**4.58**%	**2.62**%
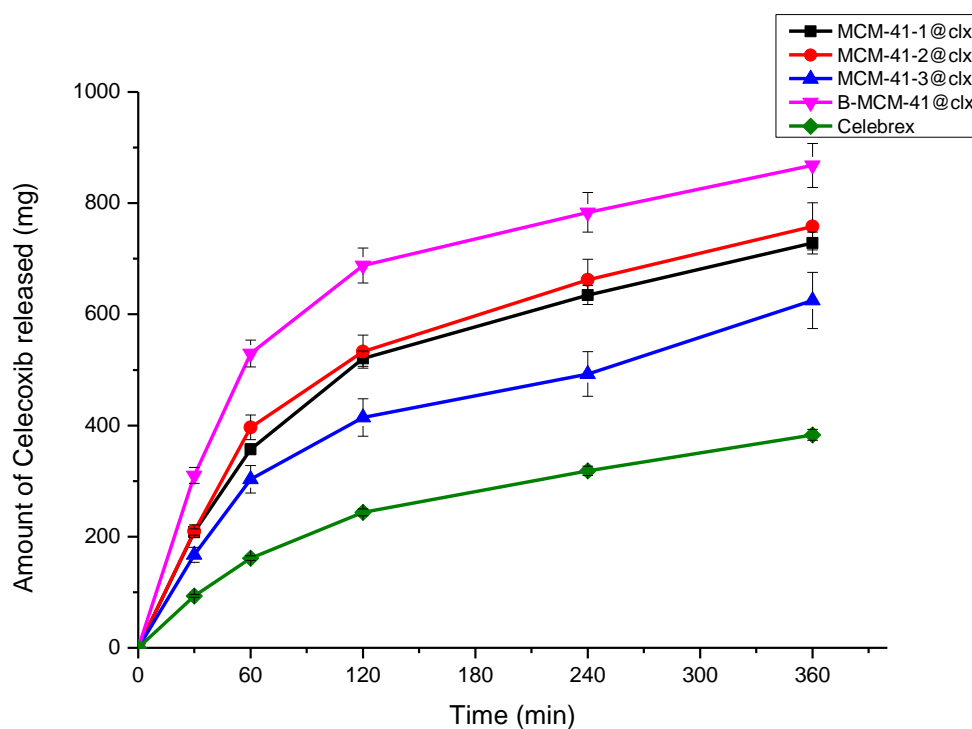
Figure 61: Amount of Celecoxib released from 1.0 g of Celecoxib loaded to MCM-41 in ethanol within 6 hours

Table 16: % Released Celecoxib of MCM-41 silica particles loaded with drug in ethanol within 6 hours and errors

Time(min)	MCM-41-1	MCM-41-2	MCM-41-3	B-MCM-41	Celebrex
0	0	0	0	0	0
30 min	23.57%	24.23%	21.22%	27.88%	10.54%
1 hour	19.11%	20.19%	24.69%	29.45%	9.77%
2 hour	20.46%	21.65%	26.88%	27.25%	10.23%
4 hour	21.56%	18.98%	20.63%	31.60%	9.67%
6 hour	23.09%	21.77%	21.04%	32.73%	8.04%
Total	**70.33**%	**69.97**%	**72.79**%	**82.97**%	**39.80**%
%Error	**0.86**%	**2.54**%	**7.06**%	**4.39**%	**1.15**%
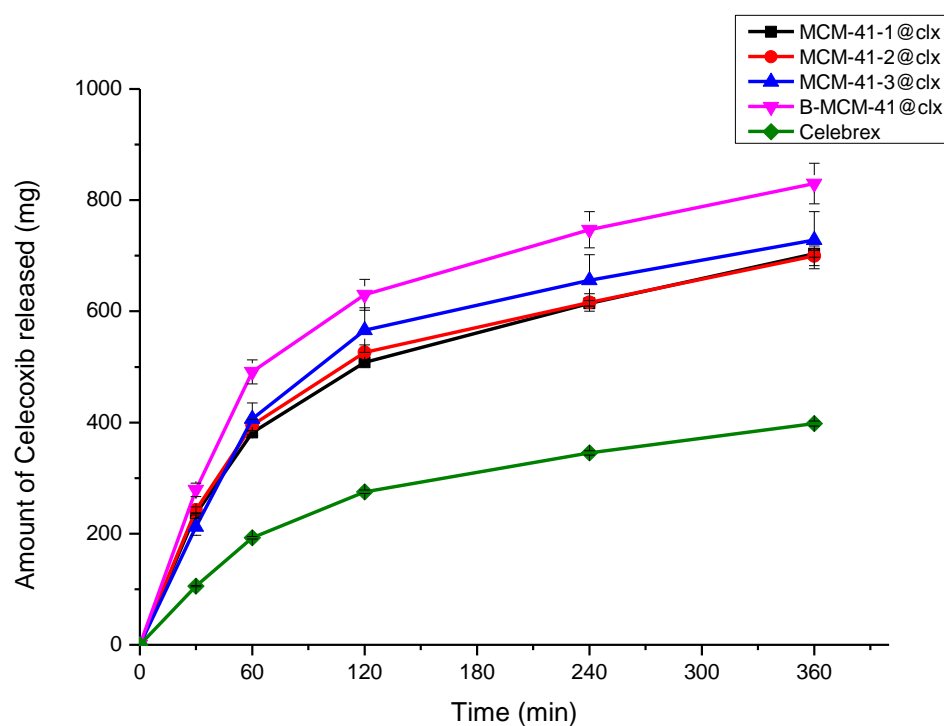
Figure 62: Amount of Celecoxib released from 1.0 g of Celecoxib loaded to MCM-41 in ethanol within 6 hours

Table 17: % Released Celecoxib of MCM-41 silica particles loaded with drug in ethanol within 6 hours and errors

Time(min)	MCM-41-1	MCM-41-2	MCM-41-3	B-MCM-41	Celebrex
0	0	0	0	0	0
30 min	21.22%	21.08%	20.07%	23.89%	10.23%
1 hour	20.08%	21.56%	19.51%	25.10%	9.12%
2 hour	21.74%	22.88%	21.11%	24.63%	11.26%
4 hour	19.25%	20.37%	22.59%	31.03%	9.33%
6 hour	23.71%	19.12	20.31%	29.81%	8.08%
Total	**69.65**%	**69.58**%	**68.69**%	**79.20**%	**39.92**%
%Error	**1.80**%	**3.08**%	**1.03**%	**4.56**%	**1.45**%
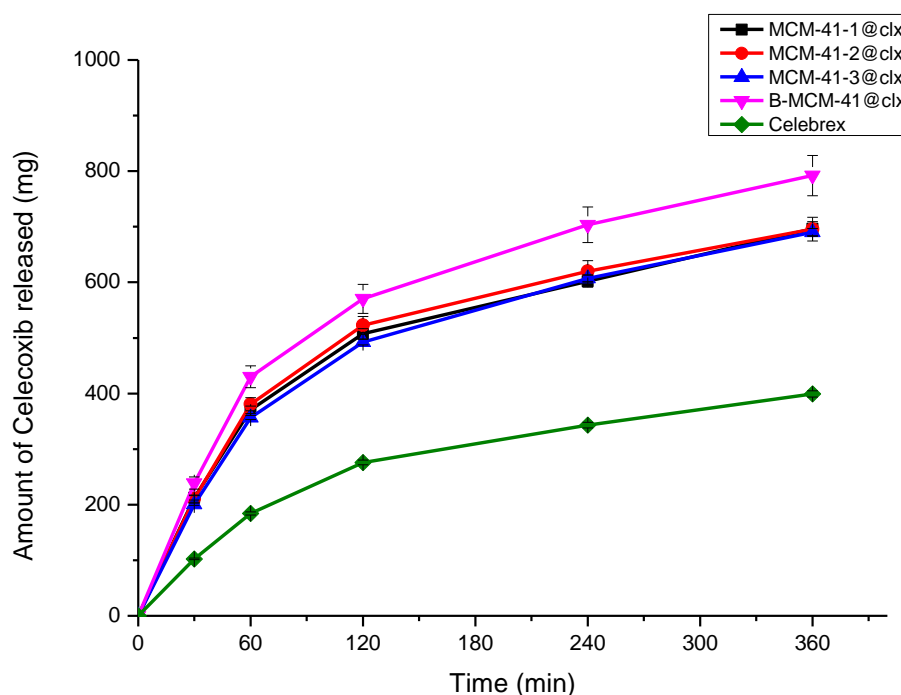
Figure 63: Amount of Celecoxib released from 1.0 g of Celecoxib loaded to MCM-41 in ethanol within 6 hours

Table 18: % Released Celecoxib of MCM-41 silica particles loaded with drug in hexane within 6 hours

Time(min)	MCM-41-1	MCM-41-2	MCM-41-3	B-MCM-41	Celebrex
0	0	0	0	0	0
30 min	35.84%	23.55%	36.78%	37.22%	9.04%
1 hour	12.06%	33.61%	14.35%	25.90%	10.36%
2 hour	12.87%	10.94%	9.02%	12.67%	11.89%
4 hour	10.63%	11.75%	9.44%	8.03%	9.48%
6 hour	9.21%	10.87%	8.36%	9.58%	7.96%
Total	**60.11**%	**64.44**%	**59.12**%	**66.22**%	**40.15**%
Error	**1.07%**	**6.38%**	**1.20%**	**0.24%**	**0.12%**
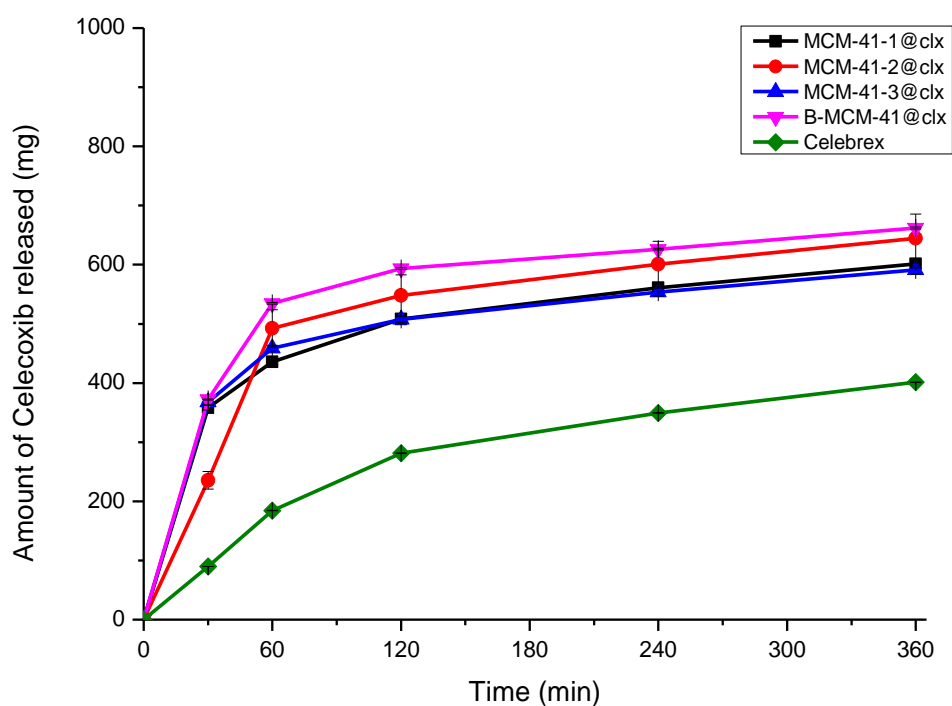
Figure 64: Amount of Celecoxib released from 1.0 g of Celecoxib loaded to MCM-41 in hexane within 6 hours

90

Table 19: % Released Celecoxib of MCM-41 silica particles loaded with drug in hexane within 6 hours

Time(min)	MCM-41-1	MCM-41-2	MCM-41-3	B-MCM-41	Celebrex
0	0	0	0	0	0
30 min	29.57%	25.52%	34.05%	39.72%	11.26%
1 hour	17.20%	11.23%	11.98%	19.39%	7.97%
2 hour	12.25%	15.97%	12.50%	10.63%	7.61%
4 hour	11.64%	11.53%	8.02%	11.74%	10.89%
6 hour	8.71%	10.22%	8.63%	9.96%	7.30%
Total	**58.68**%	**59.84**%	**57.31**%	**65.49**%	**37.67**%
Error	**3.42%**	**1.21%**	**1.90%**	**1.34%**	**6.29%**
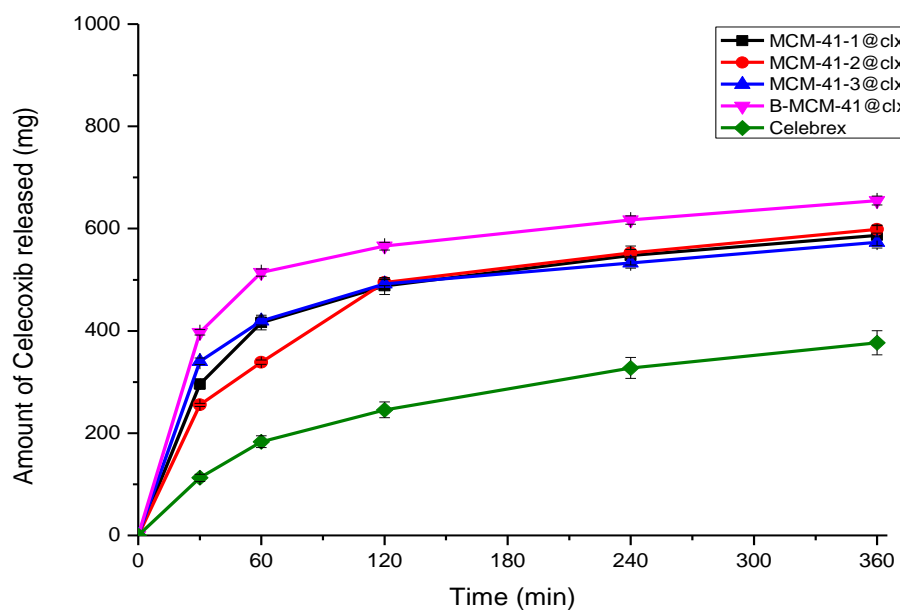
Figure 65: Amount of Celecoxib released from 1.0 g of Celecoxib loaded to MCM-41 in hexane within 6 hours

Table 20: % Released Celecoxib of MCM-41 silica particles loaded with drug in hexane within 6 hours

Time(min)	MCM-41-1	MCM-41-2	MCM-41-3	B-MCM-41	Celebrex
0	0	0	0	0	0
30 min	33.87%	31.15%	34.66%	38.73%	11.71%
1 hour	20.93%	12.78%	16.15%	27.04%	12.02%
2 hour	14.12%	13.02%	9.57%	12.59%	9.06%
4 hour	9.87%	10.36%	10.06%	10.17%	9.67%
6 hour	9.79%	9.05%	7.62%	7.25%	10.31%
Total	**63.48**%	**57.42**%	**58.83**%	**67.44**%	**42.77**%
Error	**4.48%**	**5.20%**	**0.70%**	**1.59%**	**6.39%**
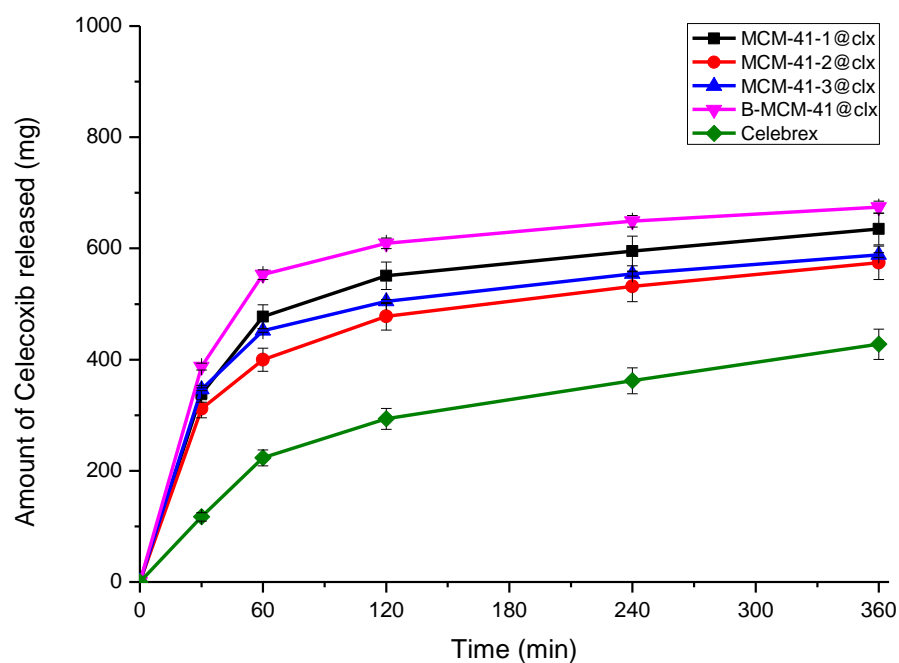
Figure 66: Amount of Celecoxib released from 1.0 g of Celecoxib loaded to MCM-41 in hexane within 6 hours

Due to results, it can be said that release rate of the Celecoxib was enhanced by using MCM-41 silica particles. The sustained release was seen in the first 6 hours. Amount of released Celecoxib was not changed significantly in the time intervals. At the end of 6 hours of mixing in PBS, while 39.35% of the Celecoxib loaded to Celebrex, commercial drug, was released, this value was increased to 82.98% by loading Celecoxib to borosilicate particles. This increase in improvement of release and dissolution rate is due to the reduction in degree of Celecoxib crystallization. According to results, borosilicate particles that held the lowest amount of Celecoxib showed the highest release rate. MCM-41-1, MCM-41-2 and MCM-41-3 held higher amount of drug than borosilicate however their releasing rates are slower. It can be explained with the loading and release processes. For poorly soluble drugs, physical adsorption such as hydrogen bonding, electrostatic and hydrophobic interaction is more favorable to enhance dissolution. Because, drug loaded to carrier should be released easily at appropriate conditions. Drug molecules adsorbed on the outer pores of MCM-41 move firstly when the dissolution medium is introduced. However, influx of dissolution medium to inner pores needs more time and these drug molecules are released slowly. On the other side, during the loading process, drug molecules firstly fill the outer pores and move to the inner arrays in MCM-41 later. Loading and release processes are reversible due to this effect. MCM-41 samples holding lower amount of Celecoxib holds it in outer pores and release it faster, however, release of the higher amount of Celecoxib molecules from the MCM-41 takes more time and release occurs slowly [16]. In the comparison between the ethanol and hexane, it can be observed that samples loaded with drug in ethanol held lower amount of drug molecules and release in the percentage of 82.97% at maximum, however samples loaded with Celecoxib in hexane held higher amount of drug and release 66.22% of them in the first 6 hours.

Another observation is the difference between the release rate of samples loaded with drug in ethanol and hexane solvents in the first 30 minutes. While 21.88% of the Celecoxib loaded to MCM-41-1 was released in the first 30 minutes in the release experiments of samples loaded with drug in ethanol, Celecoxib was released in the

percentage of 35.84% in the samples loaded with drug in hexane. This trend can be seen in every sample. Reason of this increase is the faster release of the adsorbed drug molecules to the silanol groups on the outer pores of the MCM-41 in hexane. Weak bonds between silanol groups on the surface of the MCM-41 and Celecoxib drug molecules might be broken easily in presence of suitable solvent and drug located to outer pores was released in the first 30 minutes. However, Celecoxib drug particles, that the solubility was enhanced and delivered as finely divided colloidal particles, were dispersed in the inner pores of MCM-41 particles in ethanol. After the influx of solvent to the pore surfaces, drug molecules were released. By this way, release rate of the Celecoxib was controlled [57].

According to release experiments and XRD result, it can be concluded that Celecoxib was remained as crystalline state and these molecules mainly adsorbed on the outer pores in surface of the MCM-41 samples in hexane and this adsorption accelerated release rate due to weak bonding between silanol groups and drug molecules in the first 30 min. However, Celecoxib was dispersed in the arrays of MCM-41 particle pores in ethanol and released more slowly in the first 30 min due to encapsulation in the pores of carrier.

6.9 THERMOGRAVIMETRIC ANALYSIS (TGA)

Thermogravimetric analysis is a method of thermal analysis in which the sample is heated to elevated temperature and monitoring the weight loss as a function of increasing temperature. TGA analysis can provide information about a lot of physical and chemical phenomena such as second-order transition, sublimation, absorption, adsorption, chemisorptions, dehydration, decomposition, oxidative degradation and solid-state reactions [58].

Loss in weight is mainly related with the adsorbed H_2O, formation of oxides and gases such as CO_2, NH_3, N_2, NO_x, SO_y at the temperature below 200 °C. Weight loss due to Celecoxib was occurred between the temperature of 200 °C and 600 °C.

Therefore, calculations of Celecoxib loaded to MCM-41 silica particles were done according to the weight loss in this temperature range. In the Figures 67, 68, 69 and 70, % weight loss of MCM-41 particles and MCM-41 particles loaded with Celecoxib in the ethanol can be seen.
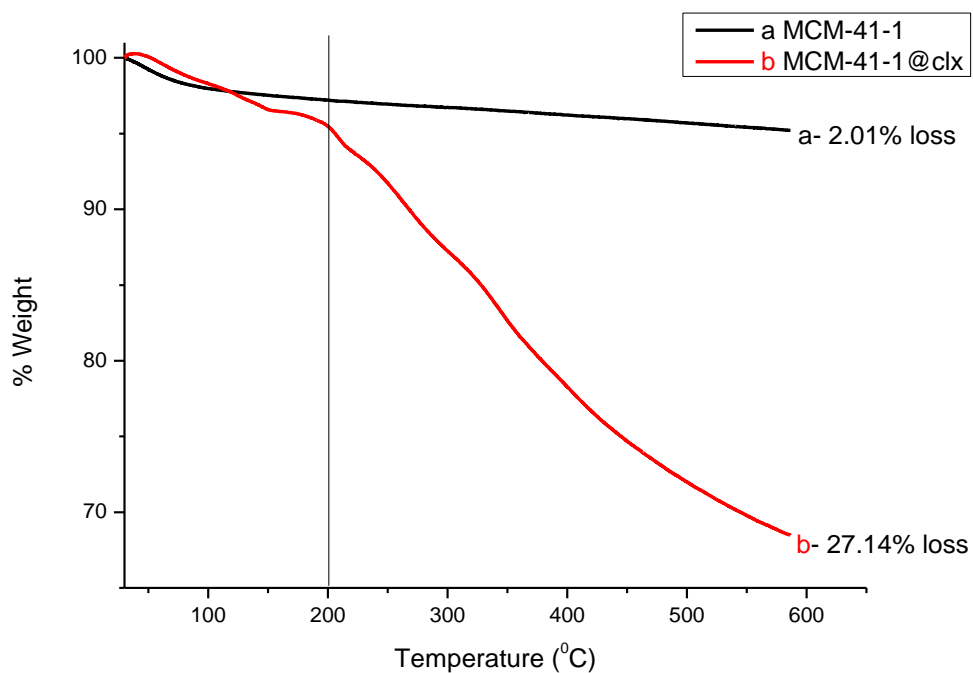
Figure 67: % Weight loss of a) MCM-41-1 b)MCM-41-1@clx samples
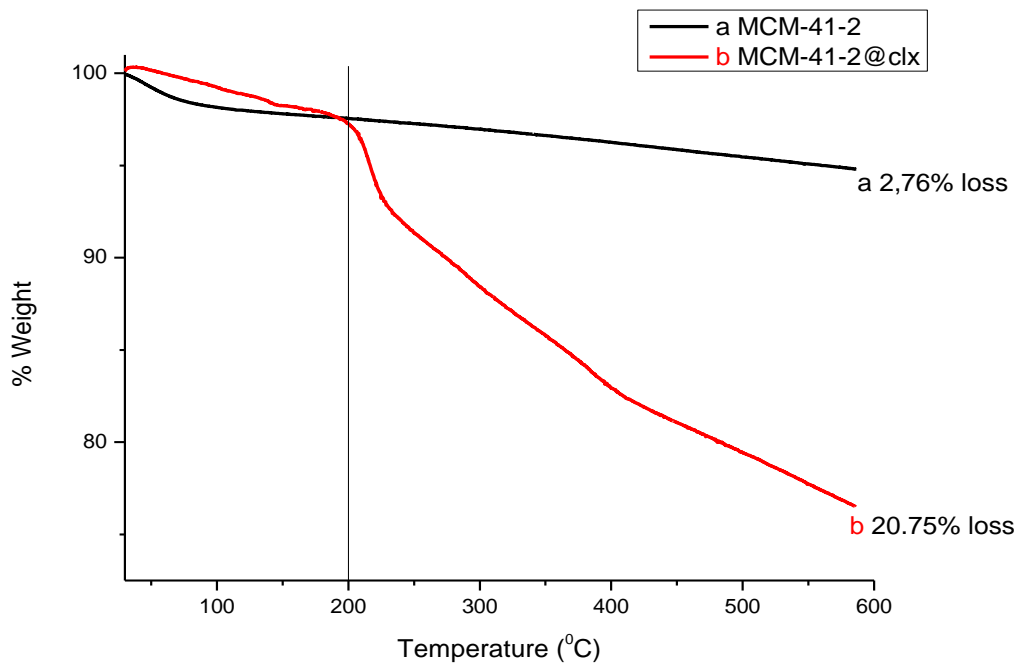
Figure 68: % Weight loss of a) MCM-41-2 b)MCM-41-2@clx samples
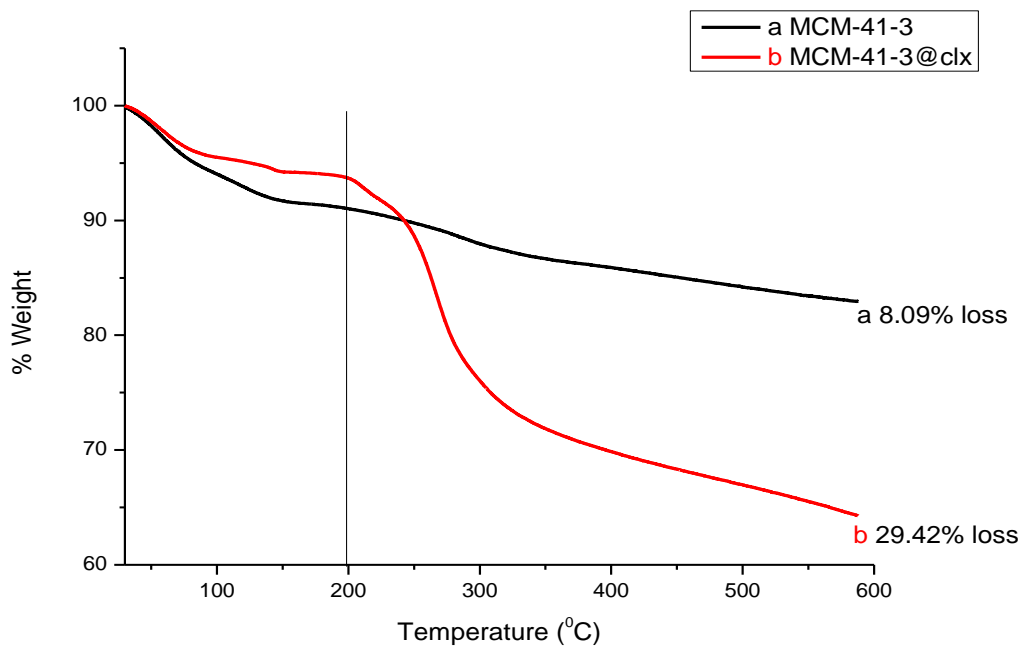
Figure 69: % Weight loss of a) MCM-41-3 b)MCM-41-3@clx samples
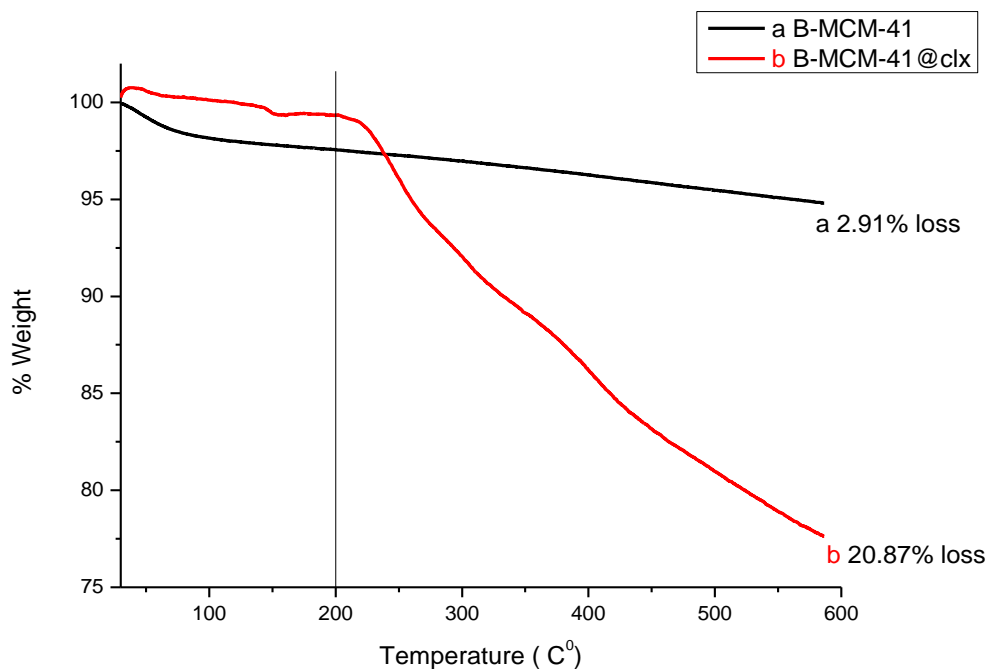
Figure 70: % Weight loss of a) B-MCM-41 b)B-MCM-41@clx samples

In the Table 21, there are data calculated of % Celecoxib loaded to carrier in ethanol due to UV analysis TGA analysis. As it can be seen, values are really close to each other. This confirms the amount the Celecoxib loaded to MCM-41 silica particles.

Table 21: % Celecoxib loaded to MCM-41 silica particles calculated due to UV analysis and TGA analysis

	UV Result	**TGA Result**
MCM-41-1	25.95%	25.13%
MCM-41-2	20.95%	17.99%
MCM-41-3	25.21%	21.33%
B-MCM-41	17.57%	17.96%

It can be seen that weight loss of the MCM-41 particles that are not loaded with Celecoxib are negligible at the temperature between 200 °C and 600 °C. There are only small weight loss due to adsorbed water or formation of gases before the temperature of 200 °C. It indicates that the ways used to remove the surfactant during the synthesis procedure are efficient.

CHAPTER 7

CONCLUSION

In order to enhance the release rate of Celecoxib and improving its biocompability, MCM-41 silica particles in different morphologies and diameters were synthesized. Surface functionalization was performed with different groups. As a model drug, Celecoxib was used. In order to investigate the solvent effect, 3 different solvents were used; methanol, ethanol and hexane.

According to XRD results, the order of pores of samples was determined as hexagonal unit cell (p6mm) 2D structure. In the small angle XRD patterns of MCM-41 particles, 3 diffraction peaks were observed. Decrease in intensity of the peaks and small shifts were explained with decrease in order and change in unit cell parameters. This is due to encapsulation of the drug molecules into the internal surface of particles. In the wide XRD patterns, after Celecoxib loading process, characteristic peaks of Celecoxib were observed for particles examined in hexane. This showed that drug molecules were stayed in crystalline state in hexane and mainly attached to the outer surface of the MCM-41 particles. However, they were finely divided in ethanol and highly dispersed into the pores and channels of the carrier particles.

In the FTIR analysis of MCM-41 samples, all the expected peaks indicating the silanol groups on the surface of the silica particles were determined. In the FTIR spectrum of samples loaded with drug in hexane, characteristic peaks of Celecoxib were observed. This confirmed that the drug molecules could not be dissolved and attached the outer surface of particles in hexane.

The pore size, pore volume and surface area were characterized by N_2 - adsorption - desorption analysis. In addition, the pore size distribution was calculated using BJH method. All the samples exhibited type IV BET isotherms that indicate mesoporous characteristic. Reversible adsorption – desorption processes and narrow hysteresis loops show the uniformity in pores and channels and small pore sizes. Decrease in pore volume and surface area was explained with successful grafting of Celecoxib molecules to the internal surface of MCM-41 particles. Narrow pore size distribution was seen in BJH method.

While the TEM images confirmed the hexagonal crystal structure composed of one - dimensional channels, SEM images proved the high degree of homogeneity in particle size and morphology. All MCM-41 samples preserved these properties, it was verified that the porous structure was not disrupted after Celecoxib loading process.

In order to do surface analysis zeta potential measurement was conducted. All the MCM-41 particles exhibited negative surface charge due to negatively charged silanol groups on the surface. Because of the high electronegativity of boron, B-MCM-41 samples showed more negative surface charge.

Due to the results of elemental analysis, it has been seen that functionalization did not increase the drug loading capacity of the carrier particles. It was explained by decrease in surface area after drug loading process and effect of chemistry of surface. PEG, APTES and YVO_4: Eu groups may prevent the interaction of silanol groups with Celecoxib molecules. In the elemental analysis, solvent effect was observed as one of the most important effect on the drug loading efficiency. This was explained with the polarity of the solvents. Polar solvents such as methanol and ethanol might form competitive adsorption with drug molecules and decrease the degree of Celecoxib loading.

UV analysis was used to confirm the amount of drug loaded to MCM-41 particles and investigate the release rate of the Celecoxib. It can be seen that release rate of the

Celecoxib was enhanced by using MCM-41 silica particles. The sustained release was observed in the first 6 hours.

TGA analysis was used to prove the amount of Celecoxib loaded to MCM-41 carrier particles. All the amounts of loaded drug were close to each other in the elemental analysis, UV analysis and TGA.

In conclusion, loaded amount of Celecoxib to the MCM-41 particles were enhanced. Maximum amount of Celecoxib loaded to silica particles was seen in hexane as solvent and MCM-41-1 that have the highest pore volume. Besides, release of the Celecoxib molecules were also highly improved according to its commercial drug capsule, Celebrex, by using MCM-41 particles as carrier.

FUTURE PROSPECTS

During the entire study, it has been seen that by making small variations in the synthesis procedure, different properties can be observed in the MCM-41 mesoporous materials. Different synthesis conditions leading to various morphologies and different surface properties can be applied in order to enhance the loading properties of the MCM-41 carrier particles in the drug delivery systems. Besides, different solvents such as chloroform can be used in order to observe the effect of solvent on the drug loading and release property of the carrier particles.

Alternatively, different support materials can be used in the controlled delivery of Celecoxib. In this way, major materials that can be investigated are other silica-based materials, fibrous ordered mesoporous carbons that have high pore volume, high surface area and high adsorption capacity, metal-organic frameworks that show high stability and high porosity with organic groups in the frameworks and silica lipid hybrid materials that combine the solubilising effect of the lipid and stabilizing effect of the silica. Bioavalibity of the Celecoxib can be enhanced by using these promising materials.

One important focus of future research will be in the biological aspects of using mesoporous particles in the delivery of Celecoxib. In order to observe the behavior of this drug delivery system in the body, experiments will be promoted to *vivo* tests and they will be conducted with cells.

REFERENCES

1) Li, W.; Zhao, D. *Chem. Commun*. **2013,** *49*, 943-946.

2) Deng, Y.; Wei, J.; Sun, Z.; Zhao, D. *Chem. Soc. Rev*. **2012**, *42*, 4054-4070.

3) Perego, C.; Millini, R. *Chem. Soc. Rev*. **2013**, *42*, 3956-3976.

4) Liu, J.; Bu, W.; Pan, L.; Shi, J. *Angew. Chem. Int. Ed*. **2013**, *52*, 4375-4379.

5) Kamarudin, N.; Jalil, A.; Triwahyono, S.; Salleh, N.; Karim, A.; Mukti, R.; Hameed, B.; Ahmad, A. *Microporous and Mesoporous Mater.* **2013**, *180*, 235-241.

6) Schumacher, K.; Gru, M.; Unger K. *Microporous and Mesoporous Mater.* **1999**, *27*, 201-206.

7) Meynen, V.; Cool, P.; Vansant, E.F. *Microporous and Mesoporous Mater.* **2009**, *125*, 170-223

8) Zhang, J.; Luz, Z.; Goldfarb, D. *J. Phys. Chem. B* **1997**, *101*, 7087-7094.

9) Ciesla, U.; Schucth, F.; Wolfgang, J. *Microporous and Mesoporous Mater.* **1999**, *27*, 131–149.

10) Yang, P.; Gai, S.; Lin, J. *Chem. Soc. Rev*. **2012**, *41*, 3679-3698.

11) Garcia, N.; Benito, E.; Guzman, J.; Tiemblo, P.; Morales, V.; Garcia, R. *Microporous and Mesoporous Mater.* **2007**, *106*, 129-139.

12) Zhao, D.; Feng, J.; Huo, O.; Melosh, N.; Fredisckson, G.; Chmelka, B.; Stucky, G. *Science* **1998**, *279*, 548-552.

13) Ying, Y.; Mehnert, C.; Wong, M. Angew. *Chem. Int. Ed*. **1999**, *38*, 56-77.

14) Stein, A.; Melde, B.; Schroden, R. *Adv. Mater.* **2000**, *12*, 1403-1419.

15) Vallet - Regi, M.; Balas, F.; Colilla, M.; Manzano, M. *Solid State Sci*. **2007**, *9*, 768-776.

16) Xu, W.; Riikonen, J.; Lehto, V. Int. *J. Pharmaceut. Sci*. **2013**, *453*, 181-197.

17) Zhang, W.; Shi, J.; Wang, L.; Yan, D. *Mater. Let*. **2000**, *46*, 35–38.

18) Wang, X.; Lin, K.; Chan, J.; Cheng, S. *J. Phys. Chem. B* **2005**, *109*, 1763-1769.

19) Lebeau, B.; Gaslain, F.; Fernandez - Martin, C.; Babonneau, F. *Elsevier B. V.* **2009**, 285.

20) Song , S.; Hidajat, K.; Kawi, S. *Am. Chem. Soc*. **2005**, *21*, 9568-9575.

21) Xu, H.; Yan, F.; Monson, E.; Kopelman, R. *J. Biomed. Mater. A* **2003**, *66*, 870-879.

22) Yu, M.; Lin, J.; Fang, J. *Chem. Mater*. **2005**, *17*, 1783-1791.

23) Yang, P.; Quan, Z.; Hou, Z.; Li, C.; Kang, X.; Cheng, Z.; Lin, J. *Biomater.* **2009**, *30*, 4786-4795.

24) Hwang, G.; Jeon, H.; Kim, Y. *J. Am. Ceram. Soc*. **2002**, *85*, 2956-60.

25) Liu, M.; Hidajat, K.; Kawi, S.; Zhao, D. *Chem. Commun*. **2000**, 1145-1146.

26) Das, D.; Lee, J.; Cheng, S. *Chem. Commun*. **2001**, 2178-2179.

27) Allen, T.; Cullis, P. *Science* **2004**, *303*, 1818-1822.

28) Horcajada, P.; Rámila, A.; Vallet-Regi, J. M. *Microporous and Mesoporous Mater*. **2004**, *68*, 105-109.

29) Perrie, Y.; Rades, T. *London: Pharmaceutical Press* **2012**, 2, 1-13.

30) Yang, P.; Quan, Z.; Li, C.; Lian, H.; Huang, S.; Lin, J. *Microporous and Mesoporous Mater*. **2008**, *116*, 524-531.

31) Wang, S. *Microporous and Mesoporous Mater*. **2009**, *117*, 1-9.

32) Liu, Y.; Sua, C.; Hao, Y.; Jiang, T.; Zheng, L.; Wang, S. *J Pharm Pharmaceut. Sci*. **2010**, *13*, 589-606.

33) Timpe, C. *Am. Pharm. Rev.* **2010**.

34) Wischke1, C.; Schwendeman, S. *Int. J. Pharmaceut*. **2008**, *364*, 298-327.

35) Chaudhary, A.; Nagaich, U.; Gulati, N.; Sharma, V.; Khosa V. *J. Adv. Pharm. Edu.* **2012**, *2*, 32-67.

36) Strickley, R. *Pharmaceut. Res*. **2004**, *21*, 202-228.

37) Hauss, D. *Adv. Drug Delivery Rev.* **2007**, *59*, 667–676.

38) Mudit, D., Panner S.; Jain A. *J. Pharma*. **2012**, 598-563.

39) Serajuddin, A. *J. Pharmaceut. Sci*. **1999**, *88*, 1058-1066.

40) Mellaerts, R.; Aerts, C.; Van Humbeeck, J.; Augustijns, P.; Van den Mooter, G.; Martens, J. *Chem Commun*. **2007**, *13,* 1375-1377.

41) Tan, A.; Davey, A.; Presditge, A. *Pharm. Res.* **2011**, *28*, 2273-2287.

42) Steinbach, G.; Lynch, P. *N. Engl. J. Med. 2000, 342,* 1946-1942.

43) Kawamori, T.; Rao, C.; Seibert, K.; Reddy, B. *J. Cancer Res.* **1998,** *58,* 409.

44) Schade, R.; Suissa, S.; Garbe, E. *Stroke* **2006**, *37*, 1725-1730.

45) Chen, L.C.; Ashcroft, D.M. *J. Clinical Pharmacy and Therapeutics* **2006**, *31*, 565-576.

46) Tan, A.; Simovic, S.; Davey, A.; Rades, T.; Prestidge, C. A. *J. Controlled Release* **2009**, *134*, 62-70.

47) Zhao, P.; Jiang, H.; Jiana, T.; Zhi, Z.; Wua, C.; Sun, C.; Zhang, J.; Wang, S. *Eu. J. Pharmaceut. Sci*. **2012**, *45*, 639-647.

48) Zheng, Q.; Hao, Y.; Ye, P.; Guo, L.; Wu, H.; Guo, Q.; Jiang, J.; Fu, F.; Chen, A. *J. Mater. Chem. B* **2013**, *1*, 1644-1648.

49) Zhanga, J.; Liua, M.; Songa, C.; Guoa, X. *Microporous and Mesoporous Mater.* **2011**,*139*, 31-37.

50) Yu, M.; Lin, J.; Fang, J. *Chem. Mater.* **2005**, *17*, 1783-1791.

51) Primo, T. F. *Acta Farm.* **2005**, *24***,** 421-4255.

52) Parida, S.; Dash, S.; Patel, S.; Mishra, B. *Adv. Colloid Interface Sci.* **2006**, *121*, 77-110.

53) Allen, T. *London; New York: Chapman and Hall* **1997**, *1*, 104 – 105.

54) Kruk, M.; Jaroniec, M. *Langmuir* **1997**, *13*, 6267-6273.

55) Ravikovitch, P.; Domhnaill, S.; Neimark, A.; Schuth, F.; Ungert, K. *J. Am. Chem. Soc*. **1995**, *11*, 4765-4772.

56) Kaminsky, R. D.; Maglara, E.; Conner, W. *J. Am. Chem. Soc*. **1994**, *10*, 1556-1565.

57) Yıldırım, A.; Ozgur, E.; Bayındır, E. *J* . *Mater. Chem. B* **2013**, *1*, 1909-2013.

58) Ambrogi, V.; Perioli, L.; Pagano, C.; Latterini, L.; Marmottini, F.; Ricci, M.; Rossi, C. *Microporous and Mesoporous Mater*. **2012**, *147*, 343-349.

59) Hudson, S.; Tanner, D. A.; Redington, W.; Magner, E.; Hodnett, K.; Nakahara, S. *Phys. Chem. Chem. Phys*. **2006**, *8*, 3467–3474.

APPENDIX A

SMALL ANGLE XRD PATTERN OF MESOPOROUS SILICA
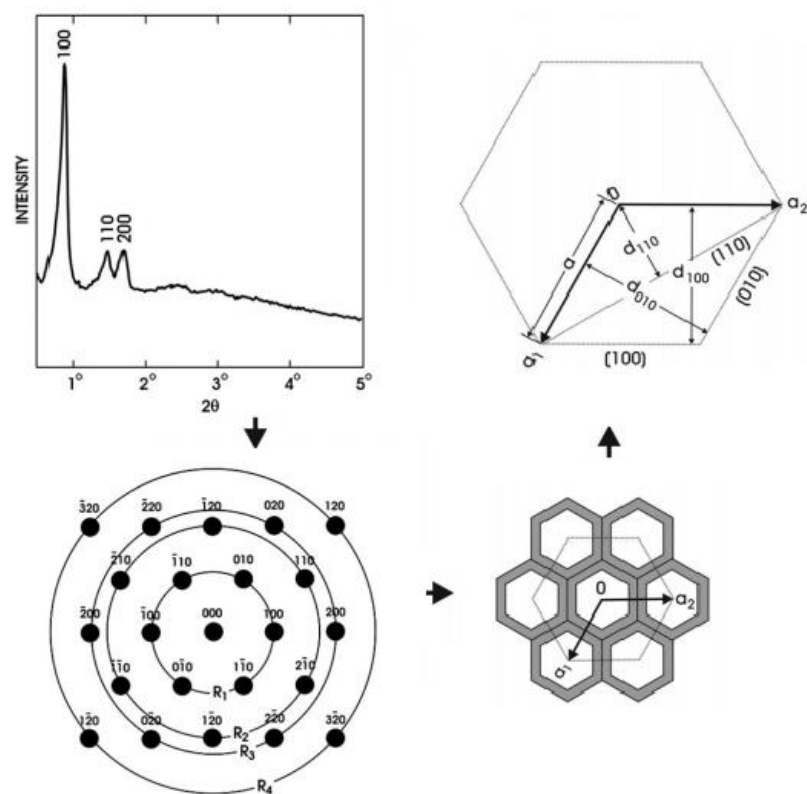
Figure A.1: Small angle XRD pattern that defines the order of pores in mesoporous silica [59]

CALCULATION OF % CELECOXIB LOADED TO MCM-41-1 PARTICLES IN HEXANE

$$A = \varepsilon \times b \times c$$

A = Absorbance (0.3246 for Celecoxib in 254 nm in UV Analysis)

ε = Molar absorptivity coefficient (87.814 L/ mol $\times$ cm for hexane)

b = Path length of the sample (1 cm for sample cell)

c = Concentration (M)

$$A / (\varepsilon \times b) = c$$

$0.3246 / \left(87.8 \frac{L}{mol \times cm} \times 1 \text{ cm}\right) = 0.00369$ M of filtrate

$0.00369 \frac{mol}{L} \times \frac{1 \text{ L}}{1000 \text{ mL}} \times \frac{1000 \text{ mmol}}{1 \text{ mol}} \times 50 \text{ mL} = 0.1848$ mmol Celecoxib in the filtrate

$0.1848 \text{ mmol} \times 381.373 \frac{mg}{mmol} = 70.49 \text{ mg}$ Celecoxib in the filtrate

$100 \text{ mg} - 70.49 \text{ mg} = 29.51 \text{ mg}$ Celecoxib loaded to MCM-41-1 particles

$(29.51 \text{ mg} / 100 \text{ mg}) \times 100\% = 29.51\% = \%$ Celecoxib loaded to MCM-41-1 particles

BET ISOTHERMS
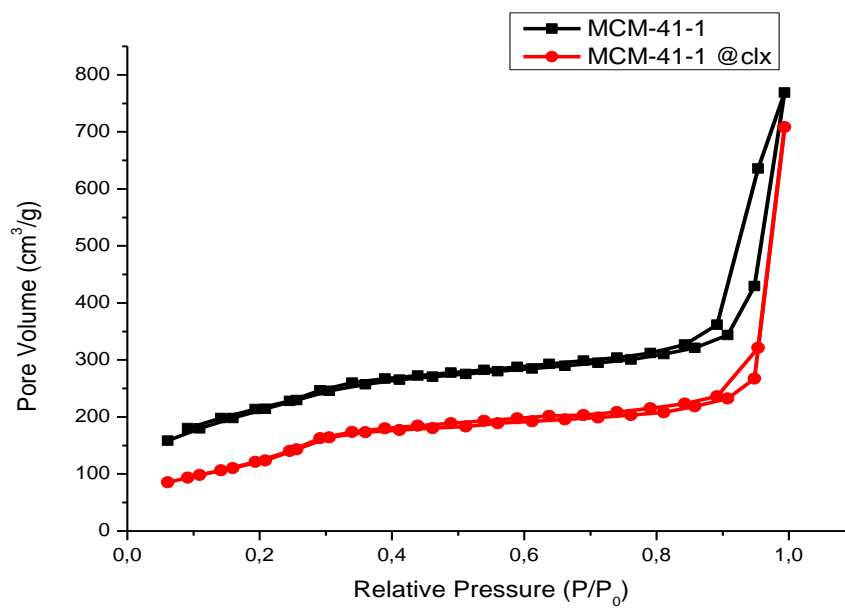
Figure A.2: BET isotherms of isotherms of MCM-41-1 and MCM-41-1@clx in ethanol
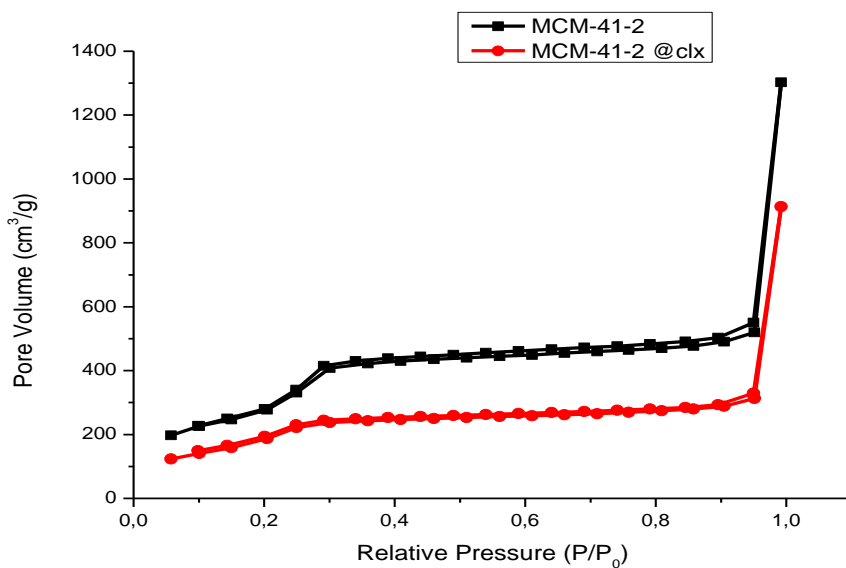
Figure A.3: BET isotherms of isotherms of MCM-41-2 and MCM-41-2@clx in ethanol
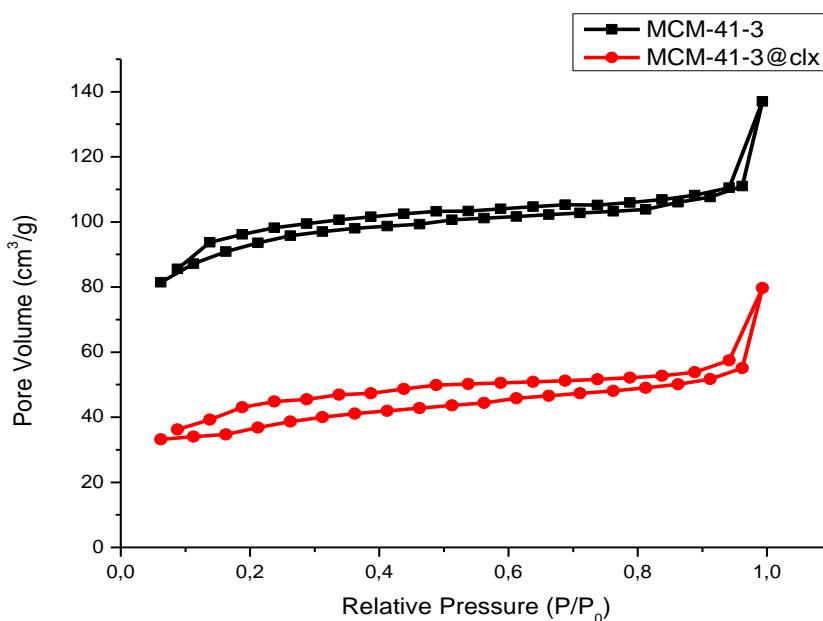
Figure A.4: BET isotherms of isotherms of MCM-41-3 and MCM-41-3@clx in ethanol
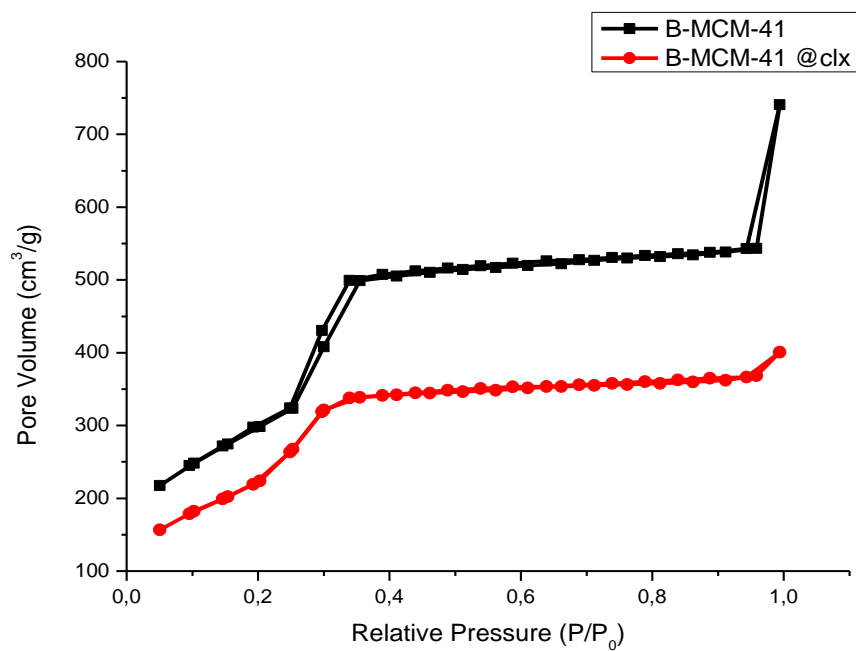
Figure A.5: BET isotherms of isotherms of B-MCM-41 and B-MCM-41@clx in ethanol